



岐阜大学機関リポジトリ

Gifu University Institutional Repository

Mechanism of Controlling Melanin Biosynthesis by the Constituents of Tropical Medicinal Plants

メタデータ	言語: English 出版者: 公開日: 2016-12-02 キーワード (Ja): キーワード (En): 作成者: YAMAUCHI, Kosei メールアドレス: 所属:
URL	http://hdl.handle.net/20.500.12099/51015

**Mechanism of Controlling Melanin Biosynthesis by the Constituents of
Tropical Medicinal Plants**

(熱帯産薬用植物成分のメラニン生合成制御機構に関する研究)

2014

The United Graduate School of Agricultural Science, Gifu University

Science of Biological Resources

(Gifu University)

YAMAUCHI, Kosei

**Mechanism of Controlling Melanin Biosynthesis by the Constituents of
Tropical Medicinal Plants**

(熱帯産薬用植物成分のメラニン生合成制御機構に関する研究)

YAMAUCHI, Kosei

Contents

Table of contents	I
List of figures	V
List of schemes	VII
List of tables	VII
Summary	VIII
學位論文要旨.....	XI
Chapter 1	1
General introduction	1
1.1 Melanin biosynthesis.....	2
1.1.1 Skin and hair pigmentation.....	2
1.1.2 Melanin biosynthesis.....	4
1.2 Transcriptional regulation of melanogenesis.....	7
1.3 Transportation of melanosomes.....	9
1.3.1 Microtubule transportation of melanosomes.....	9
1.3.2 Actin transportation of melanosomes.....	11
1.4 Melanogenesis controlling effect of medicinal plants extract.....	13
1.4.1 Indonesian medicinal plants.....	13
1.4.2 Tyrosinase inhibitor.....	14
1.4.3 Regulator on expression of melanogenic enzymes.....	17
1.5 Research objectives.....	19
Chapter2	21
Identification of quercetin glycosides as intracellular melanogenesis stimulator from <i>Helminthstachys zeylanica</i>	21

2.1 Introduction.....	22
2.2 Material and Methods.....	23
2.2.1 General.....	23
2.2.2 Material.....	24
2.2.3 Extraction and fractionation of <i>H. zeylanica</i> root powder.....	24
2.2.4 Tyrosinase activity assay.....	24
2.2.5 Cell culture.....	24
2.2.6 Measurement of cellular melanin contents.....	25
2.2.7 Cell viability.....	25
2.2.8 Identification of compound 1 and 2.....	26
2.2.9. Acid hydrolysis.....	29
2.2.10 Determination of absolute configuration of sugars from compound 1 and 2.....	29
2.3 Results and Discussion.....	30
2.3.1 Identification of compound 1 and 2.....	30
2.3.2 Intracellular melanogenesis enhancement activity.....	35
2.4 Summary.....	39
Chapter3.....	40
Synthesis of quercetin derivatives.....	40
3.1 Introduction.....	41
3.2 Material and methods.....	44
3.2.1 General.....	44
3.2.1 Synthesis of quercetin glycosides.....	45
3.2.1.1 Preparation of acetobromocellobiose.....	45

3.2.1.2 Synthesis of 3 and 4.....	45
3.2.1.3 Synthesis of 1 and 5-11.....	47
3.2.2. Synthesis of quercetin methyl ether.....	53
3.2.2.1 Synthesis of 12.....	53
3.2.2.2 Synthesis of 13, 14, and 15.....	55
3.2.2.3 Synthesis of 16, 17, and 18.....	56
3.2.3 Synthesis of 19.....	58
3.2.4 Synthesis of 20.....	59
3.3 Result and discussion.....	61
3.3.1 Synthesis of quercetin glycosides.....	61
3.3.2 Synthesis of 12-20.....	65
3.4 Summary.....	71
Chapter 4.....	72
Melanogenesis stimulatory activity of synthesized quercetin derivatives via	
p38 MAPK path way.....	72
4.1 Introduction.....	73
4.2 Material and methods.....	75
4.2.1 General.....	75
4.2.2 Tyrosinase activity assay.....	75
4.2.3 Cell culture.....	75
4.2.4 Measurement of cellular melanin content.....	76
4.2.5 Cell viability.....	76
4.2.6 Western blot analysis.....	77
4.2.7 Statistical analysis.....	78

4.3 Results and discussion.....	78
4.3.1 Melanogenesis activities of quercetin glycosides.....	78
4.3.2 Melanogenesis activities of quercetin methyl ether.....	83
4.3.3. Effect of compounds 12 and 15 on the expression of proteins involved in melanin biosynthesis.....	86
4.4 Summary.....	90
Chapter 5.....	92
Quercetin derivatives regulate transportation of melanosome via EPI64.....	92
5.1 Introduction.....	93
5.2 Material and methods.....	96
5.2.1 General.....	96
5.2.2 Cell culture.....	96
5.2.3 Observation of cell shapes.....	97
5.2.4 Western blot analysis.....	97
5.2.5 Immunofluorescence Microscopy.....	98
5.2.6 Statistical analysis.....	99
5.3 Results and discussion.....	99
5.3.1 Effects on cell shapes treated with 1, 12, and 15.....	99
5.3.2 Effects of 1, 12, and 15 on transportation of melanosome.....	106
5.4 Summary.....	112
Conclusion.....	113
References.....	115
Acknowledgments.....	129

List of figures

Fig.1.1 Mechanism of skin pigmentation.....	3
Fig.1.2 Typical hair follicle.....	4
Fig.1.3 Melanin biosynthesis path way.....	5
Fig.1.4 Catalysis mechanism of tyrosinase on oxidation of L-tyrosine and L-DOPA.....	6
Fig.1.5 Transcriptional regulation of expression of melanogenic enzymes.....	8
Fig.1.6 Transportation of melanosome in melanocyte.....	10
Fig.1.7 Actin transportation of melanosome.....	12
Fig.1.8 Interaction of melanosome with plasma membrane <i>via</i> Slp2-a.....	13
Fig.1.9 Chemical structures of tyrosinase inhibitor including 2, 4-substituted resorcinol moiety.....	16
Fig.1.10 <i>R. rosea</i>	18
Fig.1.11 Chemical structures of melanogenesis modulators.....	19
Fig.2.1 <i>Helminthostachys zeylanica</i>	22
Fig.2.2 Structures of compound 1 and 2.....	32
Fig.2.3 Total ion chromatograms of silylated D-glucose, L-rhamnose, D-arabinose, D-galactose, and sugars from compound 1.....	33
Fig.2.4 UPLC-TOFMS spectrum of compound 1.....	34
Fig.2.5 Intracellular melanogenesis activity and cell viability of compound 1 and 2.....	37
Fig.2.6 Tyrosinase activity of compound 1 and 2.....	38
Fig.3.1 Structures of quercetin derivatives.....	43
Fig.3.2 Key HMBC correlations of compound 1, 3, and 4.....	64

Fig.3.3 Key HMBC correlations of compounds 12, 15, and 20.....	70
Fig.4.1 p38 MAPK path way regulating the expressions of melanogenic enzymes.....	74
Fig.4.2 Effect of 12 and 15 on the expression of Tyrosinase, TRP1, TRP2, MITF, p-p38MAPK, and p38MAPK in B16 melanoma cells.....	89
Fig.4.3 Effects of compound 12 and 15 on expression of melanogenic enzymes..	91
Fig.5.1 Complex for actin transportation.....	95
Fig.5.2 Active/inactive switch of Rab27A on melanosomes.....	95
Fig.5.3 Cell shapes treated with 1 at 200-0 μ M for 42h or 72h.....	101
Fig.5.4 Cell shapes treated with 12 at 25-0 μ M for 42h or 72h.....	102
Fig.5.5 Cell shapes treated with 15 at 25-0 μ M for 42h or 72h.....	103
Fig.5.6 Ratio of cell length.....	104
Fig.5.7 Effect of Varp on melanogenesis in melanocyte.....	105
Fig.5.8 Effect of 1, 12, and 15 on the expression of EPI64 in B16 melanoma cells.....	108
Fig.5.9 Immunofluorescence confocal microscopy showing the distribution of Rab27A and melanosomes.....	109
Fig.5.10 Effect of 1 on transportation of melanosome.....	110
Fig.5.11 Effect of 12 and 15 on transportation of melanosome.....	111

List of Scheme

Scheme 3.1 Synthesis route of quercetin glycosides 1 and 3-11.....	63
Scheme 3.2 Synthesis route of methylquercetins 12-15.....	67
Scheme 3.3 Synthesis route of methylquercetins 16-18.....	68
Scheme 3.4 Synthesis route of methylquercetins 19, 20.....	69

List of Tables

Table 2.1 ¹ H and ¹³ C-NMR chemical shifts and key HMBC correlations of compound 1.....	27
Table 2.2 ¹ H and ¹³ C-NMR chemical shifts and key HMBC correlations of compound 2.....	28
Table 4.1 Intra and extracellular melanogenesis activity and cell viability in B16 melanoma cells by the synthesized quercetin glycosides.....	80
Table 4.2 Mushroom tyrosinase activity by the synthesized quercetin glycosides	82
Table 4.3 Intra and extracellular melanogenesis activity and cell viability in B16 melanoma cells by the synthesized quercetin derivatives 12-20.....	85

Summary

Melanin, a pigment present in several tissues in the human body, is biosynthesized in melanocytes by the catalysis of tyrosinase, tyrosinase related protein (TRP-1 and TRP-2). Melanin plays an important role in preventing skin cancer caused by ultraviolet (UV) rays. The overall level of melanogenesis is changed by aging, stress, and damage caused by the UV rays, resulting in the appearance of gray hairs, sunburn, and mottling on the skin. Therefore, controlling melanogenesis is important for maintaining the good health and cosmetic appearance of the human body. This study aims to search the active compounds exhibiting the melanogenesis modulating activity and elucidate the mechanism underlying the observed activity.

Two novel quercetin glycosides namely 4'-*O*- β -D-glucopyranosyl-quercetin-3-*O*- β -D-glucopyranosyl-(1 \rightarrow 4)- β -D-glucopyranoside (**1**) and 4'-*O*- β -D-glucopyranosyl-(1 \rightarrow 2)- β -D-glucopyranosyl-quercetin-3-*O*- β -D-glucopyranosyl-(1 \rightarrow 4)- β -D-glucopyranoside (**2**) were isolated and identified from *Helminthostachys zeylanica* roots 50% ethanol extract (Chapter 2). Compound **1** exhibited intracellular melanogenesis stimulatory activity, while **2** showed no effect even the structural similarity of the two compounds in B16 melanoma cells. This result indicates the involvement of the substituent group attached quercetin on melanogenesis stimulatory activity of quercetin derivatives. In order to understand the structure-activity relationships of quercetin derivatives, nineteen quercetin derivatives were synthesized from rutin in Chapter 3.

As the result of bioassay using synthesized nineteen quercetin derivatives in B16

melanoma cells, **1**, quercetin-3-*O*- β -D-glucopyranoside (**3**), and quercetin-3-*O*- β -D-glucopyranosyl-(1 \rightarrow 4)- β -D-glucopyranoside (**4**) stimulated the intracellular melanogenesis, while they elicited no stimulatory activity on extracellular melanogenesis. On the other hand, synthesized 3-*O*-methylquercetin (**12**) and 3,4',7-*O*-trimethylquercetin (**15**) increased the both intra and extracellular melanin contents with no cytotoxicity (Chapter 4). Compound **15** increased the phosphorylated p38 mitogen activated protein kinase (MAPK) and microphthalmia-associated transcription factor (MITF) which regulates the expression of tyrosinase, TRP-1 and TRP-2. While **12** enhanced the expression of the melanogenic enzymes without involving the MITF, as evidenced by its lack of any stimulation of the expression of MITF and p-p38 MAPK. This result indicates that **12** may stimulate the expression of tyrosinase, TRP-1, and TRP-2 by stimulating currently unidentified transcriptional factors and/or by regulating the degradation of melanogenic enzymes.

Mature melanosomes in melanocytes are specifically transported by transporter proteins on the microtubule and actin. Melanocyte elongates the dendrite and melanosomes are transferred to the keratinocytes or hair matrix cells which results in hair and skin pigmentation. Rab27A on the melanosome composes the transportation complex and the motor protein transports the complex to the periphery region of melanocyte on the actin filament. Rab27A is inactivated by EBP50-PDZ interactor of 64kDa (EPI64) and excluded from the surface of melanosome. In order to investigate the effect of **12** and **15** on transportation of melanosomes, the cell length and the expression of EPI64 in B16 melanoma cells after treatment of **12** and **15** were examined in Chapter 5. Compounds **12** and **15** elongated the dendrite of B16 melanoma cells in a dose dependent manner, and the elongation effect of **15** was stronger than **12**.

Furthermore, **12** and **15** inhibited the expression of EPI64. The inhibition of **15** was more potently than **12**, suggesting that the stimulation effect of **15** on transportation of melanosomes was stronger than **12**. The extracellular melanogenesis stimulatory activity of **15** was also higher than that of **12**, which indicated that the extracellular melanogenesis stimulatory activity of **12** and **15** is involved in the dendrite elongation effect and melanosome transportation stimulatory effect. It was also clarified that **12** and **15** induced the colocalization of Rab27A and melanosomes by the examination of immunofluorescence microscopy. This results support the effects on inhibitory activity of expression of EPI64 in B16 melanoma cells treated with **12** or **15**.

学位論文要旨

メラニンチロシンを基質として tyrosinase や tyrosinase related protein (TRP-1, TRP-2)によりメラノサイト内で生合成される色素であり, 紫外線ダメージにより生じる皮膚癌を防ぐはたらきをもつ。一方, 白髪や日焼け, しみ, そばかすを引き起こす原因となる。そのためメラニン生成を制御することは健康や美容を維持する上で重要視されている。そこで本研究はメラニン生成を制御する化合物を熱帯産植物から探索し, 活性成分の構造解析とメラニン生合成の制御機構の解明を目的とした。

本研究で新規 quercetin 配糖体である 4'-O-β-D-glucopyranosyl-quercetin-3-O-β-D-glucopyranosyl-(1→4)-β-D-glucopyranoside (1) と 4'-O-β-D-glucopyranosyl-(1→2)-β-D-glucopyranosyl-quercetin-3-O-β-D-glucopyranosyl-(1→4)-β-D-glucopyranoside (2) を *Helminthostachys zeylanica* 根 50%エタノール抽出物から単離した。化合物 1 は細胞内メラニン生成促進活性を示したが, 化合物 2 は構造が類似しているにもかかわらず活性を示さなかった。この結果から quercetin に結合する置換基が quercetin 誘導体のメラニン生成促進活性に関与していることが示された。そこで quercetin 誘導体の構造活性相関を調査するために 19 種の quercetin 誘導体を rutin から合成した。

合成した 19 種 quercetin 誘導体を用いた B16 メラノーマ細胞の活性試験を行い, その結果化合物 1 や quercetin-3-O-β-D-glucopyranoside (3), quercetin-3-O-β-D-glucopyranosyl-(1→4)-β-D-glucopyranoside (4)に細胞内メラニン生成促進活性が認められた。しかしこれらの合成物は細胞外メラニンの増加には関与しなかった。一方 3-O-methylquercetin (12) や 3, 4', 7-O-trimethylquercetin (15)は細胞内外共にメラニン生成促進活性を低細胞毒性で示した。化合物 15 は p38 mitogen activated protein kinase (MAPK)のリン酸化と microphthalmia-associated transcription factor (MITF)の発現を促進することで tyrosinase や TRP-1, TRP-2 の発現を促進した。一方化合物 12 は MITF や p-p38MAPK を増加せずにメラニン合成酵素の発現を促進した。このため化合物 12 は未知の転写因子を介することで, あるいはメラニン合成酵素の分解に関与することでメラニン合成酵素の発現を促進したと考察した。

成熟したメラノソームは特異的に微小管やアクチンを伝い輸送される。メラノサイトは樹状突起を伸長しメラノソームをケラチノサイトや毛母細胞に輸送することで, 皮膚や毛髪の色沈着が生じる。メラノソーム表面に存在する Rab27A は輸送複合体を形成し, 複合体はモータータンパク質によりアクチンを伝って細胞膜方向へ輸送される。EPI64 は Rab27A を不活性化してメラノソーム表面から排除する。化合物 12 と 15 のメラノソーム輸送への関与を調査するために本化合物で処理した細胞の EPI64 の発現量を測定した。その結果化合物 12 と 15 は B16 メラノーマ細胞の樹状突起を濃度依存的に伸長し, 化合物 15 は 12 よりも高い活性を示した。さらにこれらは EPI64 の発現を阻害し, この活性においても化合物 15 の方が高かった。化合物 15 は 12 よりも高い細胞外メラニン生成促進活性を示すことから, 樹状突起の伸長や EPI64 の発現を阻害することによるメラノソーム輸送促進が,

細胞外メラニン生成促進活性に関与することを強く示唆した。さらに化合物 **12** や **15** で処理することにより **Rab27A** とメラノソームが共局在を生じることが免疫蛍光染色顕微鏡検査により明らかとなり、本化合物が **EPI64** 発現阻害活性を示す結果を裏付けた。

Chapter 1

General introduction

1.1 Melanin biosynthesis

1.1.1 Skin and hair pigmentation

Melanin pigment is distributed in several tissues in the human body. The main function of melanin is considered to prevent skin damage by ultraviolet (UV) rays including in sunlight (Lukiewicz, 1972 and Wang, 2006). The excess accumulation of melanin or the absence of melanin production caused by aging, stress, and UV damages induces gray hairs, freckles, mottling, and senile lentiginos (Rees, 2003). Hence regulating melanogenesis is desired for maintain the good health and cosmetic appearance of the human body. Keratinocytes, existing on the skin surface, produce messengers such as α -melanocyte-stimulating hormone (α -MSH), prostaglandin, and histamine to melanocytes after get stimulated by UV irradiation (Yoshida, 2000). Then melanocyte biosynthesizes the melanin in melanosome and transports the mature melanosomes to the keratinocytes. The skin pigmentation is induced by the cornification of keratinocyte including the mature melanosomes that are biosynthesized and transported by the melanocytes (Fig.1.1). Similarly, hair pigmentation occurs due to melanin released on the outside of the melanocyte. During active growth of hair follicles, melanocytes locate in the hair bulb proliferated and differentiate to produce pigment of the hair shaft (Slominski, 2005 and Slominski, 1993) (Fig.1.2). Melanocytes begin to shut down melanogenesis in late anagen and regression phase called catagen, and it dies by apoptosis on the hair bulb in rest phase called telogen. The melanogenesis in melanocytes reappears when hair follicles reenter anagen (Tobin, 1998, Slominski, 1994, Tobin, 1999, Guo., 2012). The prevention of melanogenesis in the hair bulb on anagen is induced by the aging or stress which results in gray hair.

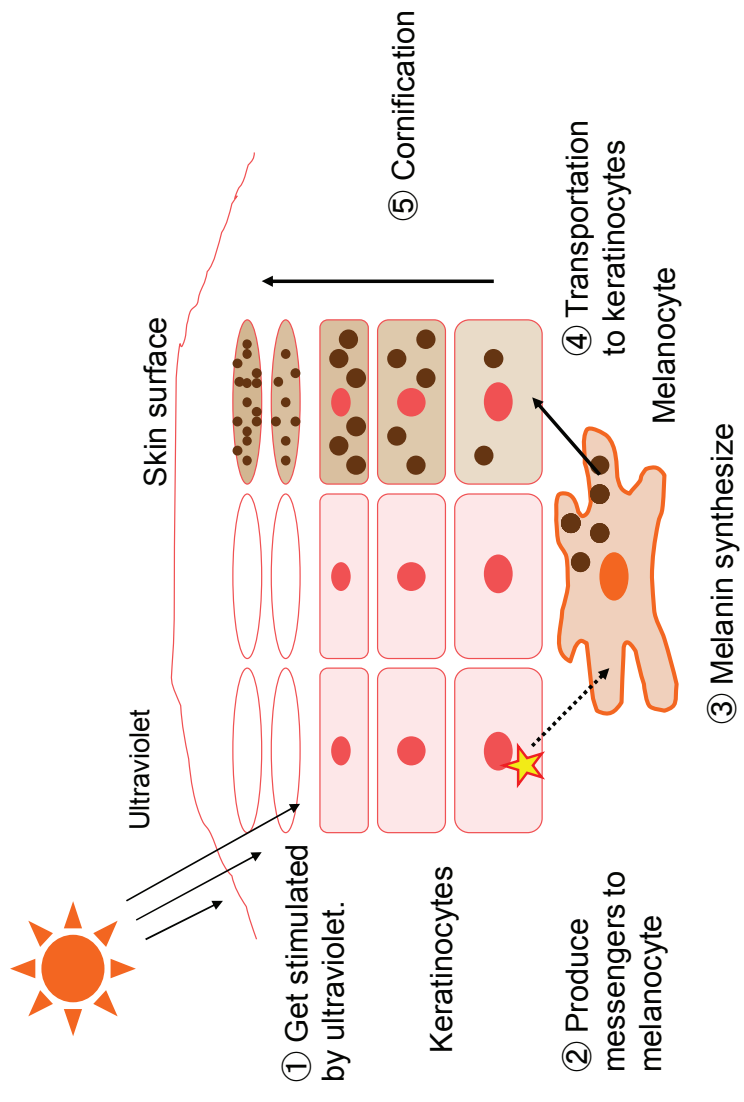


Fig.1.1 Mechanism of skin pigmentation

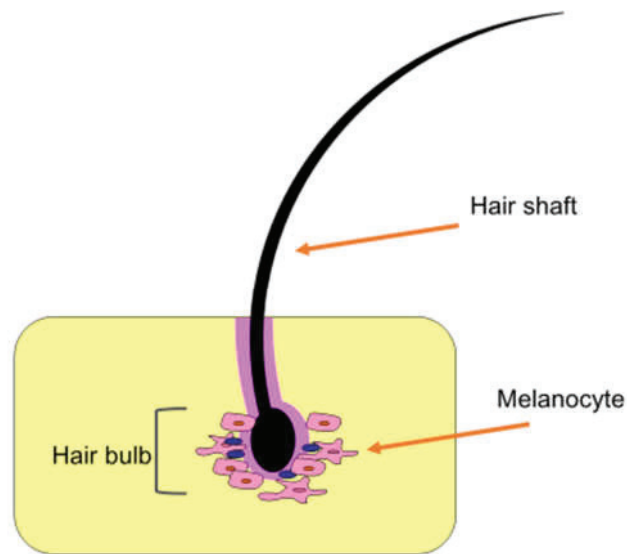
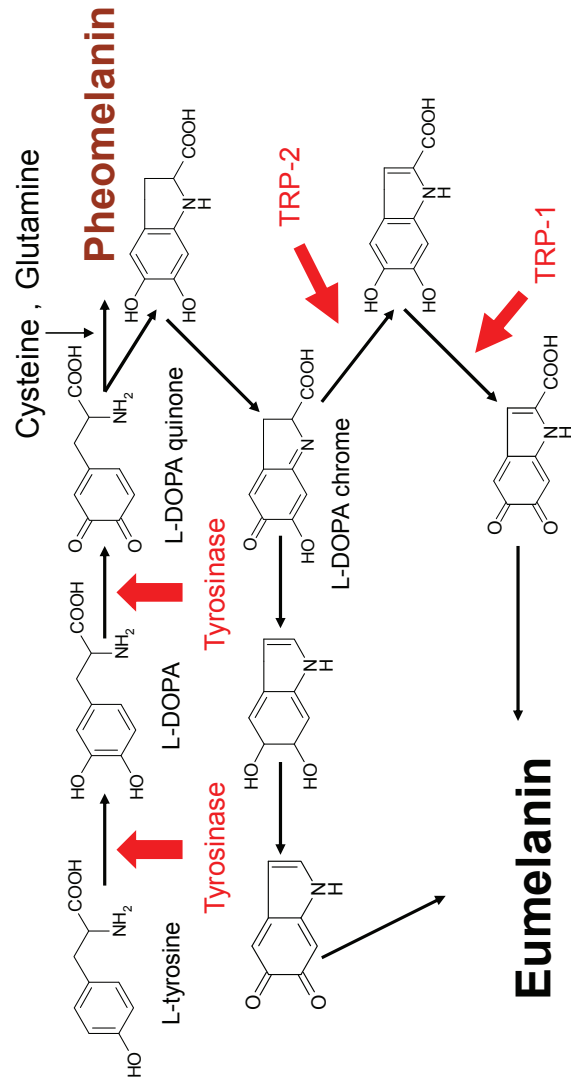


Fig.1.2 Typical hair follicle

1.1.2 Melanin biosynthesis

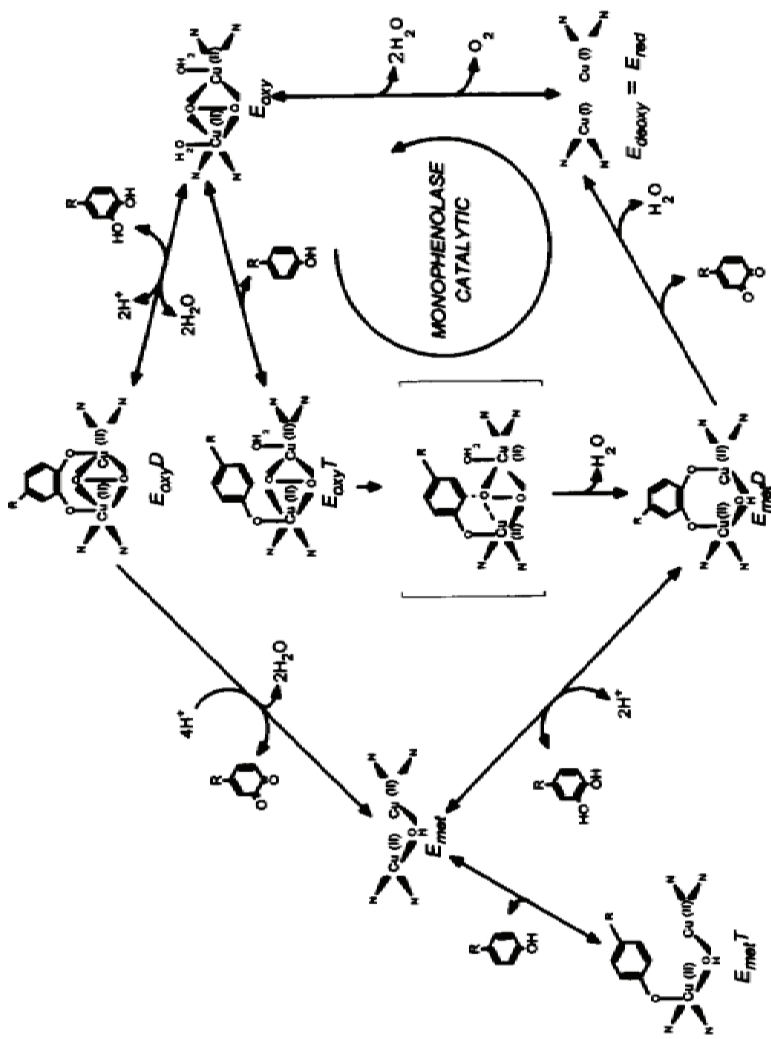
Melanin biosynthesis initially take places *via* oxidation of L-tyrosine catalyzed by tyrosinase in malanosome, a rate limiting reaction of melanin biosynthesis (Fig.1.3). Tyrosinase catalyzes the hydroxylation of L-tyrosine to L-3,4-dihydroxyphenylalanine (L-DOPA), as well as the subsequent oxidation of L-DOPA to L-DOPA quinone (Prota 1995 and Alvaro, 1995). Tyrosinase contains two copper ions, and inactive tyrosinase is activated *via* taking in oxygen and H₂O (Fig.1.4). The active tyrosinase binds with tyrosine or L-DOPA and release the oxidized product *via* constitution of intermediate. Two types of melanin are ultimately biosynthesized, reddish-orange and blackish-brown pigments called pheomelanin and eumelanin respectively, with the enzymes tyrosinase related protein (TRP)-1 and TRP-2 playing a key role in the biosynthesis of eumelanin (Cooksey, 1998). Then regulation of tyrosinase, TRP-1, and TRP-2 activity and/or expressions plays an important role to control melanin production.



Alvaro Sanchez-Ferrer *et al.*, BBA (1995)

Slominski Andrzej *et al.*, Physiological Reviews (2003)

Fig.1.3 Melanin biosynthesis path way



Alvaro Sanchez-Ferrer et al., BBA (1995)

Fig.1.4 Catalysis mechanism of tyrosinase on oxidation of L-tyrosine and L-DOPA

1.2 Transcriptional regulation of melanogenesis

The expressions of melanogenic enzymes, tyrosinase, TRP-1, and TRP-2, are transcriptionally regulated by microphthalmia-associated transcription factor (MITF) and several kinds of kinase path way (Ye, 2010b, Aksan, 1998, Bertolotto, 1998a, and Tachibana, 1996). The amounts of cyclic adenosine monophosphate (cAMP) in melanocyte is increased by the messenger such as histamine, α -MSH, tumor necrosis factor (TNF)- α , interleukin (IL)-1 β , and prostaglandin released by keratinocyte after get stimulated by UV (Yoshida, 2000, Karin., 1995, Weston, 2007). The effects of messengers are induced *via* interaction with receptors on the melanocytes. Melanocortin 1 receptor (MC1R), a receptor of α -MSH, leads to elevation of cAMP contents by the interaction with α -MSH.

The increase of cAMP contents results in the regulation of the expression on protein kinase A (PKA), p38 mitogen activated protein kinase (MAPK), extracellular signal-regulated kinase (ERK), and c-Jun N-terminal kinase (JNK) which regulate the expressions of melanogenic enzymes (Buscà, 2000). PKA phosphorylates the cAMP response element binding protein (CREB), which is known to be an activator of MITF expression (Bertolotto, 1998a, Bertolotto, 1998b, Bertolotto, 1998c, and Jang, 2011). Phosphorylated p38 MAPK stimulates the expression of melanogenic enzymes *via* activating the MITF expression (Jiang, 2009, Park, 2010). Additionally p38 MAPK regulates melanogenesis by stimulating proteasomal degradation of melanogenic enzymes (Ballei, 2010). ERK phosphorylates more than 160 proteins, including transcription factors, enzymes, protein kinase relating to signal transduction, and so on, and it ultimately down regulates the expression of MITF and melanogenesis (Englaro,

1998, Roberts, 2007, Yoon, 2006, and Lopez-Bergami 2011). JNK, involved in proliferation and apoptosis cancer cells, also controls the melanogenesis by down regulating the expression of MITF (Bu, 2008, Mingo-Sion, 2004, and Uzgare, 2004) (Fig.1.5).

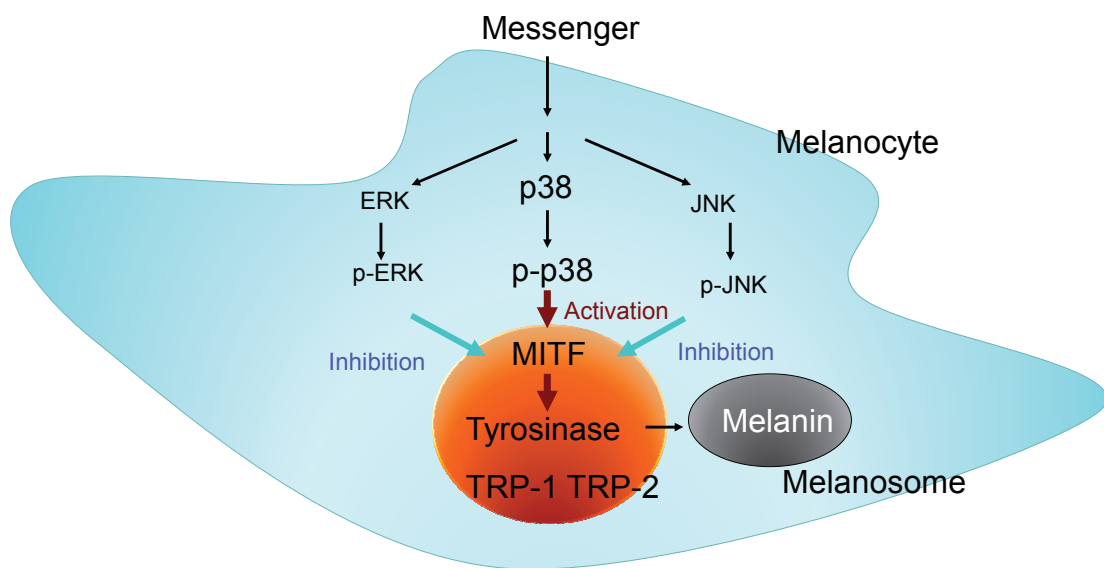


Fig.1.5 Transcriptional regulation of expression of melanogenic enzymes

1.3 Transportation of melanosomes

1.3.1 Microtubule transportation of melanosomes

Melanin is biosynthesized in melanosome by tyrosinase, TRP-1, and TRP-2 which transcriptionally regulated by MITF (Fig.1.3 and Fig.1.5). Mature melanosomes in melanocytes are specifically transported by transporter proteins on the microtubule and actin. Melanosomes are transferred to the keratinocytes or hair matrix cells which results in hair and skin pigmentation (Fig.1.1). Then the transportation of melanosomes as well as the expression or activity of melanogenic enzymes in melanocyte is essential process to regulate the pigmentation. Melanin is biosynthesized on perinuclear region in melanosome and the melanosome is transported to periphery of the cell by several kinds of transporter proteins through reversible microtubule transportation and irreversibly actin transportation. On the anterograde microtubule transportation, melanosome and kinesin, a motor protein, compose the transport complex *via* Rab1A on the melanosome (Ishida, 2012). Melanoregulin (Mreg), localized on the mature melanosome, forms the complex with Rab-interacting lysosomal protein (RILP) and dynein-dynactin motor proteins, which retrogradely transports melanosome to perinuclear region on the microtubule (Ohbayashi, 2012a) (Fig.1.6).

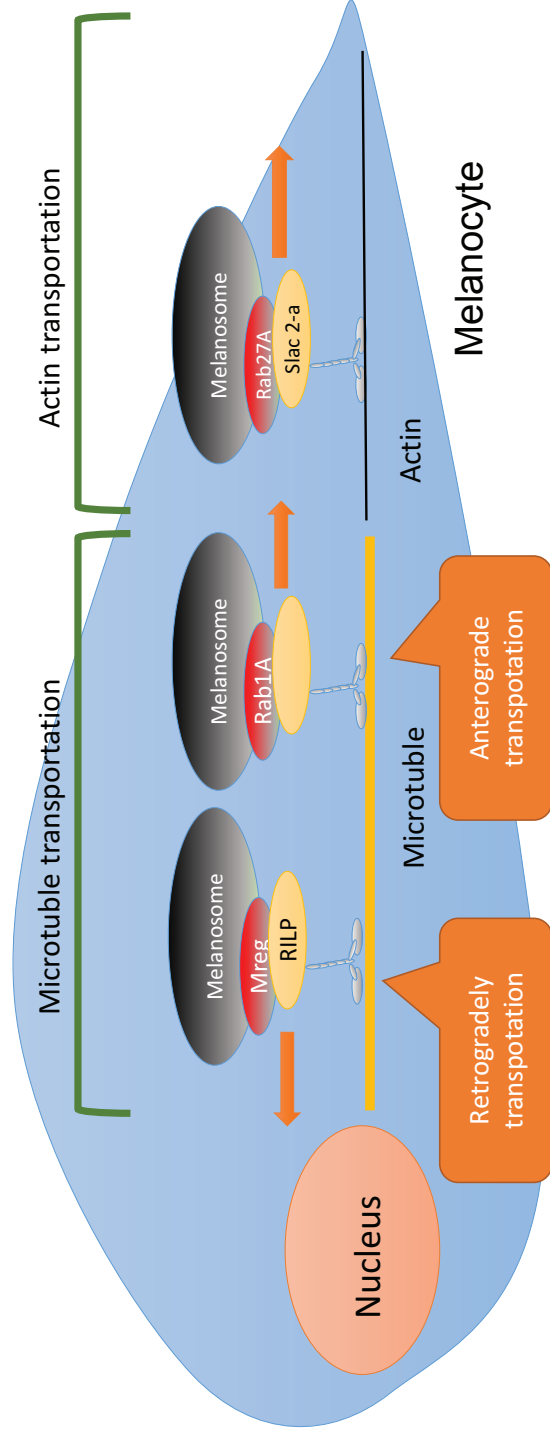
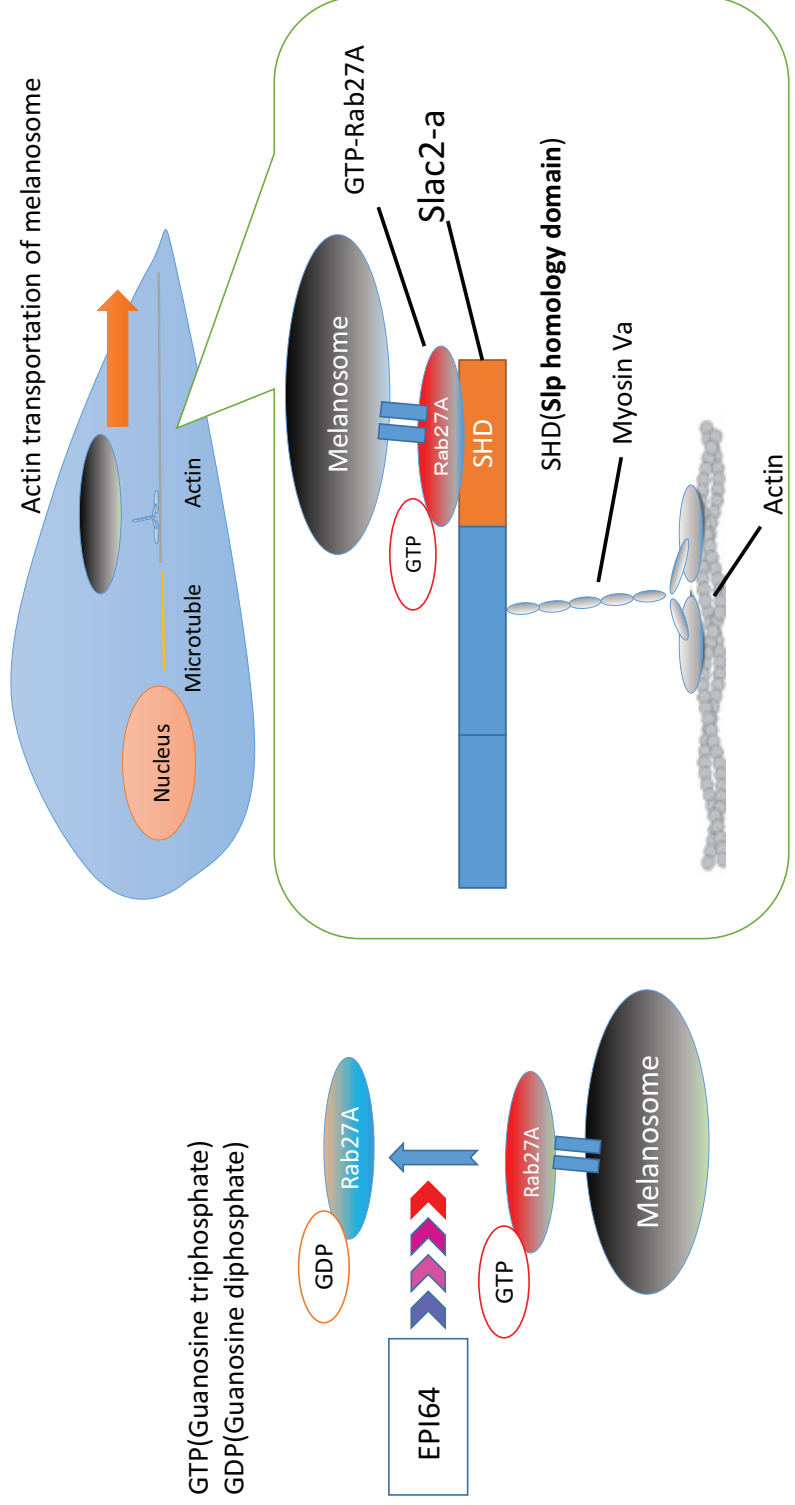


Fig.1.6 Transportation of melanosome in melanocyte

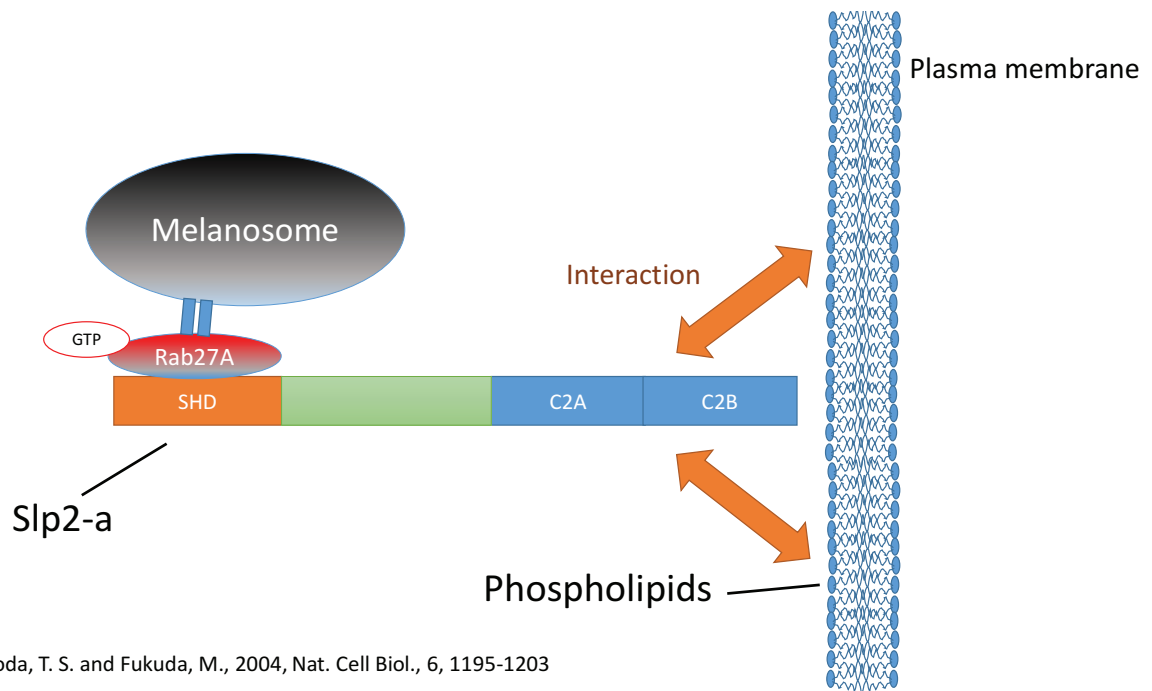
1.3.2 Actin transportation of melanosomes

Activated Rab27A, localized on melanosomes, attaches with its effectors, Slac2-a/melanophilin and Slp2-a (Kuroda, 2004 and Fukuda, 2005). Slac 2-a attaches with myosin Va which is a motor protein on actin transportation and the melanosome/Rab27A/Slac 2-a/myosin Va complex translates to the periphery of the cell from the perinuclear region on the actin cable (Fukuda, 2002, Wu, 2002, Kuroda, 2003, Itoh, 2006). Rab27A occurs in a guanosine triphosphate (GTP)-bound active state and a guanosine diphosphate (GDP)-bound inactive state. The GTP-bound active Rab27A is localized on the melanosome which elicits transportation of melanosome by interacting with Slac 2-a and myosin Va, while GDP-bound inactivated Rab27A is excluded from the surface of melanosome, which inhibits the transportation of melanosome. Then the active and inactive cycling of Rab27A plays an essential role to regulate the melanosome transportation. Guanine nucleotide exchange factors deprives the GDP and stimulates GTP loading to Rab27A. Conversely EPI64, a GTPase-activating protein of Rab27A, promotes the GDP-bounding and inactivates Rab27A (Itoh and Fukuda, 2006) (Fig.1.7). On the peripheral region in melanocyte, Rab27A interacts with Rab27-binding domain (Slp-homology domain: SHD) of Slp2-a. C2A and C2B domains in the Slp2-a bind to phospholipids including in plasma membrane, which keep attachment of melanosome to the plasma membrane (Kuroda and Fukuda, 2004).



Fukuda M. et al., 2002, Journal of Biological chemistry, 277, 12432-12436.
 Itoh. et al., 2006, Journal of Biological chemistry, 281, 31823-31831.

Fig.1.7 Actin transportation of melanosome



Kuroda, T. S. and Fukuda, M., 2004, Nat. Cell Biol., 6, 1195-1203

Fig. 1.8 Interaction of melanosome with plasma membrane *via* Slp2-a

1.4 Melanogenesis controlling effect of medicinal plants extract

1.4.1 Indonesian medicinal plants

Medicinal plants have been traditionally used to maintain good health and beauty on human body such as curing the inflammatory, preventing microbial infection, skin whitening etc. Indonesian tropical forests, contain 28,000 plant species, covers about 143 million hectares and is home to about 80% medicinal plants in the world (Elfahmi, 2014). Jamu, an Indonesian traditional herbal medicine, have been generally used in Indonesia so far. For instance, a Jamu including *Trigonella foenum graecum*, *Tribulus terrestris*, *Yohimbe*, *Talinum paniculatum*, and *Plantago major* have been used to treat liver and kidney disturbance. *Orthosiphonis*, *Phyllanthi*, *Plantaginis*, *Blumeae*,

Centellae, *Morindae*, *Alstoniae*, *Andrographidis*, and *Cercospora apii* have been used for treating mild hypertension, and *Morindae fructus*, *Orthosiphonis folium*, *Syzygii polyanthi*, *Andrographidis*, *Centellae*, and *Curcumae* have been used to treat diabetes mellitus (Elfahmi, 2014).

In order to clarify the mechanism of the biological activity of Jamu, the biological activity of Indonesian medicinal plants extracts have been investigated and isolation and identification of bioactive components including Indonesian medicinal plants have been performed in the world because of its valuable pharmaceutical potential. A number of bioactivity of Indonesian medicinal plants have been reported and novel compounds and bioactive components have been isolated from Indonesian herbal medicinal plants used as Jamu. Kamiya *et al.*, isolated five novel flavonoid glucuronides from fruit of *Helicteres isora* which is called Ulet-Ulet in Java island and used as Jamu in Indonesia. A novel anthraquinone glucoside was isolated from the root of *Rheum pulmatum*, an Indonesian Jamu (Kubo, 1992). The extracts of traditional Indonesian medicinal plants, *Cinnamomum massoiae*, *Eucalyptus globulus*, *Vitex trifolia*, *Eucalyptus globulus*, *Plantago major* L., and *Vitex trifolia* L. inhibit the histamine release from rat basophilic leukemia cells (Ikawati, 2001). In this study, the lead compounds exhibiting melanogenesis controlling effect was searched using *Helminthstachys zeylanica*, an Indonesian medicinal plant.

1.4.2 Tyrosinase inhibitor

Traditional medicinal plants have been used for cosmetics especially for whitening

agents. As described above, melanin is synthesized *via* rate limiting reaction by tyrosinase catalysis from L-tyrosine as a starting material. Hence a number of extracts of medicinal plants and the components have been treated to determine the tyrosinase inhibitory activity in order to search the whitening agents. Morin (Fig.1.9), one of the flavonol and widely distributed in plants including onion, guava leaves and seaweeds, exhibits potent tyrosinase inhibitory activity (Mendoza-Wilson, 2011 and Wang, 2014). Glabridin (Fig.1.9), an isoflavan derivatives, was isolated from *Allamanda cathartica* stem as potent tyrosinase inhibitor (Yamauchi, 2011 and Nerya, 2003). Artocarbene, chlorophorin, norartocarpanone, and 4-propylresorcinol (Fig.1.9) including 2, 4-substituted resorcinol moiety induce high tyrosinase inhibitory activity (Shimizu, 1998 and 2000). Catechol moiety of chalcone exhibits tyrosinase inhibitory activity, and it is reported that the catechol chelates with the copper ions, present in the active site of tyrosinase. While the 2, 4-substituted resorcinol shows no chelate with the copper ions and inhibits tyrosinase activity more potently than catechol by competitive binding with the copper ions in tyrosinase (Khatib, 2005). The tyrosinase activity and melanogenesis of prenylated flavonoids from *Artocarpus altilis* were determined (Lan, 2013). *A. altilis* is popularly known as the breadfruit tree in English. Besides the leaves, roots, and root bark are used as traditional medicines in West Indies to relieve asthma, decrease blood pressure, cure liver disorders, and decrease fever (Adewole, 2007). Norartocarpetin (Fig.1.9) from *A. altilis* also including 2, 4-substituted resorcinol moiety exhibits potent tyrosinase inhibitory activity as well as melanaogenesis inhibitory activity in B16 melanoma cells. While artocarpin (Fig.1.9) which has 2, 4-substituted moiety shows less potent tyrosinase inhibitory activity than norartocarpetin because of its low polarity substituent groups. However it should be noted that artocarpin exhibits higher

melanogenesis inhibitory activity in melanoma cells than norartocarpetin even though artocarpitin shows low tyrosinase inhibitory activity, suggesting that it is necessary to consider the expressions of melanogenic enzymes as well as tyrosinase activity in melanoma cells. As described above, a lot of tyrosinase inhibitors have been obtained and investigated the mechanism. However there are few reports focusing on the compounds stimulating tyrosinase activity thus far.

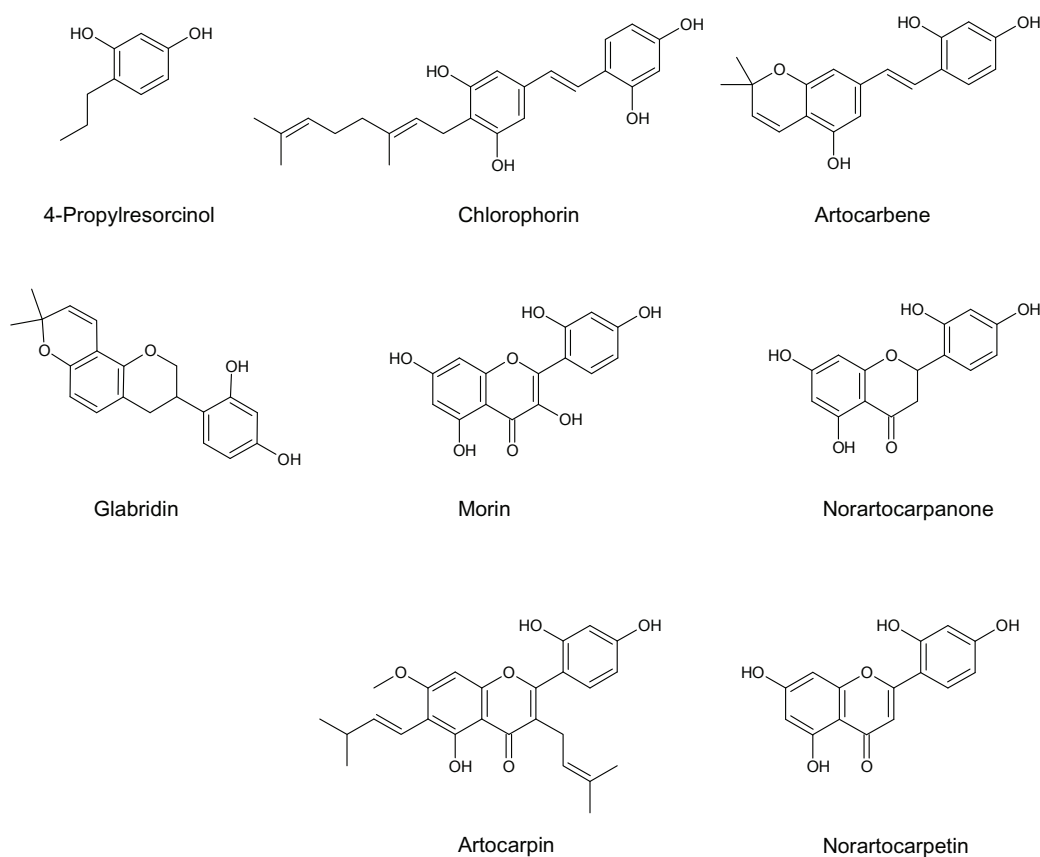


Fig.1.9 Chemical structures of tyrosinase inhibitor including 2, 4-substituted resorcinol moiety

1.4.3 Regulator on expression of melanogenic enzymes

Tyrosinase is transcriptionally regulated by MITF, and MITF expression is regulated by a number of kinase pathways. Recently the melanogenesis regulating activity of compounds have been evaluated by determining the tyrosinase expression as well as tyrosinase activity. Besides in order to clarify the mechanism, the expressions of MITF and kinases have been investigated by western blot analysis. 1-*O*-Methyl-fructofuranose (Fig.1.11) from the fruit of *Schisandra chinensis* is a traditional Korean medicinal herb, and the effects of 1-*O*-methyl-fructofuranose on melanogenesis, expressions of melanogenic enzymes, and related signaling pathways were investigated. 1-*O*-Methyl-fructofuranose inhibits melanogenesis by suppressing the expressions of tyrosinase, TRP-1, and MITF. Additionally the study also elucidated the compound increases the phosphorylation of ERK, suggesting 1-*O*-methyl-fructofuranose inhibits melanogenesis by stimulating the ERK pathway (Oh, 2010). Citrus fruits press cake was reported as melanogenesis inhibitor by suppressing MITF expression (Kim, 2013). *Rhodiola rosea* (Fig.1.10) extracts was studied as melanogenesis suppressor. The acetone extract of *R. rosea* exhibits tyrosinase inhibitory activity (Chen, 2009). Besides *R. rosea* root containing phenylethanol derivatives, phenylpropanoids, monoterpenes, flavanoids, phenolic acids, and triterpenes (Saratikov, 1967 and Kurkin, 1985) decreases melanin content in B16 melanoma cells *via* suppressing the expressions of MC1R, a receptor of α -MSH, MITF, TRP-1, and tyrosianse (Chiang, 2014).

On the other hand melanogenesis stimulator also have been studied. Diethylstilbestrol (Fig.1.11) was reported to exhibit potent melanogenesis stimulatory

activity. Diethylstilbestrol increases the tyrosinase, TRP-1, TRP-2, and MITF mRNA as well as tyrosinase activity (Jian, 2011). Cilostazol (6-[4-(1-cyclohexyl-1H-tetrazol-5-yl)butoxy]-3,4-dihydro-2-(1H)-quinolinone) (Fig.1.11), known as an inhibitor of cAMP degrading enzyme, promotes melanogenesis by increasing the expressions of MITF *via* PKA/CREB pathway (Wei, 2014).



From <http://ja.wikipedia.org/wiki/%E3%82%A4%E3%83%AF%E3%83%99%E3%83%B3%E3%82%B1%E3%82%A4>

Fig.1.10 *R. rosea*

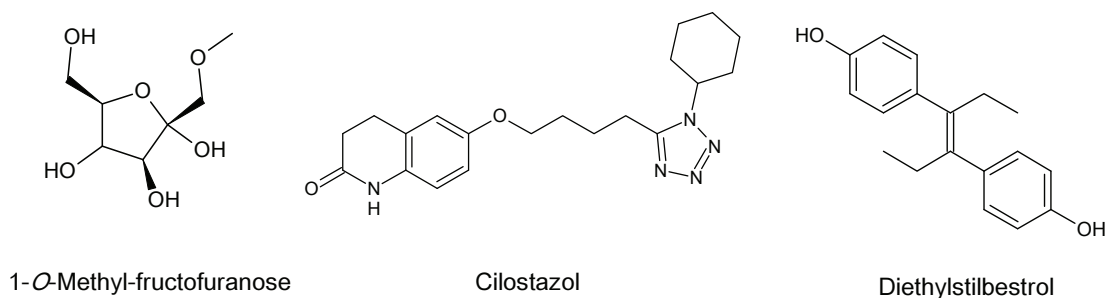


Fig.1.11 Chemical structures of melanogenesis modulators

1.5 Research objectives

Recently a number of papers have focused on the modulation of tyrosinase activity and expressions of melanogenic enzymes in order to control the skin and hair pigmentation. The skin and hair pigmentation takes place by the melanosomes transported and released from melanocyte. However few studies have treated the compounds which could control the transportation of melanosomes as well as the expressions of melanogenic enzymes. Several proteins, involved in the transportation of melanosomes, have been identified and a lot of the mechanism of the transportation have been already clarified. Therefore the investigation of regulators on transportation of malanosomes is desired.

In this study, isolation and identification of compounds in *Helminthostachys*

zeylanica extract which exhibited potent intracellular melanogenesis stimulatory activity were performed in order to search the lead compounds as melanogenesis modulators. Moreover the structure-activity relationships of the bioactive compounds were investigated. Additionally the effects of the bioactive compounds on transportation of melanosomes as well as expressions of melanogenic enzymes were investigated by using western blot analysis and immunofluorescence microscopy in order to clarify the mechanisms of the activity.

Chapter 2

Identification of quercetin glycosides as intracellular melanogenesis stimulator from *Helminthstachys zeylanica*

2.1 Introduction

In order to search the lead compounds modulating the melanogenesis activity, *Helminthostachys zeylanica* (Fig.2.1) root extract has been focused on because of the melanogenesis stimulatory activity on the screening assay. *H. zeylanica*, belongs to Ophioglossaceae family, has been used for pain relief, germ killing, wound care, and promotion of bone healing after fracture (Lee, 2011 and 2012). Besides it has been used as an antipyretic, antiphlogistic, and anodyne (Chiu, 1992) and used to treat sciatica, boils, ulcers and malaria (Suja, 2004). The bioactive components including *H. zeylanica* have been isolated and identified so far. Four flavonoids, ugonins A–D were isolated from the rhizomes of *H. zeylanica* (Murakami, 1973a and b). Moreover, it is reported that ugonins E–T were isolated from the root of *H. zeylanica* and identified as well as their antioxidant and anti-inflammatory activity by Huang *et al.*, (2003, 2009). Ugonin K, isolated from *H. zeylanica*, reported to promote osteoblastic differentiation and mineralization *via* activating of p38 MAPK and ERK path way (Lee, 2011). In this chapter reports the isolation and identification of novel quercetin glycosides from *H. zeylanica* root extract and the potent intracellular melanogenesis enhancement activity in B16 melanoma cells.



From http://homepage2.nifty.com/yucca_ueno/miyakojima.html

Fig.2.1 *Helminthostachys zeylanica*

2.2 Material and Methods

2.2.1 General

^1H and ^{13}C NMR spectra were recorded in methanol- d_4 with Bruker Biospin AVANCE III 800MHz NMR and JEOL EC600MHz NMR. Coupling constants were expressed in Hz, and chemical shifts were given on a δ (ppm) scale. UPLC-TOFMS (Waters Waters[®]XevoTM QToF MS) was performed using column C18 (2.1mm ϕ \times 100mmL, Waters). GC-MS (Shimadzu GCMS-QP 5050A) was performed using a DB-5 MS column (0.25mm ϕ \times 30m L, J&W scientific). Column chromatography was performed with Sephadex LH-20 (18–111 μm , GE Healthcare).

2.2.2 Material

The sample was collected from Samarinda, Indonesia in 2006. The sample and the voucher specimen were deposited in Herbarium wanariset, Samboja, East Kalimantan, Indonesia identified no. WAN0017365

2.2.3 Extraction and fractionation of *H. zeylanica* root powder

H. zeylanica root powder ca.100g was extracted with 50% ethanol. The 50% ethanol extract was separated with Sephadex LH-20 gel column (25mmφ×820mmL) chromatography eluting with the solvent (water:MeOH = 1:1 v/v) to obtain compound **1** (yellow powder 52.5mg) and **2** (yellow powder 771mg).

2.2.4 Tyrosinase activity assay

The tyrosinase activity method was performed based on Batubara,(2010). The sample 70μL was put in 96-well plate. Tyrosinase 30μl (333unit/ml in phosphate buffer 50mM pH 6.5) and 110 μL of substrates (L-tyrosine 2mM or L-DOPA 2mM) were added. After incubation at 37°C for 30min, the absorbance at 510nm was measured using a micro plate reader. IC₅₀ is expressed as the concentration of inhibitor showing 50% inhibition.

2.2.5 Cell culture

Murine melanoma B16-F0 cells (DS Pharma Biomedical, USA) grown in DMEM medium supplementing with 10% fetal bovine serum, 1% penicillin/streptomycin, were cultured at 37°C in a humidified atmosphere of 5% CO₂.

2.2.6 Measurement of cellular melanin contents

Measurement of cellular melanin contents was performed according to the method (Arung., 2011). In brief, confluent cultures of B16 melanoma cells were rinsed in phosphate-buffered saline (PBS) and removed using 0.25% trypsin/EDTA. The cells were placed in 10cm petri dishes (1.0×10^5 cells / dish) and allowed to adhere at 37°C for 24h. After adding samples, cells were incubated for 72h and then washed with PBS following lysed in 200µl of 2M NaOH by 40min heating at 80°C to solubilize the melanin. Resulting lysate 150µL was put in a 96-well microplate, and the absorbance was measured at 405nm with a microplate reader. Each experiment was repeated twice. Enhancement of melanine production is expressed as percentage to that of control cells treated with the solvent DMSO/water without sample materials.

2.2.7 Cell viability

Cell viability was determined using the hemocytometer (Erma, Tokyo). B16 cells were cultured and added samples as shown in 2.2.6 section. After 72h incubation B16 melanoma cells were removed using 0.25% trypsin/EDTA solution, and then for the 200µL of the solution 10µL trypan blue solution was added in 1.5ml tube. The 10µL of mixed solution was put in to the hemocytometer to count the cells number. Each

experiment was repeated twice. Enhancement of melanine production is expressed as percentage to that of control cells treated with the solvent DMSO/water without sample.

2.2.8 Identification of compound 1 and 2

Compound **1** and **2** were identified by ^1H NMR, ^{13}C NMR, ^1H ^1H COSY, HMQC, HMBC, and UPLC-TOFMS. Methanol- d_4 was used as the NMR solvent. NMR measurements were performed by using Bruker Biospin AVANCE III 800MHz NMR and JEOL EC600MHz NMR. UPLC-TOFMS (Waters Waters[®]XevoTM QToF MS) was performed using column C18 (2.1mm ϕ \times 100mmL) with MeOH/water = 5/95 (0min), 100/0 (10min), 100/0 (13min) as eluent. The data were collected in negative ionization modes. The capillary voltage was 3.0kV. Cone and desolvation gas flow rates were set at 50 and 1000 liters/h respectively, and the source and desolvation temperature was 150°C and 500°C respectively.

The NMR data of the compounds isolated from *H. zeylanica* roots are shown in Table 2.1 and 2.2.

Compound **1**: yellow powder, UPLC-TOFMS ES⁻ : [M-1]⁻ 787.2029, 625.1410, 463.0890, 301.0372 (m/z). UV $\lambda^{\text{MeOH}}_{\text{max}}$: 207, 265, 345 (nm). $[\alpha]^{20}_{\text{D}}$: -33.4°(c=0.84, MeOH:H₂O 1:1 v/v). IR (KBr): 3402, 1655, 1612, 1499, 1457, 1365, 1260, 1205, 1072 (cm⁻¹).

Compound **2**: yellow powder, UPLC-TOFMS ES⁻ : [M-1]⁻ 949.2466 (m/z).

UV $\lambda^{\text{MeOH}}_{\text{max}}$: 207, 265, 342 (nm). $[\alpha]^{20}_{\text{D}}$: -41.0° (c=0.83, H₂O). IR (KBr): 3402, 1642, 1615, 1519, 1466, 1343, 1312, 1162, 1087 (cm⁻¹).

Table 2.1 ¹H and ¹³C-NMR chemical shifts and key HMBC correlations of compound **1**

Position	δ_{H} (ppm)	J(Hz)	δ_{C} (ppm)	HMBC
2			156.8	
3			134.6	
4			178.1	
4a			104.4	
5			161.7	
6	6.18 d	2.04	98.6	C-5, C-7
7			164.9	
8	6.36 d	2.10	93.4	C-7, C-8a
8a			157.1	
1'			121.5	
2'	7.67 d	2.04	116.6	C-2, C-4'
3'			146.2	
4'			147.6	
5'	7.25 d	8.94	115.8	C-3', C-4'
6'	7.62 dd	8.94, 2.04	121.5	C-2, C-4'
	3-glucose			
A1	5.28 d	7.56	102.6	C-3, C-A5
A2	3.49 t	8.22	75.0	
A3	3.57 m		76.4	C-A2, C-A4
A4	3.33 m		79.0	C-A5, C-A6, C-B1
A5	3.33 m		75.6	C-A4
A6	3.70(2H) m		60.3	C-A4
	(1→4)-glucose			
B1	4.37 d	7.56	103.2	C-A4, C-B5
B2	3.19 t	8.94	73.5	
B3	3.30 m		76.7	
B4	3.31 m		69.9	
B5	3.29 m		76.4	
B6	3.63(2H) m		61.0	C-B4
	4'-glucose			
C1	4.91 d	7.56	101.9	C-4'
C2	3.56 t	8.94	73.4	
C3	3.68 m		74.3	
C4	3.52 m		69.9	
C5	3.57 m		76.7	
C6	3.90, 3.86 m, m		61.2	

Table 2.2 ¹H and ¹³C-NMR chemical shifts and key HMBC correlations of compound 2

Position	δ_{H} (ppm)	J(Hz)	δ_{C} (ppm)	HMBC
2			156.8	
3			134.7	
4			178.1	
4a			104.4	
5			161.7	
6	6.18 d	2.04	98.8	C-5, C-7
7			165.1	
8	6.36 d	2.04	93.5	C-7, C-8a
8a			157.2	
1'			125.6	
2'	7.66 d	2.04	116.3	C-2, C-4'
3'			146.6	
4'			147.7	
5'	7.29 d	8.28	116.3	C-3', C-4'
6'	7.60 dd	8.22, 2.04	121.5	C-2, C-4'
	3-glucose			
A1	5.29 d	7.56	102.5	C-3
A2	3.50 t	8.94	74.4	
A3	3.57 m		76.5	C-A2, C-A4
A4	3.33 m		79.0	C-A5, C-A6, C-B1
A5	3.33 m		75.6	C-A4
A6	3.71(2H) m		60.5	C-A4
	(1→4)-glucose			
B1	4.37 d	8.22	103.2	C-A4, C-B5
B2	3.19 dd	8.94, 7.56	73.5	
B3	3.28 m		76.5	
B4	3.30 m		70.0	
B5	3.29 m		76.5	
B6	3.68(2H) m		61.1	C-B4
	4'-glucose			
C1	4.97 d	7.56	101.2	C-4', C-C2
C2	3.80 t	7.56	81.8	
C3	3.68 m		74.1	
C4	3.52 m		69.9	
C5	3.59 m		76.8	
C6	3.90, 3.86 m, m		61.1	
	(1→2)-glucose			
D1	4.75 d	8.22	104.2	C-C2
D2	3.27 t	8.94	75.0	
D3	3.39 dd	13.7, 8.93	76.3	
D4	3.47 m		69.6	
D5	3.31 m		77.0	
D6	3.68, 3.65 m, m		60.9	

2.2.9. Acid hydrolysis

Acid hydrolysis was performed according to the previous method (Koz, 2010). 5ml of 1N HCl was added to a 10mg of compound **1**, and the mixture was stirred at 80°C for 4h. After cooling down to room temperature, the solution was partitioned between H₂O and EtOAc. The H₂O layer was freeze dried, and the EtOAc layer was analyzed by JEOL EC600MHz NMR. The freeze dried product from H₂O layer was dissolved in 1-(trimethylsilyl)-imidazole 0.4ml and pyridine 5.0ml to trimethylsilylate. The solution was stirred at 60°C for 5min. After drying the solution with a stream of N₂, the residue was partitioned between H₂O and CHCl₃. The CHCl₃ layer was analysed by GC-MS (Shimadzu GCMS-QP 5050A) using a DB-5 MS column (J&W scientific 0.25mmφ×30mL). Temperatures of the injector and detector were 250°C. A temperature gradient of column oven was follows, starting at 80°C for 2min and increasing up to 250°C over a period of 9min. The hydrolysis of standard monosaccharides D-glucose, D-galactose, D-arabinose and L-rhamnose were performed by the same method of compound **1**.

2.2.10 Determination of absolute configuration of sugars from compound **1** and **2**

Five milliliter of 1N HCl was added to a 5mg of compound **1** and **2** respectively, and the mixtures were stirred at 80°C for 4h. After cooling down to room temperature, the solutions were partitioned between H₂O and EtOAc by a separatory funnel. The sugars from compound **1** and **2** were obtained by the drying of H₂O layer in vacuo, and its specific optical rotation were $[\alpha]_D^{20}$: +83.0°(c=0.23, H₂O), +86.7°(c=0.19, H₂O) respectively.

2.3 Results and Discussion

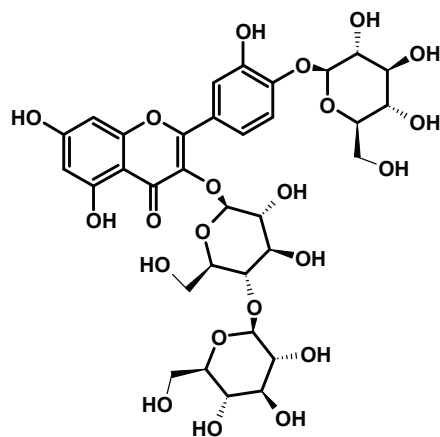
2.3.1 Identification of compound 1 and 2

Compound **1** (Fig.2.2) was obtained from a water/EtOH extract of *H. zeylanica* root was using LH-20 gel column chromatography, and the structure was analyzed by NMR and UPLC-TOFMS. Also, compound **1** was hydrolyzed with acid to determine the constitution of sugars and aglycon in compound **1**. The sugars were analyzed using GC-MS after trimethylsilylation, and the aglycon was determined using NMR. The total ion chromatograms of trimethylsilylated D-glucose, L-rhamnose, D-arabinose, D-galactose and hydrolysates of compound **1** are shown in Fig.2.3 The peaks of trimethylsilylated D-glucose at standard were observed at 24.5, 25.5, and 27.7 (min) of retention time which are completely the same retention times of hydrolysates of compound **1**. Moreover, the mass spectrum of compound **1** showed four major peaks appeared at 787.2029 [M-1]-, 625.1410 [M-1-162] -, 463.0890 [M-1-324] -, 301.0372 [M-1-466] - (m/z) by UPLC-TOFMS (Fig.2.4). Considering the 162m/z differences of each peak depend on the fragment of glucose, compound **1** contained three molecules of D-glucoses.

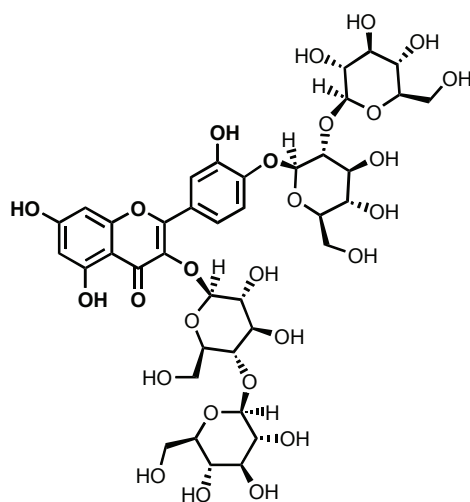
According to the NMR data of aglycon, it accorded the NMR data of quercetin reported by Lasse *et al.*, (2009) and Moon *et al.*, (2001). In order to elucidate the binding position of three glucoses of compound **1**, HMBC correlations in Table 2.1 were determined using 800MHz NMR. HMBC of compound **1** gave the correlations between H-C1 and C-4', and between H-A1 and C-3. These correlations result in the presence of C-C1 to C-4' and C-A1 to C-3 bonds respectively via oxygen. Additionally the correlation

between H-B1 and C-A4 was observed, so that the compound **1** was identified as 4'-*O*- β -D-glucopyranosyl-quercetin-3-*O*- β -D-glucopyranosyl-(1 \rightarrow 4)- β -D-glucopyranoside.

Compound **2** (Fig.2.2) was identified by comparing to the NMR and UPLC-TOFMS data of compound **1**. The NMR data of compound **2** shown in Table 2.2 was related to that of compound **1**. According to HMBC data, the proton signal at 4.75ppm of compound **2** which was not appeared in compound **1** correlated with C-C2. The coupling constant of H-D3 was more than 7Hz, so that H-D2, H-D3 and H-D4 were therefore shown to be in axial positions. Further, UPLC-TOFMS data of compound **2** was 949 [M-1]- m/z which was 162 m/z higher than that of compound **1** (787m/z). Therefore compound **2** is identified as 4'-*O*- β -D-glucopyranosyl-(1 \rightarrow 2)- β -D-glucopyranosyl-quercetin-3-*O*- β -D-glucopyranosyl-(1 \rightarrow 4)- β -D-glucopyranoside.



Compound **1**: 4'-O- β -D-glucopyranosyl-quercetin-3-O- β -D-glucopyranosyl-(1 \rightarrow 4)- β -D-glucopyranoside



Compound **2**: 4'-O- β -D-glucopyranosyl-(1 \rightarrow 2)- β -D-glucopyranosyl-quercetin-3-O- β -D-glucopyranosyl-(1 \rightarrow 4)- β -D-glucopyranoside

Fig.2.2 Structures of compound **1** and **2**

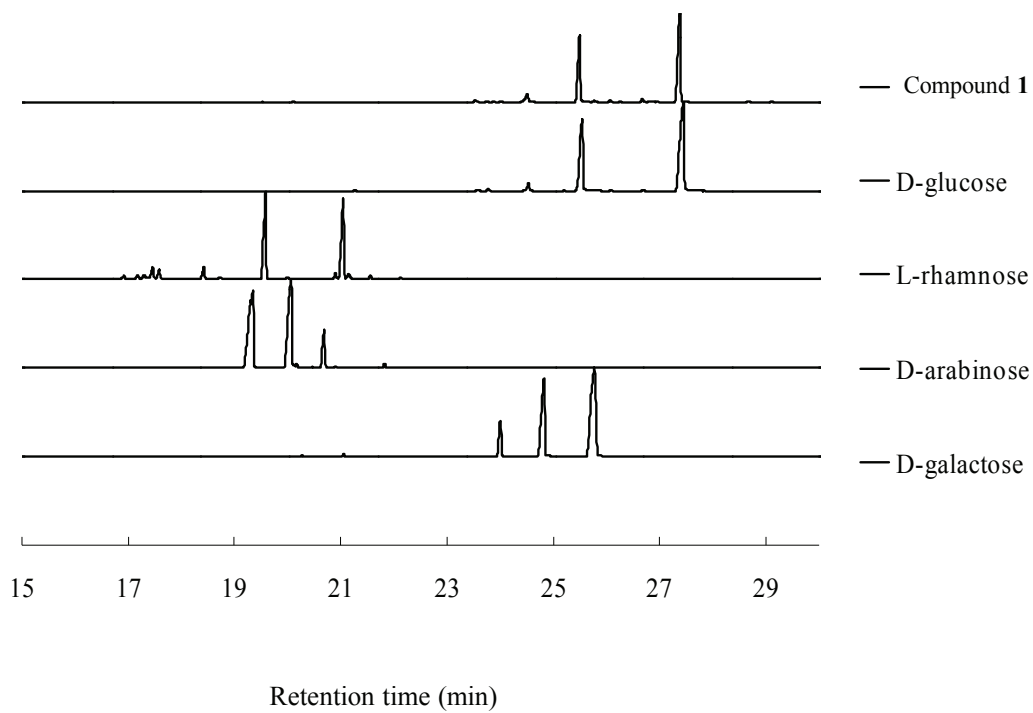


Fig.2.3 Total ion chromatograms of silylated D-glucose, L-rhamnose, D-arabinose, D-galactose, and sugars from compound 1

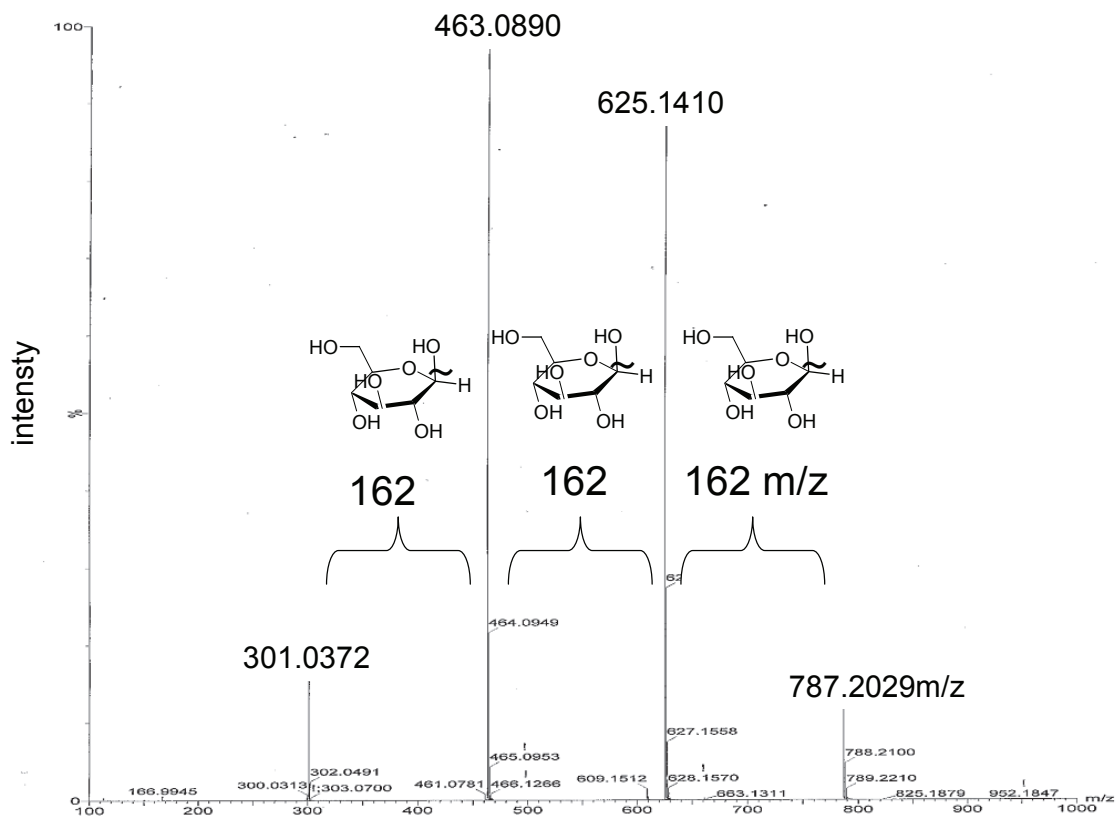


Fig.2.4 UPLC-TOFMS spectrum of compound 1

2.3.2 Intracellular melanogenesis enhancement activity

The intracellular melanogenesis enhancement activity of compound **1** and **2** at 10 μ M of concentration was shown in Fig.2.5. The intracellular melanogenesis activity and cell viability of compound **1** were 270 and 93% respectively, while compound **2** did not exhibit an intracellular intracellular melanogenesis enhancement activity. Quercetin, the aglycon of compound **1** and **2**, was reported to have high intracellular melanogenesis inhibitory activity. However, quercetin-4'-*O*- β -D-glucoside, quercetin-3-*O*- β -D-glucoside, quercetin-3, 4'-*O*- β -D-glucoside, and rutin showed a lower inhibitory activity than quercetin (Arung, 2011). Furthermore, it was demonstrated that quercetin-3-*O*- β -D-glucoside enhances melanogenesis by accelerating the expression of TRP-1 and -2 (Ye, 2010a). Our results added the intracellular melanogenesis activities of quercetin glycosides, especially glycoside attached to C-3 and 4' of quercetin had no melanogenesis inhibitory activity. Compound **1** showed intracellular melanogenesis acceleration activity of 2.7 times to control, while interestingly compound **2** had no intracellular melanogenesis enhancement activity in spite of the similarity of the structure. This result means the number of sugar connecting C-4' may play an important role in the melanogenesis activity.

Since melanogenesis related to the tyrosinase activity, we also determined the tyrosinase activity of compound **1** and **2**. The activity of compound **1** and **2** at 10 μ M of concentration is presented in Fig.2.6. The tyrosinase activity of compound **1** was 115% and 117% using L-tyrosine and L-DOPA as substrate respectively. No enhancement activity of tyrosinase was shown for compound **1** in spite of dramatic activity of melanin

biosynthesis.

Tyrosinase is transcriptionally regulated by microphthalmia-associated transcription factor (MITF) and its expression is activated by the p38 MAPK cascade. On the other hand, extracellularly responsive kinase (ERK) and c-Jun N-terminal kinase (JNK) pathway have been reported to be related to the down-regulation of melanin synthesis (Ye, 2010b). Some melanogenic enhancing agents have been examined at several points of melanogenesis such as expression of tyrosinase, p38, JNK, ERK and MITF as well as tyrosinase activity. A study suggested that p38 MAPK was stimulated by cubebin, which enhanced melanogenesis activity in murine B16 melanoma cells (Hirata, 2007). Compound **1** may also enhance the activity or expression of MITF by regulating kinase mentioned above, because it did not show tyrosinase accelerate activity in spite of its high intracellular melanogenesis stimulation activity in B16 melanoma cells (Fig. 2.6). Moreover, considering the structures of two novel quercetin glycosides, the glucoses connecting quercetin C4' may play an important role in the intracellular melanogenesis stimulation activity. These results are described in the previous published (Yamauchi, 2013). We need to elucidate the mechanism of intracellular melanogenesis enhancement activity of compound **1** by way of determining the tyrosinase and MITF expression in B16 melanoma cells.

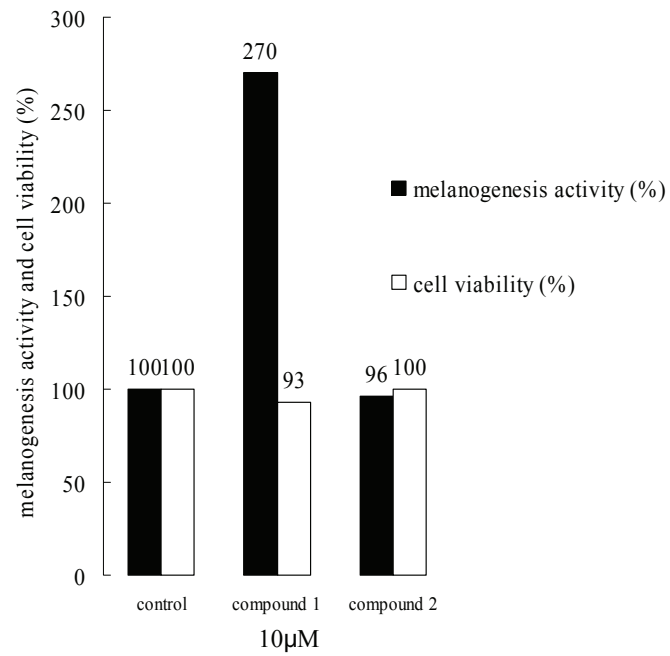


Fig.2.5 Intracellular melanogenesis activity and cell viability of compound 1 and 2

■: intracellular melanogenesis activity of B16 melanoma cells treated with samples
□: cell viability of B16 melanoma cells treated with samples

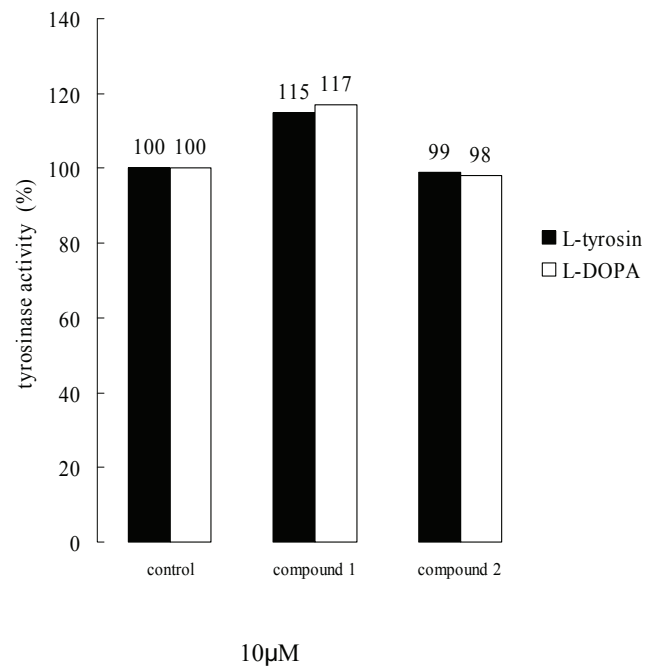


Fig.2.6 Tyrosinase activity of compound **1** and **2**

- : tyrosinase activity using L-tyrosin as substrate
- : tyrosinase activity using L-DOPA as substrate

2.4 Summary

Two novel quercetin glycosides namely 4'-O- β -D-glucopyranosyl-quercetin-3-O- β -D-glucopyranosyl-(1 \rightarrow 4)- β -D-glucopyranoside (compound **1**) and 4'-O- β -D-glucopyranosyl-(1 \rightarrow 2)- β -D-glucopyranosyl-quercetin-3-O- β -D-glucopyranosyl-(1 \rightarrow 4)- β -D-glucopyranoside (compound **2**) were isolated from *H. zeylanica* root 50% ethanol extract. Structural analysis of isolated compounds was achieved mainly by 600MHz, 800MHz NMR, UPLC-TOFMS, and GC-MS. Among the two quercetin glycosides, compound **1** showed high intracellular melanogenic stimulatory effect which was 2.7 times higher than a control in murine B16 melanoma cells with no cytotoxic effect even though **2** exhibited no stimulatory activity as the similar compound. This results indicated the importance of the substituent moieties attached to quercetin on melanogenesis stimulatory activity.

Chapter 3

Synthesis of quercetin derivatives

3.1 Introduction

Quercetin is a flavonoid present as a glycoside in various fruits and vegetables (Hertog, 1992, Hollman, 1999, and Manach, 2004). A number of studies have demonstrated that quercetin exhibits a variety of pharmacological effects, including antioxidant and anti-cancer activities (Gibellini, 2009 and Chen, 2002), while some reports relate to effectiveness in controlling melanogenesis. Quercetin is recognized as a potent inhibitor of tyrosinase activity and melanogenesis, as evidenced by the studies performed in the mouse B16 melanoma cells (Fuji, 2009). However, quercetin has been reported to elicit the opposite effect and accelerate melanogenesis in human melanoma cells (Nagata, 2004). Furthermore, it was reported that the direction of its melanogenesis-regulating activity depends on the concentration of quercetin used (Yang, 2011). A small number of studies have shown that quercetin derivatives can control melanogenesis. Quercetin-3-*O*- β -D-glucoside enhances melanogenesis by stimulating the expression of TRP-1 and TRP-2 (Ye, 2010). In our previous study, we evaluated the effect on melanogenesis of two quercetin glycosides, 4'-*O*- β -D-glucopyranosyl-quercetin-3-*O*- β -D-glucopyranosyl-(1 \rightarrow 4)- β -D-glucopyranoside (**1**) and 4'-*O*- β -D-glucopyranosyl-(1 \rightarrow 2)- β -D-glucopyranosyl-quercetin-3-*O*- β -D-glucopyranosyl-(1 \rightarrow 4)- β -D-glucopyranoside (**2**) isolated from *Helminthostachys zeylanica* root extract (Yamauchi, 2013, Chapter 2). While compound **1** was found to stimulate melanogenesis, the latter compound had no effect, suggesting that the structure and positions of the sugars in the quercetin glycosides may affect their melanogenesis-modulating activity in B16 melanoma cells.

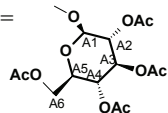
Chemical synthesis of compounds isolated from natural products plays an important role to obtain the abundant amount of the compounds and to identify the exact chemical

structure of the compounds. The synthesis strategy of quercetin derivatives have been studied so far because of their high potency on biological activity. For instance, quercetin 3-*O*- β -D-glucuronide was synthesized from rutin as a starting material (Kajjout, 2011). Regiospecific synthesis of quercetin-*O*- β -D-glucosylated and quercetin-*O*- β -D-glucuronidated isomers using dichlorodiphenylmethane to protect hydroxyl groups of catechol moiety on B ring (Kajjout, 2011). Additionally five *O*-monomethylated analogues of quercetin (3'-*O*-methylquercetin, 4'-*O*-methylquercetin, 3-*O*-methylquercetin, 5-*O*-methylquercetin, and 7-*O*-methylquercetin) were synthesized through sequential protection using dichlorodiphenylmethane (Bouktaib, 2002).

In this chapter, compound **1**, a novel quercetin glycoside isolated from Indonesian medicinal plant, was synthesized using rutin as a starting material. Moreover eighteen structurally distinct quercetin derivatives (Fig.3.1) were synthesized in order to investigate the structure-activity relationships of quercetin glycosides on melanogenesis stimulatory activity.

quercetin $R_1=R_2=R_3=OH$

Compound

- | | | | |
|-----------|---|-----------|--|
| 1 | $R_1=$ cellobiose, $R_2=$ glucose, $R_3=OH$ | 12 | $R_1=OCH_3$, $R_2=R_3=OH$ |
| 2 | $R_1=$ cellobiose, $R_2=$ sophorose, $R_3=OH$ | 13 | $R_1=R_2=OCH_3$, $R_3=OH$ |
| 3 | $R_1=$ glucose, $R_2=R_3=OH$ | 14 | $R_1=R_3=OCH_3$, $R_2=OH$ |
| 4 | $R_1=$ cellobiose, $R_2=R_3=OH$ | 15 | $R_1=R_2=R_3=OCH_3$ |
| 5 | $R_1=$ cellobiose, $R_2=OH$, $R_3=$ glucose | 16 | $R_2=OCH_3$, $R_1=R_3=OH$ |
| 6 | $R_1=$ cellobiose, $R_2=$ cellobiose, $R_3=OH$ | 17 | $R_3=OCH_3$, $R_1=R_2=OH$ |
| 7 | $R_1=$ cellobiose, $R_2=OH$, $R_3=$ cellobiose | 18 | $R_1=OH$, $R_2=R_3=OCH_3$ |
| 8 | $R_1=$ glucose, $R_2=$ glucose, $R_3=OH$ | 19 | $R_1=OAc$, $R_2=R_3=OH$ |
| 9 | $R_1=$ glucose, $R_2=OH$, $R_3=$ glucose | 20 | $R_1=$  , $R_2=R_3=OH$ |
| 10 | $R_1=$ glucose, $R_2=$ cellobiose, $R_3=OH$ | | |
| 11 | $R_1=$ glucose, $R_2=OH$, $R_3=$ cellobiose | | |

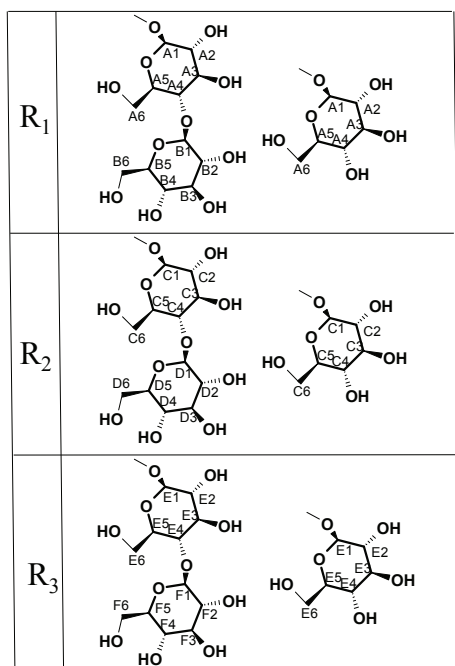
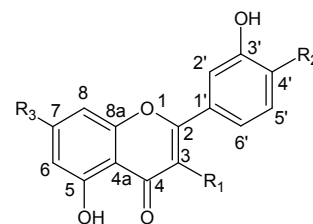


Fig.3.1 Structures of quercetin derivatives

3.2 Material and methods

3.2.1 General

¹H and ¹³C NMR spectra were recorded in methanol-*d*₄ or DMSO-*d*₆ by using JEOL EC600M Hz NMR. Coupling constants were expressed in Hz, and chemical shifts were determined on a δ (ppm) scale. Ultra performance liquid chromatography time-of-flight mass spectrometry (UPLC-TOFMS) (Waters®Xevo™ QT for MS) was performed using a C₁₈ column (2.1 mm ϕ \times 100 mm L; Waters, Milford, MA). UPLC-TOFMS data were collected in negative ionization modes. The capillary voltage was 3.0 kV. Cone and desolvation gas flow rates were set at 50 and 1000 L/h respectively, and the source and desolvation temperatures were 150°C and 500°C, respectively. Matrix assisted laser desorption/ionization TOFMS (MALDI-TOFMS) spectra were measured on a Shimadzu AXIMA-Resonance spectrometer (Kyoto, Japan) equipped with a nitrogen laser (λ = 337 nm). Samples were mixed with matrix (2,3-dihydroxybenzoic acid in 30% acetonitrile, 10 mg/mL) and loaded onto a 384-well MALDI sample plate. Preparative HPLC (SHIMAZU LC-6AD) was performed using an Inertsil ODS-3 column (20 ϕ \times 250 mm; GL Sciences, Tokyo, Japan). Cellobiose was purchased from Sigma-Aldrich (St. Louis, MO), and 30% hydrobromic acid was purchased from Merck (Whitehouse Station, NJ). Other commercially available products were purchased from Wako Chemicals (Richmond, VA). IR spectra were recorded on a PerkinElmer Spectrum 100 FT-IR system (Waltham, MA). UV spectra were recorded on a Shimadzu SPD-M20A diode array detector. Optical rotations were measured using a JASCO P-2300 system (Easton, MD).

3.2.1 Synthesis of quercetin glycosides

3.2.1.1 Preparation of acetobromocellobiose

Cellobiose (3.00 g, 8.76 mmol) was dissolved in anhydrous acetic acid (10 mL); then, 14 mL of pyridine was added, and the mixture was stirred overnight at room temperature. The resulting mixture was diluted with 50 mL of chloroform and was washed with water (3 × 50 mL). The chloroform phase was dried using Na₂SO₄, and acetocellobiose (3.17 g, 53.4% yield) was obtained after solvent evaporation.

Acetocellobiose was dissolved in 10 mL of chloroform, and 4 mL of 30% hydrobromic acid-acetic acid (20.00 mmol) was added at 0°C. The mixture was stirred overnight at room temperature. The resulting mixture was diluted with 50 mL of EtOAc and was washed with water (5 × 40 mL). The EtOAc phase was dried using Na₂SO₄, and acetobromocellobiose (3.11 g, 95.1% yield) was obtained after solvent evaporation.

3.2.1.2 Synthesis of 3 and 4

Rutin (5.00 g, 8.19 mmol), K₂CO₃ (9.04 g, 65.52 mmol), and BnBr (7.79 mL, 65.52 mmol) were added to 60 mL of dimethylformamide (DMF), and the mixture was then stirred for 10 h under argon at room temperature. The resulting mixture was diluted with 150 mL of EtOAc and washed with water (2 × 150 mL). The residue obtained after evaporation of the solvent was dissolved in 100 mL of 1 N HCl, and the mixture was refluxed at 80°C for 2 h.

After the precipitate was cooled, it was filtered. Next, 1.0 g of the precipitate, K₂CO₃

(417 mg, 3.02 mmol), and acetobromocellobiose or acetobromoglucose (2.11 g or 1.24 g respectively, 3.02 mmol) were added to 20 mL of DMF, and the mixture was stirred for 6 h at room temperature. The reaction mixture was diluted with 80 mL of EtOAc and washed with water (2 × 80 mL). After the EtOAc phase was dried using Na₂SO₄, the reactant was obtained by evaporating the solvent.

The reactant was dissolved in a 30-mL mixture of methanol (MeOH)/tetrahydrofuran (THF) (1/1, v/v), and 10 mL of 28% sodium methoxide/MeOH (1:50, v/v) was added. After the solution was stirred for 6 h at room temperature, it was neutralized by adding 2.0 g of an ion-exchange resin (H⁺ form) and stirred for 30 min. The resin was filtered off, and the reactant was obtained after the solvent was evaporated.

Next, 60 mg of reactant was dissolved in 40 mL of EtOH/THF (1:1, v/v), and 100 mg of 10% Pd/C was added. The mixture was stirred for 2 h at room temperature under 0.1 MPa H₂. The Pd/C was filtered off, and the solvent was evaporated. The quercetin-3-*O*-β-D-glucopyranosyl-(1→4)-β-D-glucopyranoside (**4**) and quercetin-3-*O*-β-D-glucopyranoside (**3**) obtained from rutin were yellow powders, with yields of 68.2% and 71.3%, respectively. They were purified using preparative HPLC with an ODS-3 column (20 mm φ × 250 mm L) eluted using a linear gradient of MeOH/0.05% TFA aq. soln. = 50/50 (0 min), 100/0 (30 min), 100/0 (40 min). The structures of the synthesized quercetin glycosides **3** and **4** were confirmed using NMR and UPLC or MALDI-TOFMS, UV spectra, IR, and specific optical rotation.

3: Yellow powder; UV λ_{max} 204, 255, 355 nm; [α]_D²⁰ -2.1° (c 1.30, MeOH); IR (KBr) ν_{max} 3402, 1658, 1610, 1498, 1364, 1309, 1081 cm⁻¹; ¹H NMR (CD₃OD, 600 MHz) δ_H 3.20 (1H, m, H-A5), 3.32 (1H, t, *J*=9.66 Hz, H-A4), 3.41 (1H, t, *J*=8.9 Hz, H-A3), 3.46

(1H, t, $J = 8.9$ Hz, H-A2), 3.56 (1H, dd, $J = 11.7, 5.5$ Hz, one of the H-A6), 5.22 (1H, d, $J = 7.6$ Hz, H-A1), 6.18 (1H, br s, H-6), 6.37 (1H, br s, H-8), 6.84 (1H, d, $J = 8.22$ Hz, H-5'), 7.56 (1H, dd, $J = 8.3, 1.4$ Hz, H-6'), 7.69 (1H, br s, H-2'); ^{13}C NMR (CD_3OD , 150 MHz) δ_{C} 61.2 (C-A6), 69.9 (C-A4), 74.4 (C-A2), 76.8 (C-A3), 77.1 (C-A5), 93.4 (C-8), 98.5 (C-6), 103.0 (C-A1), 104.4 (C-4a), 114.7 (C-5'), 116.2 (C-2'), 121.7 (C-1'), 121.9 (C-6'), 134.3 (C-3), 144.6 (C-3'), 148.5 (C-4'), 157.1 (C-2), 157.7 (C-8a), 161.7 (C-5), 164.7 (C-7), 178.2 (C-4); MALDI-TOFMS m/z 487.0260 $[\text{M}+\text{Na}]^+$.

4: Yellow powder; UV λ_{max} 204, 256, 356 nm; $[\alpha]_{\text{D}}^{20} -14.8^\circ$ (c 0.97, MeOH); IR (KBr) ν_{max} 3402, 1655, 1611, 1498, 1433, 1203, 1071 cm^{-1} ; ^1H NMR (CD_3OD , 600 MHz) δ_{H} 3.19 (1H, t, $J = 8.22$ Hz, H-B2), 3.33-3.36 (4H, m, H-A4, A5, B3, B5), 3.54 (1H, t, $J = 8.3$ Hz, H-A2), 3.57 (1H, m, H-A3), 3.70 (2H, m, H-A6), 4.38 (1H, d, $J = 7.6$ Hz, H-B1), 5.27 (1H, d, $J = 6.8$ Hz, H-A1), 6.17 (1H, d, $J = 1.4$ Hz, H-6), 6.36 (1H, d, $J = 2.1$ Hz, H-8), 6.85 (1H, d, $J = 8.94$ Hz, H-5'), 7.55 (1H, dd, $J = 8.3, 2.0$ Hz, H-6'), 7.67 (1H, d, $J = 1.4$ Hz, H-2'); ^{13}C NMR (CD_3OD , 150 MHz) δ_{C} 60.4 (C-A6), 61.1 (C-B6), 70.0 (C-B4), 73.5 (C-B2), 74.1 (C-B5), 75.1 (C-A2), 75.5 (C-A5), 76.5 (C-A3), 76.8 (C-B3), 78.9 (C-A4), 93.4 (C-8), 98.6 (C-6), 102.8 (C-A1), 103.2 (C-B1), 104.3 (C-4a), 114.7 (C-5'), 116.2 (C-2'), 121.7 (C-1'), 121.9 (C-6'), 134.2 (C-3), 144.6 (C-3'), 148.5 (C-4'), 157.1 (C-2), 157.6 (C-8a), 161.7 (C-5), 164.6 (C-7), 178.1 (C-4); UPLC-TOFMS ES $^-$ m/z 625.1404 $[\text{M}-1]^-$.

3.2.1.3 Synthesis of **1** and **5-11**

First, quercetin glycoside **4** (200 mg, 0.320 mmol), K_2CO_3 (265 mg, 1.92 mmol),

and acetobromoglucose or acetobromocellobiose (790 mg or 1.34 g respectively, 1.92 mmol) were added to 4 mL of DMF. The mixture was stirred for 6 h at room temperature under argon. Next, K_2CO_3 (265 mg, 1.92 mmol) and BnBr (0.305 ml, 2.56 mmol) were added, and then the mixture was stirred overnight at room temperature under argon. The resulting mixture was diluted with 30 mL of EtOAc and washed with water (2×30 mL). After solvent evaporation, the residue was dissolved in 10 mL of THF, and 10 mL of 28% sodium methoxide/MeOH (1:50, v/v) was added. The mixture was stirred for 6 h at room temperature. The solution was neutralized by adding 2.0 g of an ion-exchange resin (H^+ form) and stirred for 30 min. The resin was filtered off, and the reactant was obtained after solvent evaporation. The reactant was dissolved in 20 mL of EtOH/THF (1:1, v/v), and 100 mg of 10% Pd/C was added. The mixture was stirred for 2 h at room temperature under 0.1 MPa H_2 . The Pd/C was filtered off, and the solvent was evaporated. The compounds **1**, **5**, **6**, and **7** obtained were yellow powders with yields of 10.3%, 9.68%, 4.91%, and 3.13%, respectively; they were obtained from rutin from the reactant mixture by preparative HPLC with an ODS-3 column (20 mm $\phi \times 250$ mm L) eluted with the linear gradient MeOH/0.05% TFA aq. soln. = 25/75 (0 min), 100/0 (60 min), 100/0 (80 min).

Compounds **8**, **9**, **10**, and **11** obtained from **3** were yellow powders with yields of 4.18%, 3.30%, 6.78%, and 5.01%, respectively, and were synthesized using the same method as for **1**, **5**, **6**, and **7**. The structures of synthesized quercetin glycosides were confirmed using NMR, UPLC or MALDI-TOFMS, UV spectra, IR, and specific optical rotation.

1: Yellow powder; UV λ_{max} 207, 265, 345 nm; $[\alpha]_D^{20}$ -34.4°(c 0.32, MeOH:H₂O=1:1

v/v); IR (KBr) ν_{\max} 3416, 1655, 1612, 1498, 1433, 1366, 1258, 1204, 1074 cm^{-1} ; ^1H NMR (CD_3OD , 600 MHz) δ_{H} 3.19 (1H, t, $J = 8.22$ Hz, H-B2), 3.29-3.33 (5H, m, H-A4, A5, B3, B4, B5), 3.49 (1H, t, $J = 7.6$ Hz, H-A2), 3.52 (1H, m, H-C4), 3.56 (1H, t, $J = 8.3$ Hz, H-C2), 3.58-3.59 (2H, m, H-A3, C5), 3.70 (1H, m, H-C3), 3.71 (2H, m, H-A6), 3.86-3.90 (2H, m, H-C6), 4.38 (1H, d, $J = 8.3$ Hz, H-B1), 4.92 (1H, d, $J = 7.6$ Hz, H-C1), 5.32 (1H, d, $J = 7.6$ Hz, H-A1), 6.19 (1H, d, $J = 1.4$ Hz, H-6), 6.38 (1H, br s, H-8), 7.25 (1H, d, $J = 8.9$ Hz, H-5'), 7.63 (1H, dd, $J = 8.9, 2.0$ Hz, H-6'), 7.68 (1H, d, $J = 2.0$ Hz, H-2'); ^{13}C NMR (CD_3OD , 150 MHz) δ_{C} 60.5 (C-A6), 61.1 (C-B6, C6), 69.9 (C-B4), 70.1 (C-C4), 73.5 (C-B2, C2), 74.1 (C-C3), 75.0 (C-A2), 75.6 (C-A5), 76.5 (C-A3, B5), 76.8 (C-B3, C5), 79.0 (C-A4), 93.4 (C-8), 98.7 (C-6), 101.9 (C-C1), 102.5 (C-A1), 103.2 (C-B1), 104.5 (C-4a), 115.9 (C-5'), 116.7 (C-2'), 121.6 (C-1'), 125.2 (C-6'), 134.7 (C-3), 146.3 (C-3'), 147.7 (C-4'), 156.9 (C-2), 157.2 (C-8a), 161.8 (C-5), 164.8 (C-7), 178.2 (C-4); UPLC-TOFMS ES $^-$ m/z 787.1973 [M-1].

5: Yellow powder; UV λ_{\max} 204, 255, 353 (nm); $[\alpha]_{\text{D}}^{20}$ -41.4° (c 0.17, MeOH:H₂O=1:4 v/v); IR (KBr) ν_{\max} 3447, 1651, 1494, 1338, 1202, 1073 cm^{-1} ; ^1H NMR (CD_3OD , 600 MHz) δ_{H} 3.19 (1H, t, $J = 8.3$ Hz, H-B2), 3.28-3.33 (6H, m, H-A4, A5, B3, B4, B5, E3), 3.46 (1H, m, H-E4), 3.47 (1H, m, H-E2) 3.55-3.59 (3H, m, H-A2, A3, E5), 3.71 (2H, m, H-A6), 3.86-3.89 (2H, m, H-E6), 4.38 (1H, d, $J = 6.9$ Hz, H-B1), 5.04 (1H, d, $J = 6.2$ Hz, H-E1), 5.35 (1H, d, $J = 7.6$ Hz, H-A1), 6.47 (1H, br s, H-6), 6.74 (1H, br s, H-8), 6.84 (1H, d, $J = 8.3$ Hz, H-5'), 7.56 (1H, br d, $J = 7.6$ Hz, H-6'), 7.69 (1H, br s, H-2'); ^{13}C NMR (CD_3OD , 150 MHz) δ_{C} 60.4 (C-A6), 60.8 (C-E6), 61.1 (C-B6), 69.9 (C-B4), 70.0 (C-E4), 73.5 (C-B2, C2), 74.1 (C-E3), 75.1 (C-A2), 75.6 (C-A5), 76.5 (C-A3, B5), 76.8 (C-B3), 77.0 (C-E5), 79.0 (C-A4), 94.3 (C-8), 100.3 (C-6), 101.9 (C-E1), 102.4 (C-A1), 103.2 (C-B1), 106.1 (C-4a), 114.7 (C-5'), 116.2 (C-2'), 121.5 (C-1'), 122.0

(C-6'), 134.4 (C-3), 144.6 (C-3'), 148.7 (C-4'), 156.6 (C-2), 158.2 (C-8a), 161.4 (C-5), 163.5 (C-7), 177.1 (C-4); UPLC-TOFMS ES⁻ m/z 787.1978 [M-1]⁻.

6: Yellow powder; UV λ_{\max} 205, 264, 345 nm; $[\alpha]_{\text{D}}^{20}$ -35.9° (c 0.55, MeOH:H₂O=1:4 v/v); IR (KBr) ν_{\max} 3437, 1655, 1498, 1204, 1076 cm⁻¹; ¹H NMR (CD₃OD, 600 MHz) δ_{H} 3.19 (1H, t, J = 8.2 Hz, H-B2), 3.25 (1H, t, J = 8.2 Hz, H-D2), 3.27-3.30 (2H, m, H-B4, D4), 3.30-3.37 (6H, m, H-A5, B3, B5, C5, D3, D5), 3.51 (1H, t, J = 8.3 Hz, H-A2), 3.58-3.68 (6H, m, H-A3, A4, C2, C3, one of B6, D6), 3.69 (1H, m, H-C4), 3.69-3.73 (2H, m, one of the H-A6, C6), 3.85-3.90 (2H, m, one of the H-B6, D6), 3.92-3.94 (2H, m, one of the H-A6, C6), 4.37 (1H, d, J = 9.4 Hz, H-B1), 4.45 (1H, d, J = 7.6 Hz, H-D1), 4.95 (1H, d, J = 7.6 Hz, H-C1), 5.30 (1H, d, J = 7.6 Hz, H-A1), 6.17 (1H, br s, H-6), 6.35 (1H, br s, H-8), 7.21 (1H, d, J = 8.2 Hz, H-5'), 7.62 (1H, br d, J = 8.9 Hz, H-6'), 7.66 (1H, br s, H-2'); ¹³C NMR (CD₃OD, 150 MHz) δ_{C} 60.2 (C-C6), 60.4 (C-A6), 61.1 (C-B6, D6), 70.0 (C-B4, D4), 73.2 (C-C2), 73.5 (C-B2), 73.6 (C-D2), 74.0 (C-A2), 74.5 (C-C3), 75.0 (C-A3), 75.5 (C-B3), 75.6 (C-D3), 76.5 (C-B5, D5), 76.8 (C-A5, C5), 78.8 (C-C4), 78.9 (C-A4), 93.5 (C-8), 98.7 (C-6), 101.6 (C-C1), 102.6 (C-A1), 103.3 (C-B1, D1), 104.4 (C-4a), 115.9 (C-5'), 116.7 (C-2'), 121.6 (C-1'), 125.2 (C-6'), 134.7 (C-3), 146.3 (C-3'), 147.6 (C-4'), 156.8 (C-2), 157.1 (C-8a), 161.7 (C-5), 164.8 (C-7), 178.1 (C-4); MALDI-TOFMS m/z 973.1037 [M+Na]⁺.

7: Yellow powder; UV λ_{\max} 204, 255, 353 nm; $[\alpha]_{\text{D}}^{20}$ -30.7° (c 0.46, MeOH:H₂O=1:4 v/v); IR (KBr) ν_{\max} 3409, 1656, 1601, 1496, 1342, 1204, 1072 cm⁻¹; ¹H NMR (CD₃OD, 600 MHz) δ_{H} 3.19 (1H, t, J = 8.9 Hz, H-B2), 3.24 (1H, t, J = 7.6 Hz, H-F2), 3.27-3.30 (2H, m, H-B4, F4), 3.30-3.39 (6H, m, H-A5, B3, B5, E5, F3, F5), 3.53 (1H, t, J = 8.9 Hz, H-A2), 3.56-3.68 (6H, m, H-A3, A4, E2, E3, one of B6, F6), 3.70 (1H, m, H-E4), 3.70-

3.73 (2H, m, one of the H-A6, E6), 3.83-3.91 (2H, m, one of the H-B6, F6), 3.92-3.94 (2H, m, one of the H-A6, E6), 4.37 (1H, d, $J = 8.2$ Hz, H-B1), 4.43 (1H, d, $J = 8.2$ Hz, H-F1), 5.09 (1H, d, $J = 7.6$ Hz, H-C1), 5.36 (1H, d, $J = 7.6$ Hz, H-A1), 6.47 (1H, d, $J = 2.0$ Hz, H-6), 6.73 (1H, d, $J = 1.4$ Hz, H-8), 6.85 (1H, d, $J = 8.3$ Hz, H-5'), 7.59 (1H, br d, $J = 8.9$ Hz, H-6'), 7.69 (1H, d, $J = 2.0$ Hz, H-2'); ^{13}C NMR (DMSO- d_6 , 150 MHz) δ_{C} 60.5 (C-E6), 60.9 (C-A6), 61.6 (C-B6, F6), 70.6 (C-B4, F4), 73.3 (C-E2), 73.8 (C-B2, F2), 74.3 (C-A2), 75.3 (C-E3), 75.4 (C-A3), 75.6 (C-B3), 76.0 (C-F3), 77.0 (C-B5, F5), 77.3 (C-A5, C-E5), 80.3 (C-E4), 80.9 (C-A4), 94.9 (C-8), 99.7 (C-6), 100.1 (C-E1), 103.7 (C-A1), 103.7 (C-B1, F1), 106.2 (C-4a), 115.6 (C-5'), 116.9 (C-2'), 121.4 (C-1'), 122.2 (C-6'), 134.0 (C-3), 145.4 (C-3'), 149.4 (C-4'), 156.5 (C-2), 157.5 (C-8a), 161.4 (C-5), 163.2 (C-7), 178.0 (C-4); MALDI-TOFMS m/z 973.1037 $[\text{M}+\text{Na}]^+$.

8: Yellow powder; UV λ_{max} 206, 265, 344 nm; $[\alpha]_{\text{D}}^{20} -31.3^\circ$ (c 0.60, MeOH); IR (KBr) ν_{max} 3430, 1656, 1498, 1364, 1204, 1076 cm^{-1} ; ^1H NMR (CD_3OD , 600 MHz) δ_{H} 3.20 (1H, m, H-A5), 3.30 (1H, t, $J = 9.7$ Hz, H-A4), 3.38-3.43 (2H, m, H-C4, C5), 3.46-3.55 (3H, m, H-A2, A3, C2, C3), 3.69-3.73 (3H, m, H-A6, one of the C6), 3.91 (1H, br d, $J = 10.3$ Hz, one of the H-C6), 4.91 (1H, d, $J = 7.6$ Hz, H-C1), 5.29 (1H, d, $J = 7.6$ Hz, H-A1), 6.19 (1H, br s, H-6), 6.38 (1H, br s, H-8), 7.26 (1H, d, $J = 8.9$ Hz, H-5'), 7.63 (1H, br d, $J = 8.9$ Hz, H-6'), 7.69 (1H, br s, H-2'); ^{13}C NMR (CD_3OD , 150 MHz) δ_{C} 61.1 (C-C6), 61.2 (C-A6), 70.0 (C-A4, C4), 73.4 (C-C2), 74.3 (C-A2), 76.2 (C-A3), 76.7 (C-C3), 77.1 (C-A5, C5), 89.5 (C-8), 93.4 (C-6), 101.9 (C-C1), 102.6 (C-A1), 103.3 (C-4a), 115.9 (C-5'), 116.7 (C-2'), 121.5 (C-1'), 125.3 (C-6'), 134.7 (C-3), 146.3 (C-3'), 147.7 (C-4'), 153.4 (C-2), 157.2 (C-8a), 161.8 (C-5), 165.3 (C-7), 178.2 (C-4); MALDI-TOFMS m/z 649.1273 $[\text{M}+\text{Na}]^+$.

9: Yellow powder; UV λ_{\max} 204, 255, 354 nm; $[\alpha]^{20}_{\text{D}} -14.4^{\circ}$ (*c* 0.10, MeOH); IR (KBr) ν_{\max} 3402, 1656, 1608, 1498, 1304, 1203, 1071 cm^{-1} ; ^1H NMR (CD_3OD , 600 MHz) δ_{H} 3.20 (1H, m, H-A5), 3.32-3.42 (3H, m, H-A4, E4, E5), 3.46 (2H, m, H-A2, E2), 3.49-3.57 (2H, m, H-A3, E3), 3.83-3.91 (2H, m, one of the H-A6, E6), 4.19-4.21 (2H, m, one of the H-A6, E6), 5.04 (1H, d, $J = 7.6$ Hz, H-E1), 5.32 (1H, d, $J = 7.6$ Hz, H-A1), 6.48 (1H, d, $J = 2.0$ Hz, H-6), 6.74 (1H, d, $J = 1.4$ Hz, H-8), 6.85 (1H, d, $J = 8.9$ Hz, H-5'), 7.60 (1H, dd, $J = 8.2, 1.4$ Hz, H-6'), 7.70 (1H, d, $J = 2.1$ Hz, H-2'); ^{13}C NMR (CD_3OD , 150 MHz) δ_{C} 61.1 (C-E6), 61.2 (C-A6), 70.0 (C-A4, E4), 73.4 (C-E2), 74.4 (C-A2), 76.5 (C-A3), 76.7 (C-E3), 77.0 (C-E5), 77.1 (C-A5), 94.4 (C-8), 99.5 (C-6), 100.3 (C-C1), 102.5 (C-A1), 106.1 (C-4a), 114.7 (C-5'), 116.2 (C-2'), 121.6 (C-1'), 122.0 (C-6'), 134.4 (C-3), 144.6 (C-3'), 148.7 (C-4'), 155.7 (C-2), 158.2 (C-8a), 161.4 (C-5), 163.4 (C-7), 178.4 (C-4); MALDI-TOFMS m/z 649.3783 $[\text{M}+\text{Na}]^+$.

10: Yellow powder; UV λ_{\max} 207, 265, 346 nm; $[\alpha]^{20}_{\text{D}} -28.6^{\circ}$ (*c* 0.70, MeOH:H₂O=1:4 v/v); IR (KBr) ν_{\max} 3402, 1655, 1611, 1499, 1308, 1204, 1076 cm^{-1} ; ^1H NMR (CD_3OD , 600 MHz) δ_{H} 3.23 (1H, t, $J = 7.6$ Hz, H-D2), 3.27-3.30 (2H, m, H-A4, D4), 3.30-3.37 (3H, m, H-A5, D3, C5, D5), 3.37-3.44 (2H, m, H-A3, A2), 3.58-3.68 (4H, m, H-C2, C3, one of the D6), 3.69 (1H, m, H-C4), 3.85-3.96 (5H, m, H-A6, C6, one of the D6), 4.43 (1H, d, $J = 8.3$ Hz, H-D1), 4.97 (1H, d, $J = 8.3$ Hz, H-C1), 5.30 (1H, d, $J = 7.6$ Hz, H-A1), 6.19 (1H, br s, H-6), 6.38 (1H, br s, H-8), 7.23 (1H, d, $J = 8.3$ Hz, H-5'), 7.64 (1H, br d, $J = 8.3$ Hz, H-6'), 7.69 (1H, br s, H-2'); ^{13}C NMR (CD_3OD , 150 MHz) δ_{C} 60.2 (C-C6), 61.1 (C-A6), 61.2 (C-D6), 69.9 (C-D4), 70.0 (C-A4), 73.1 (C-C2), 73.6 (C-D2), 74.4 (C-A2), 74.6 (C-C3), 75.5 (C-A3), 75.6 (C-D3), 76.5 (C-D5), 76.7 (C-A5), 76.8 (C-C5), 78.7 (C-C4), 93.5 (C-8), 98.6 (C-6), 101.6 (C-C1), 102.6 (C-A1), 103.3 (C-D1), 104.5 (C-4a), 115.8 (C-5'), 116.8 (C-2'), 121.5 (C-1'), 125.2 (C-6'), 134.7 (C-3),

146.7 (C-3'), 147.5 (C-4'), 156.9 (C-2), 157.2 (C-8a), 161.8 (C-5), 164.8 (C-7), 178.3 (C-4); MALDI-TOFMS m/z 811.0673 [M+Na]⁺.

11: Yellow powder; UV λ_{\max} 205, 255, 354 nm; $[\alpha]^{20}_{\text{D}}$ -9.3° (c 0.16, MeOH:H₂O=1:4 v/v); IR (KBr) ν_{\max} 3401, 1655, 1498, 1205, 1074 cm⁻¹; ¹H NMR (CD₃OD, 600 MHz) δ_{H} 3.24 (1H, t, J = 8.9 Hz, H-F2), 3.27-3.30 (2H, m, H-A4, F4), 3.30-3.39 (4H, m, H-A5, E5, F3, F5), 3.53-3.58 (3H, m, H-A2, one of the A6, F6), 3.64-3.71 (6H, m, H-A3, E2, E3, E4 one of the A6, F6), 3.86-3.93 (2H, m, H-E6), 4.43 (1H, d, J = 7.6 Hz, H-F1), 5.09 (1H, d, J = 6.2 Hz, H-C1), 5.30 (1H, d, J = 7.6 Hz, H-A1), 6.47 (1H, br s, H-6), 6.73 (1H, br s, H-8), 6.85 (1H, d, J = 7.6 Hz, H-5'), 7.59 (1H, br d, J = 7.6 Hz, H-6'), 7.70 (1H, br s, H-2'); ¹³C NMR (CD₃OD, 150 MHz) δ_{C} 60.3 (C-F6), 61.1 (C-A6) 61.2 (C-E6), 70.0 (C-A4), 70.1 (C-F4), 73.1 (C-E2), 73.5 (C-F2), 73.6 (C-A2), 74.4 (C-E3), 74.8 (C-A3), 76.6 (C-F3), 76.7 (C-F5), 76.8 (C-A5), 77.1 (C-E5), 78.7 (C-E4), 94.4 (CS-8), 99.4 (C-6), 99.9 (C-E1), 102.6 (C-A1), 103.2 (C-F1), 106.2 (C-4a), 114.7 (C-5'), 116.3 (C-2'), 121.6 (C-1'), 122.0 (C-6'), 134.5 (C-3), 144.6 (C-3'), 148.7 (C-4'), 156.7 (C-2), 158.3 (C-8a), 161.5 (C-5), 163.3 (C-7), 178.4 (C-4); MALDI-TOFMS m/z 811.0888 [M+Na]⁺.

3.2.2. Synthesis of quercetin methyl ether

3.2.2.1 Synthesis of compound 12

Rutin (5.00 g, 8.19 mmol), K₂CO₃ (9.04 g, 65.52 mmol), and BnBr (7.79 mL, 65.52 mmol) were added to 60 mL of dimethylformamide (DMF), and the mixture was stirred for 10 h under argon at room temperature. The resulting mixture was diluted with 150 mL

of ethyl acetate (EtOAc) and washed with water (2×150 mL). The residue obtained after evaporation of the solvent was dissolved in 100 mL of 1 N HCl, and the mixture was refluxed at 80°C for 2 h.

The precipitate was allowed to cool and filtered. Next, 1.0 g of the precipitate, K_2CO_3 (22.5 g, 163 mmol), and dimethylsulfate (17.5 mL, 184 mmol) were added to 26 mL of DMF, and the mixture was stirred for 6 h at 65°C. The reaction mixture was diluted with 150 mL of EtOAc and washed with water (2×150 mL). After the EtOAc phase was dried using Na_2SO_4 , the reactant was obtained by evaporating the solvent.

The reactant was dissolved in 40 mL of ethanol (EtOH) / tetrahydrofuran (THF) (1:1, v/v), and 200 mg of 10% Pd/C was added. The mixture was stirred for 1 h at room temperature under 0.05 MPa hydrogen. The Pd/C was filtered off. After the solvent was evaporated, 3-*O*-methylquercetin (**12**) was isolated by preparative HPLC with an ODS-3 column (20 mm $\phi \times 250$ mm). Elution was performed with a linear gradient of MeOH/0.05% aqueous solution TFA (0 min, 50/50; 50 min, 100/0; 60 min, 100/0) to obtain **12** as a yellowish powder with 41.1% yield. The structure of the synthesized methylquercetin **12** was confirmed using NMR, UPLC-TOFMS, UV, and IR spectra, and by measuring the specific optical rotation: UV λ_{max} 204, 255, 357 nm; $[\alpha]_D^{25} -3.75^\circ$ (c 0.75, MeOH); IR (KBr) ν_{max} 3402, 1655, 1607, 1505, 1440, 1361 cm^{-1} ; 1H NMR (CD_3OD , 600 MHz) δ_H 3.75 (3H, s, 3-OCH₃), 6.16 (1H, d, $J = 2.04$ Hz, H-6), 6.36 (1H, d, $J = 2.04$ Hz, H-8), 6.88 (1H, d, $J = 8.28$ Hz, H-5'), 7.50 (1H, dd, $J = 8.22, 2.04$ Hz, H-6'), 7.59 (1H, d, $J = 2.04$ Hz, H-2'); ^{13}C NMR (CD_3OD , 150 MHz) δ_C 59.2 (3-OCH₃), 93.4 (C-8), 98.4 (C-6), 104.5 (C-4a), 115.1 (C-2', 5'), 121.0 (C-6'), 121.6 (C-1'), 138.2 (C-3), 145.1 (C-3'), 148.6 (C-4'), 156.6 (C-2), 157.1 (C-8a), 161.7 (C-5), 164.5 (C-7), 178.7 (C-4);

UPLC-TOFMS m/z 315.049 [M-H]⁻.

3.2.2.2 Synthesis of **13**, **14**, and **15**

Methylquercetin **12** (100 mg, 0.316 mmol), K₂CO₃ (43.7 mg, 0.316 mmol), and dimethylsulfate (35.1 μL, 0.316 mmol) were added to 10 mL of DMF. The mixture was stirred for 6 h at 65°C. The resulting mixture was diluted with 30 mL of EtOAc and washed with water (2 × 30 mL). After evaporating the solvent, 3,4'-*O*-dimethylquercetin (**13**), 3,7-*O*-dimethylquercetin (**14**), and 3,4', 7-*O*-trimethylquercetin (**15**) were obtained by preparative HPLC with an ODS-3 column (20 mm φ × 250 mm). Compounds were eluted with the linear gradient MeOH/0.05% aqueous solution TFA (0 min, 50/50; 50 min, 100/0; 60 min, 100/0) to obtain **13**, **14** and **15** as yellowish powders with yields of 11.9, 9.1, and 9.1%, respectively. The structures of synthesized methylquercetins were confirmed using NMR, UPLC -TOFMS, UV, and IR spectra, and by measuring the specific optical rotation.

13: UV λ_{\max} 208, 254, 355 nm; $[\alpha]_{\text{D}}^{25}$ -0.51° (*c* 0.90, MeOH); IR (KBr) ν_{\max} 3402, 1654, 1609, 1507, 1441, 1364 cm⁻¹; ¹H NMR (CD₃OD, 600 MHz) δ_{H} 3.76 (3H, s, 3-OCH₃), 3.91 (3H, s, 4'-OCH₃), 6.16 (1H, dr s, H-6), 6.36 (1H, br s, H-8), 7.02 (1H, d, *J* = 8.22 Hz, H-5'), 7.57 (1H, br s, H-2'), 7.60 (1H, br d, *J* = 8.28 Hz, H-6'); ¹³C NMR (CD₃OD, 150 MHz) δ_{C} 55.0 (4'-OCH₃), 59.2 (3-OCH₃), 93.4 (C-8), 98.4 (C-6), 104.6 (C-4a), 114.8 (C-2', 5'), 120.8 (C-6'), 122.8 (C-1'), 138.5 (C-3), 146.3 (C-3'), 150.3 (C-4'), 156.2 (C-2), 157.1 (C-8a), 161.8 (C-5), 164.6 (C-7), 178.7 (C-4); UPLC-TOFMS m/z 329.0645 [M-H]⁻.

14: UV λ_{\max} 209, 256, 357 nm; $[\alpha]_{\text{D}}^{25}$ -19.6° (*c* 0.10, THF); IR (KBr) ν_{\max} 3415, 1657, 1595, 1498, 1441, 1350 cm^{-1} ; ^1H NMR (Acetone-*d*₆, 600 MHz) δ_{H} 3.84 (3H, s, 3-OCH₃), 3.89 (3H, s, 7-OCH₃), 6.28 (1H, dr s, H-6), 6.62 (1H, br s, H-8), 6.97 (1H, d, *J* = 8.22 Hz, H-5'), 7.57 (1H, br d, *J* = 8.22 Hz, H-6'), 7.70 (1H, br s, H-2'); ^{13}C NMR (Acetone-*d*₆, 150 MHz) δ_{C} 55.6 (7-OCH₃), 59.3 (3-OCH₃), 91.9 (C-8), 97.6 (C-6), 105.7 (C-4a), 115.4 (C-2'), 115.6 (C-5'), 121.3 (C-6'), 122.1 (C-1'), 138.6 (C-3), 145.0 (C-3'), 148.3 (C-4'), 156.1 (C-2), 156.9 (C-8a), 162.0 (C-5), 165.7 (C-7), 178.8 (C-4); UPLC-TOFMS *m/z* 329.0653 [M-H]⁻.

15: UV λ_{\max} 209, 255, 354 nm; $[\alpha]_{\text{D}}^{25}$ -26.1° (*c* 0.52, THF); IR (KBr) ν_{\max} 3420, 1656, 1595, 1501, 1441, 1333 cm^{-1} ; ^1H NMR (Dimethylsulfoxide-*d*₆, 600 MHz) δ_{H} 3.76 (3H, s, 3-OCH₃), 3.83 (6H, s, 4'-OCH₃, 7-OCH₃), 6.33 (1H, dr s, H-6), 6.69 (1H, br s, H-8), 7.07 (1H, d, *J* = 8.22 Hz, H-5'), 7.54 (2H, br s, H-6', 2'); ^{13}C NMR (Dimethylsulfoxide-*d*₆, 150 MHz) δ_{C} 56.2 (4'-OCH₃), 56.6 (7-OCH₃), 60.2 (3-OCH₃), 92.8 (C-8), 98.3 (C-6), 105.7 (C-4a), 115.6 (C-2', 5'), 121.0 (C-6'), 122.7 (C-1'), 138.7 (C-3), 146.9 (C-3'), 150.8 (C-4'), 156.1 (C-2), 156.8 (C-8a), 161.4 (C-5), 165.7 (C-7), 178.6 (C-4); UPLC-TOFMS *m/z* 343.0825 [M-H]⁻.

3.2.2.3 Synthesis of 16, 17, and 18

Rutin (200 mg, 0.328 mmol), K₂CO₃ (90.6 mg, 0.656 mmol), and dimethylsulfate (62.2 μL , 0.656 mmol) were added to 10 mL of DMF, and the mixture was stirred for 6 h at 65°C. The resulting mixture was added to 50 mL of 2.5 N HCl and refluxed at 80°C for 2 h. The reaction mixture was diluted with 150 mL of EtOAc and washed with water

(2 × 150 mL). The reaction mixture was obtained by drying the EtOAc phase using Na₂SO₄. After evaporating the solvent, 4'-*O*-methylquercetin (**16**), 7-*O*-methylquercetin (**17**) and 4', 7-*O*-dimethylquercetin (**18**) were obtained by preparative HPLC with an ODS-3 column (20 mm φ × 250 mm). Compounds were eluted with the linear gradient MeOH/0.05% aqueous solution of TFA (0 min, 60/40; 50 min, 100/0; 60 min, 100/0) to obtain **16**, **17** and **18** as yellowish powders with yields of 4.1, 10.0, and 7.7%, respectively. The structures of the synthesized compounds **16**, **17**, and **18** were confirmed using NMR, MALDI-TOFMS, UV and IR spectra, and by the measurements of specific optical rotation.

16: UV λ_{max} 207, 254, 368 nm; [α]²⁵_D -26.9°(c 0.20, MeOH); IR (KBr) ν_{max} 3430, 1655, 1617, 1499, 1456 cm⁻¹; ¹H NMR (Dimethylsulfoxide-*d*₆, 600 MHz) δ_H 3.81 (3H, s, 4'-OCH₃), 6.15 (1H, d, *J* = 2.04 Hz, H-6), 6.39 (1H, d, *J* = 2.04 Hz, H-8), 7.05 (1H, d, *J* = 8.22 Hz, H-5'), 7.62 (1H, dd, *J* = 8.22, 2.76 Hz, H-6'), 7.63 (1H, d, *J* = 2.10 Hz, H-2'); ¹³C NMR (Dimethylsulfoxide-*d*₆, 150 MHz) δ_C 56.1 (4'-OCH₃), 93.9 (C-8), 98.7 (C-6), 103.6 (C-4a), 112.4 (C-5'), 115.1 (C-2'), 120.3 (C-6'), 123.9 (C-1'), 136.7 (C-3), 146.7 (C-3'), 146.8 (C-2), 149.9 (C-4'), 156.7 (C-8a), 161.3 (C-5), 164.5 (C-7), 176.5 (C-4); MALDI-TOFMS *m/z* 317.0494 [M+H]⁺.

17: UV λ_{max} 206, 255, 371 nm; [α]²⁵_D -17.3°(c 0.20, THF); IR (KBr) ν_{max} 3402, 1656, 1593, 1502, 1442, 1324 cm⁻¹; ¹H NMR (Dimethylsulfoxide-*d*₆, 600 MHz) δ_H 3.82 (3H, s, 7-OCH₃), 6.31 (1H, d, *J* = 2.04 Hz, H-6), 6.60 (1H, d, *J* = 1.38 Hz, H-8), 6.86 (1H, d, *J* = 8.22 Hz, H-5'), 7.56 (1H, dd, *J* = 8.22, 2.04 Hz, H-6'), 7.69 (1H, d, *J* = 2.04 Hz, H-2'); ¹³C NMR (Dimethylsulfoxide-*d*₆, 150 MHz) δ_C 56.5 (7-OCH₃), 92.4 (C-8), 98.0 (C-6), 104.5 (C-4a), 115.6 (C-2'), 116.1 (C-5'), 120.5 (C-6'), 122.4 (C-1'), 136.6 (C-3), 145.6

(C-3'), 147.8 (C-2), 148.4 (C-4'), 156.6 (C-8a), 160.9 (C-5), 165.4 (C-7), 176.5 (C-4); MALDI-TOFMS m/z 317.0274 [M+H]⁺.

18: UV λ_{\max} 206, 254, 368 nm; $[\alpha]_{\text{D}}^{25}$ -3.72° (c 0.23, THF); IR (KBr) ν_{\max} 3420, 1656, 1594, 1501, 1441, 1332 cm^{-1} ; ¹H NMR (Dimethylsulfoxide- d_6 , 600 MHz) δ_{H} 3.82 (3H, s, 7-OCH₃), 3.83 (3H, s, 4'-OCH₃), 6.32 (1H, d, J = 2.10 Hz, H-6), 6.68 (1H, d, J = 2.04 Hz, H-8), 7.05 (1H, d, J = 8.94 Hz, H-5'), 7.65 (1H, dd, J = 8.94, 2.04 Hz, H-6'), 7.69 (1H, d, J = 2.04 Hz, H-2'); ¹³C NMR (Dimethylsulfoxide- d_6 , 150 MHz) δ_{C} 56.2 (4'-OCH₃), 56.6 (7-OCH₃), 92.5 (C-8), 98.0 (C-6), 104.6 (C-4a), 115.3 (C-2'), 112.3 (C-5'), 120.3 (C-6'), 123.8 (C-1'), 137.0 (C-3), 146.7 (C-3'), 147.3 (C-2), 150.0 (C-4'), 156.7 (C-8a), 160.9 (C-5), 165.5 (C-7), 176.6 (C-4); MALDI-TOFMS m/z 331.0608 [M+H]⁺.

3.2.3 Synthesis of 19

Rutin (5.00 g, 8.19 mmol), K₂CO₃ (9.04 g, 65.52 mmol), and BnBr (7.79 mL, 65.52 mmol) were added to 60 mL of DMF, and the mixture was stirred for 10 h under argon at room temperature. The resulting mixture was diluted with 150 mL of EtOAc and washed with water (2 × 150 mL). The residue obtained by evaporating the solvent was dissolved in 100 mL of 1 N HCl and refluxed at 80°C for 2 h. The obtained precipitate was filtered after cooling, and 100 μg was acetylated overnight using acetic anhydride (1.0 mL, 10.6 mmol) in 1.0 mL of pyridine at room temperature. The reaction mixture was diluted with 50 mL of EtOAc and washed with water (2 × 50 mL). After the EtOAc phase was dried using Na₂SO₄, the reactant was obtained by evaporating the solvent.

The reaction mixture was dissolved in 40 mL of EtOH / THF (1:1, v/v), and 100 mg

of 10% Pd/C was added. The mixture was stirred for 1 h at room temperature under 0.05 MPa hydrogen. After the Pd/C was removed by filtration, the solvent was evaporated to obtain 3-*O*-acetylquercetin (**19**) as a yellowish powder with 39.0% yield from original rutin. It was purified using preparative HPLC with an ODS-3 column (20 mm ϕ \times 250 mm L). Compound **19** was eluted using a linear gradient of MeOH / 0.05% aqueous solution of TFA (0 min, 50/50; 50 min, 100/0; 60 min, 100/0). The structure of the synthesized **19** was confirmed using NMR, UPLC-TOFMS, UV, and IR spectra, and the measurement of specific optical rotation: UV λ_{\max} 204, 255, 350 nm; $[\alpha]_{\text{D}}^{25}$ -2.67° (*c* 0.55, MeOH); IR (KBr) ν_{\max} 3402, 1656, 1604, 1507, 1444, 1367 cm^{-1} ; ^1H NMR (CD_3OD , 600 MHz) δ_{H} 2.30 (3H, s, 3-OAc), 6.20 (1H, d, J = 2.10 Hz, H-6), 6.40 (1H, d, J = 2.04 Hz, H-8), 6.88 (1H, d, J = 8.94 Hz, H-5'), 7.27 (1H, dd, J = 8.94, 2.04 Hz, H-6'), 7.32 (1H, d, J = 2.10 Hz, H-2'); ^{13}C NMR (CD_3OD , 150 MHz) δ_{C} 19.1 (3-OAc), 93.7 (C-8), 98.8 (C-6), 103.9 (C-4a), 114.8 (C-2'), 115.2 (C-5'), 120.8 (C-6'), 120.7 (C-1'), 130.1 (C-3), 145.3 (C-3'), 149.1 (C-4'), 157.0 (C-2), 157.3 (C-8a), 161.7 (C-5), 164.9 (C-7), 168.5 (3-OAc), 175.9 (C-4); UPLC-TOFMS m/z 343.043 $[\text{M}-\text{H}]^-$.

3.2.4 Synthesis of **20**

Rutin (5.00 g, 8.19 mmol), K_2CO_3 (9.04 g, 65.52 mmol), and BnBr (7.79 mL, 65.52 mmol) were added to 60 mL of DMF, and the mixture was stirred for 10 h under argon at room temperature. The resulting mixture was diluted with 150 mL of EtOAc and washed with water (2×150 mL). The residue obtained after evaporation of the solvent was dissolved in 100 mL of 1 N HCl and refluxed at 80°C for 2 h.

After the mixture was cooled and the precipitate filtered, 200 mg of the precipitate, K_2CO_3 (83.4 mg, 0.604 mmol), and acetobromoglucose (250 mg, 0.604 mmol) were added to 2.0 mL of DMF, and the mixture was stirred for 6 h at room temperature under argon. The reaction mixture was diluted with 30 mL of EtOAc and washed with water (2 \times 30 mL). After the EtOAc phase was dried using Na_2SO_4 , the reactant was obtained by evaporating the solvent.

The reaction mixture was dissolved in 40 mL of EtOH / THF (1:1, v/v). Following addition of 100 mg of 10% Pd/C, the mixture was stirred for 2 h at room temperature under 0.05 MPa hydrogen. Pd/C was filtered, and, after the solvent was evaporated, quercetin-3-*O*-tetra-*O*-acetyl- β -D-glucopyranoside (**20**) was obtained by preparative HPLC with an ODS-3 column (20 mm ϕ \times 250 mm). Fractions were eluted with the linear gradient MeOH / 0.05% TFA aqueous solution (0 min, 50/50; 50 min, 100/0; 60 min, 100/0) to obtain **20** as a yellowish powders with a yield of 25.2%. The structure of the synthesized **20** was confirmed using NMR, UPLC-TOFMS, UV, and IR spectra, and the measurement of specific optical rotation: UV λ_{max} 205, 255, 354 nm; $[\alpha]_D^{25}$ -68.1° (c 0.86, MeOH); IR (KBr) ν_{max} 3436, 1747, 1656, 1609, 1498, 1442, 1368 cm^{-1} ; 1H NMR (CD_3OD , 600 MHz) δ_H 1.89 (3H, s, A2-OAc), 1.93 (3H, s, A4-OAc), 1.96 (3H, s, A3-OAc), 2.14 (3H, s, A6-OAc), 3.92 (1H, m, H-A5), 3.94 (1H, m, H-A6), 4.03 (1H, m, H-A6), 5.01 (1H, m, H-A4), 5.21 (1H, dd, $J = 9.66, 8.28$ Hz, H-A2), 5.35 (1H, t, $J = 9.66$ Hz, H-A3), 5.56 (1H, d, $J = 8.28$ Hz, H-A1), 6.02 (1H, d, $J = 2.04$ Hz, H-6), 6.24 (1H, d, $J = 2.10$ Hz, H-8), 6.85 (1H, d, $J = 8.22$ Hz, H-5'), 7.48 (1H, dd, $J = 8.28, 2.10$ Hz, H-6'), 7.56 (1H, d, $J = 2.04$ Hz, H-2'); ^{13}C NMR (CD_3OD , 150 MHz) δ_C 19.2 (A2-OAc, A4-OAc), 19.3 (A3-OAc), 19.7 (A6-OAc), 61.3 (C-A6), 68.6 (C-A4), 71.4 (C-A5), 71.7 (C-A2), 72.8 (C-A3), 93.5 (C-8), 98.4 (C-6), 99.5 (C-A1), 104.4 (C-4a), 114.6 (C-2'), 116.2 (C-5'),

121.9 (C-1'), 122.0 (C-6'), 133.3 (C-3), 144.5 (C-3'), 148.3 (C-4'), 157.0 (C-2), 158.3 (C-8a), 161.5 (C-5), 164.4 (C-7), 169.9 (A4-OAc), 170.3 (A6-OAc), 170.6 (A3-OAc), 171.1 (A2-OAc), 177.4 (C-4) ; UPLC-TOFMS m/z 631.126 [M-H]⁻.

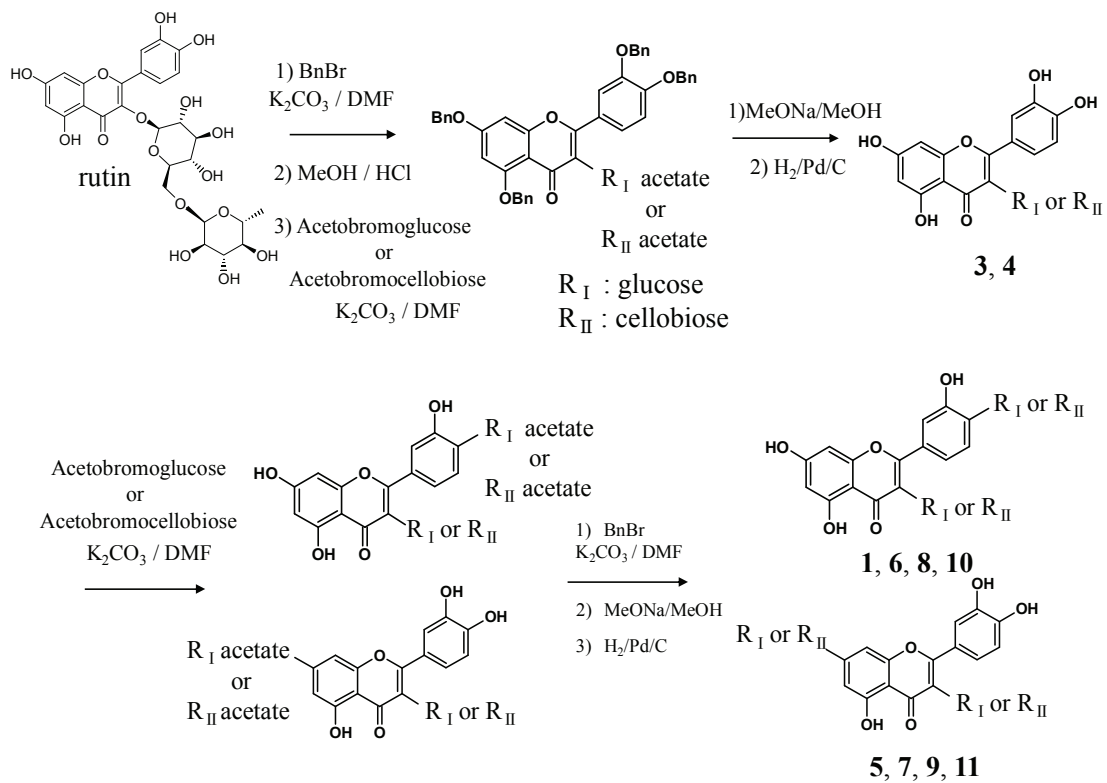
3.3 Result and discussion

3.3.1 Synthesis of quercetin glycosides

The synthetic method for quercetin glycosides in their experiments are shown in Scheme 3.1. The first strategy is to combine cellobiose or glucose at the C-3 position of quercetin. Commercially available rutin was used as the starting material. All phenolic hydroxyl group of rutin were protected by benzylation. After removing rutinose by acid hydrolysis, the free C-3 hydroxyl group was glycosylated using acetobromocellobiose or acetobromoglucose. After deacetylation with sodium methoxide, debenylation was conducted by hydrogenation using palladium carbon to obtain quercetin-3-*O*- β -D-glucopyranoside **3** or quercetin-3-*O*- β -D-glucopyranosyl-(1 \rightarrow 4)- β -D-glucopyranoside **4** from rutin.

Quercetin glycoside **3** or **4** was glycosylated using acetobromoglucose or acetobromocellobiose as shown in Schemes 3.1. After benzylation of these compounds, deacetylation was performed following debenylation. Finally, **1** and **3-11** were purified using preparative high-performance liquid chromatography (HPLC). Structural analysis for all synthesized compounds were performed by nuclear magnetic resonance (NMR), mass spectrometry (MS), infrared spectroscopy (IR), UV spectroscopy, and specific optical rotation. Compound **1**, stimulating melanine biosynthesis in the B16 melanoma

cells, was isolated from *H. zeylanica* and identified completely with the analytical data of synthesized **1** (Table 2.1). The other synthesized quercetin glycosides were also identified by using the same analytical instruments, and the position of sugars connected with quercetin was clarified by using Hetero-nuclear Multiple-Bond Connectivity (HMBC). The protons existing anomeric position of glucose or cellobiose constructing **3** or **4** respectively were correlated with C-3 as shown in Fig. 3.1 indicated that the glucose or cellobiose is bonded to C-3 position as a glycoside. The key HMBC correlations of **1** were also shown in Fig.3.1, which also showed the binding position of sugars in **1**. These results are described in the previous published (Yamauchi, 2014a). Similarly, the HMBC correlations were observed to clear the exact position of sugars in the other synthesized quercetin glycosides (not shown).



Scheme 3.1 Synthesis route of quercetin glycosides **1** and **3-11**

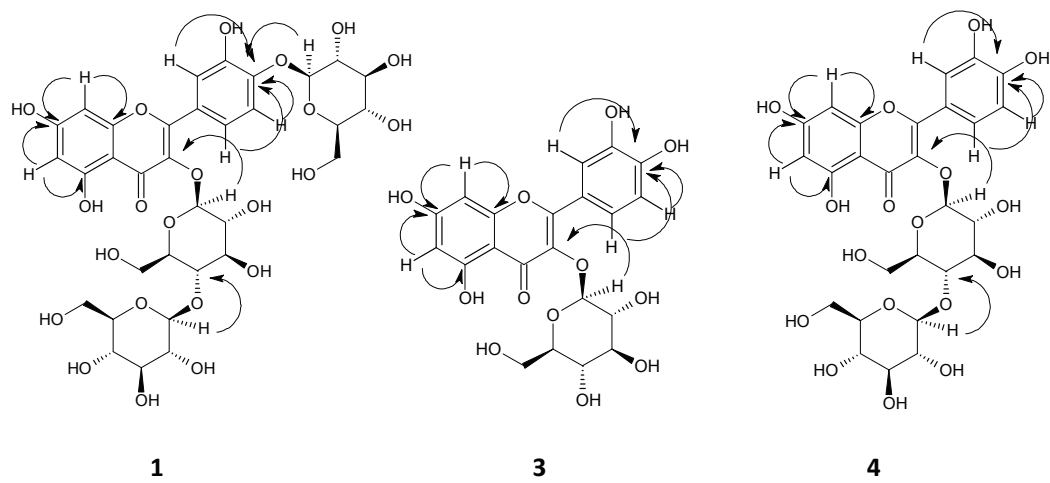


Fig.3.2 Key HMBC correlations of compound 1, 3, and 4

3.3.2 Synthesis of 12-20

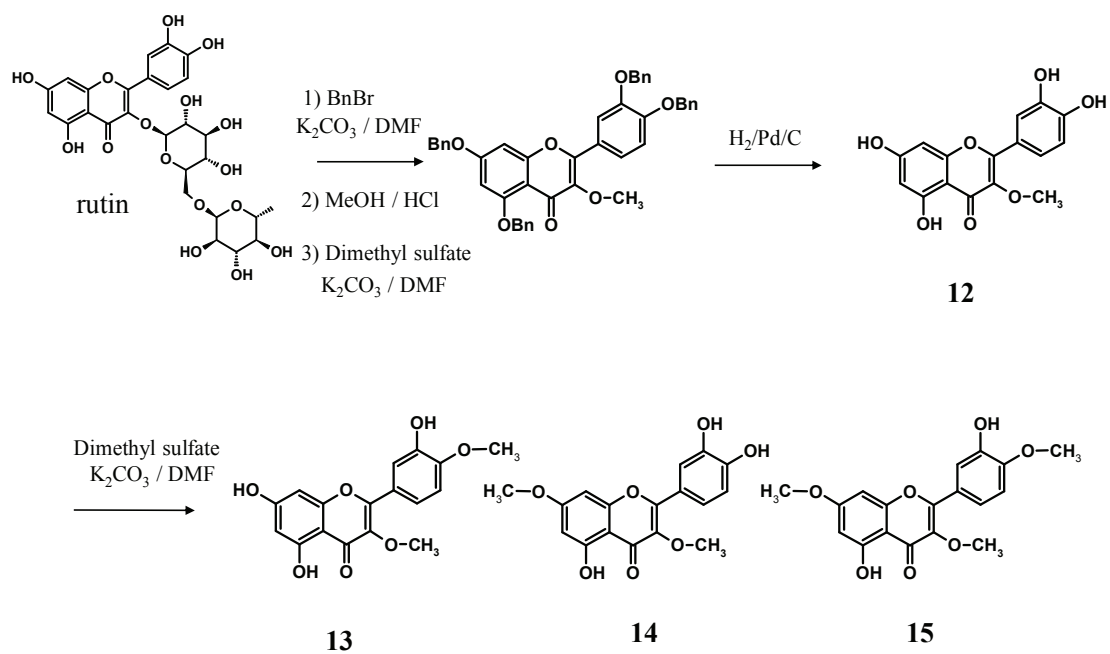
Quercetin derivatives **12–20** were synthesized using commercially available rutin as the starting material. The methylquercetin derivatives **12–15** were synthesized according to the synthesis route shown in Scheme 3.2. The first step in this synthetic approach involved append the methyl group at the C-3 hydroxyl group of quercetin. All phenolic hydroxyl groups of rutin were protected by benzylation. After removing rutinose by acid hydrolysis, the free C-3 hydroxyl group was methylated using dimethylsulfate. Debzylation was subsequently performed by hydrogenation using palladium on carbon (Pd/C), yielding 3-*O*-methylquercetin **12**. Further methylation of **12** was performed to obtain compounds **13–15**.

Compounds **16–18** were synthesized according to the route shown in Scheme 3.3. Following methylation of rutin by dimethylsulfate, rutinose was removed by acid hydrolysis to obtain **16–18**.

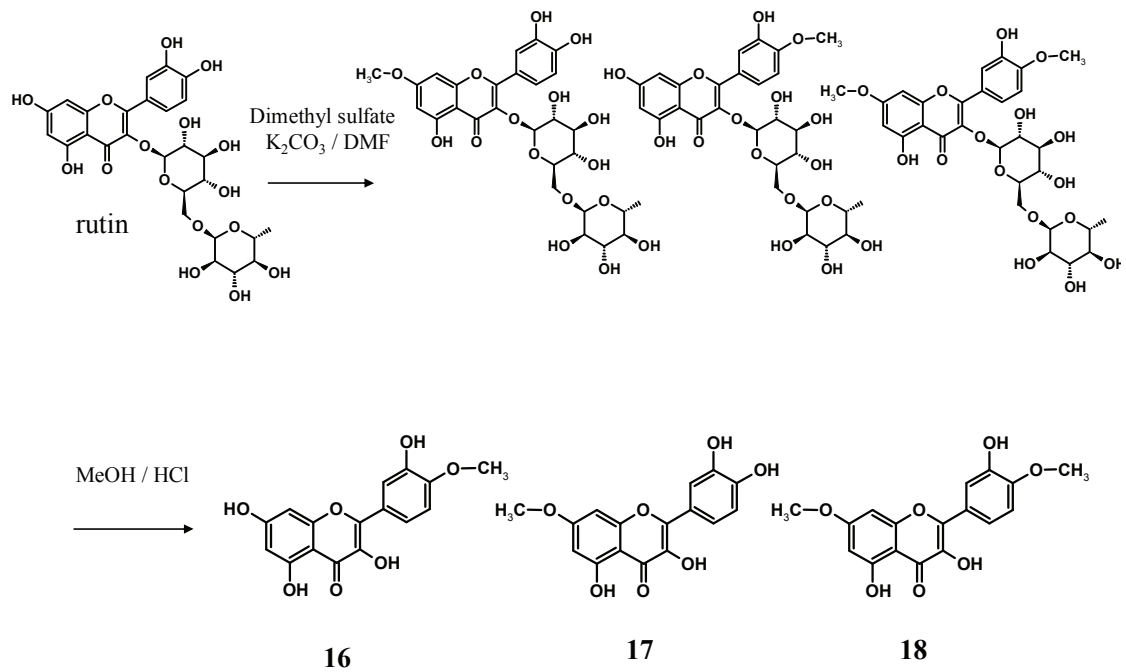
Compounds **19** and **20** were synthesized according to the route shown in Scheme 3.4. In order to specifically append the acetyl group or acetoglucose at the C-3 hydroxyl group, the phenolic hydroxyl group of rutin was protected by benzylation using the method described above. Following acid hydrolysis, the C-3 hydroxyl group was acetylated or glucosylated by acetic acid anhydride or acetobromoglucose to yield **19** or **20**, respectively.

Compounds **12–20** were purified using p-HPLC. Structural analysis of compounds **12–20** was performed by NMR, MS, IR spectroscopy, UV spectroscopy, and the measurement of specific optical rotation. These results are described in the previous

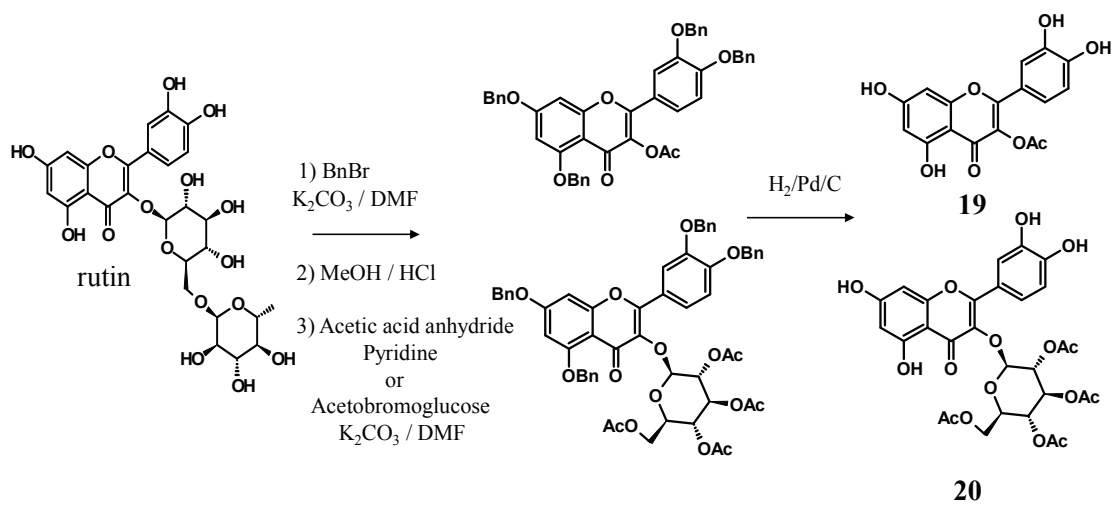
published (Yamauchi, 2014b). The protons existing in the methoxyl group of compound **12** were correlated with C-3, as shown in Fig. 3.2, indicating that the methoxyl group is bonded to the C-3 position. The key HMBC within compound **15** are also presented in Fig.3.2, showing the binding position of the methoxyl group. The anomeric proton of acetoglucose of **20** was correlated with C-3, as shown in Fig.3.2, indicating that acetoglucose binds to the C-3 position as a glycoside. Similarly, HMBC correlations indicated the exact position of the substituent groups in the other synthesized quercetin derivatives (not shown). Comparing the data with the spectrum of quercetin itself (Olejniczak, 2004 and Wagner, 1976) the position of the acetyl group in **19** is likely to be at C-3, as suggested by the observed chemical shift of the C-3 carbon (130.1 ppm).



Scheme 3.2 Synthesis route of methylquercetins **12-15**.



Scheme 3.3 Synthesis route of methylquercetins **16-18**



Scheme 3.4 Synthesis route of methylquercetins **19**, **20**.

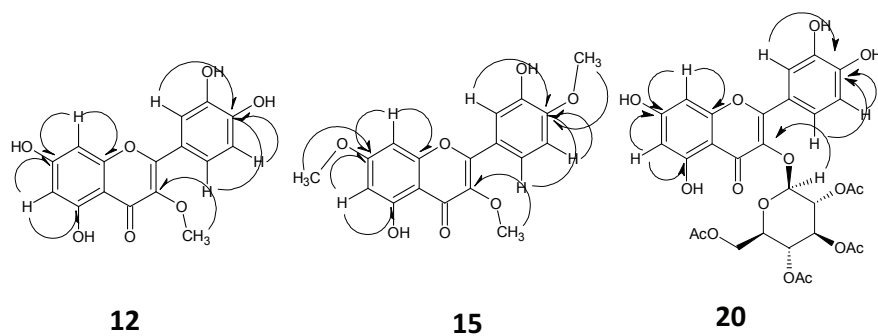


Fig.3.3 Key HMBC correlations of compounds **12**, **15**, and **20**

3.4 Summary

3-*O*-substituent quercetin derivatives **3**, **4**, **12**, **19**, and **20** were regiospecifically synthesized using rutin as the starting material. Other synthesized quercetin glycosides were obtained from **3** or **4** by the glycosylation using acetobromoglucose or acetobromocellobiose. Compounds **13**, **14**, and **15** were synthesized from **12** by methylation using dimethylsulfate. The chemical structure of synthesized compounds were confirmed by using NMR, UPLC or MALDI-TOFMS, UV spectra, IR, and specific optical rotation. The data of instrumental analysis of **1**, isolated from *H. zeylanica* root 50% EtOH extract as novel quercetin glycoside in Chapter 2, conformed to that of synthesized **1**, which supports the identification result of isolated **1** in Chapter 2.

Chapter 4

Melanogenesis stimulatory activity of synthesized quercetin derivatives *via* p38 MAPK path way

4.1 Introduction

Melanin is biosynthesized in the melanosome in the perinuclear region of the melanocyte and transported in the mature melanosome to the periphery of the cell (Kuroda and Fukuda, 2004, Fukuda, 2005, and Marks and Seabra, 2001). The melanosome is further transported to the hair matrix or the keratinocyte present above the melanocyte. The keratinocyte that receives the melanin undergoes cornification, resulting in skin pigmentation. Similarly, hair pigmentation occurs due to melanin released on the outside of the melanocyte which is described in Chapter 1.1. Despite the importance of the extracellular pigment stores, an evaluation of melanogenesis activity using melanin-controlling agents has only been performed on intracellular melanin in B16 melanoma cells thus far (Lan, 2013, Chan, 2011, and Diwakar, 2012). The present study focused on evaluating extracellular melanin released from B16 melanoma cells and investigated the levels of melanin released from the B16 melanoma cells in addition to measuring the intracellular melanin content in order to understand the structure-activity relationships of quercetin derivatives synthesized in Chapter 3.

Melanogenesis in melanocyte is regulated by the contents of melanogenic enzymes which is modulated by MITF, a transcriptional factor of melanogenic enzymes. A number of kinase pathways regulate expression of MITF. p38 MAPK is well known as one of the regulation kinase pathway on the expressions of melanogenic enzymes (Fig.4.1), and we investigated the contents of p38 MAPK, p-p38 MAPK, MITF, tyrosinase, TRP-1, and TRP-2 in B16 melanoma cells after treating with synthesized quercetin derivatives for understanding the mechanisms underlying the observed activity.

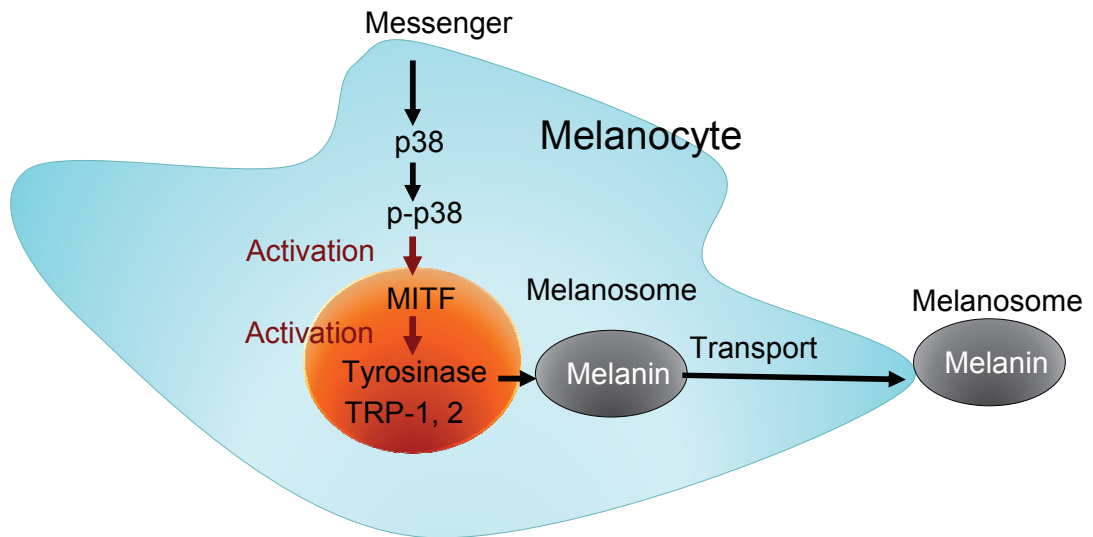


Fig.4.1 p38 MAPK path way regulating the expressions of melanogenic enzymes

4.2 Material and methods

4.2.1 General

Microculture tetrazolium technique (MTT) assay kit and bovine serum albumin (BSA) was purchased from Sigma-Aldrich (St. Louis, MO, USA). Antibodies against tyrosinase (H-109), TRP-1 (H-90), TRP-2 (H-150), p38 MAPK (H-147), and p-p38 MAPK (D-8) were purchased from Santa Cruz Bio technology (Santa Cruz, CA, USA). Horseradish peroxidase (HRP)-conjugated anti-rabbit IgG donkey antibody (NA934) and HRP-conjugated anti-mouse IgG sheep antibody (NA931) were purchased from GE Healthcare (Piscataway, NJ, USA), while MITF-specific antibody (EPR9731) and glyceraldehyde-3-phosphate dehydrogenase (GAPDH)-specific antibody (GTX100118) were purchased from Abcam (Cambridge, MA, USA) and GeneTex (Irvine, CA, USA) respectively. Radioimmunoprecipitation assay (RIPA) buffer (ab156034) and protease inhibitors cocktail (539134) were purchased from Abcam (Cambridge, MA, USA) and Merck Millipore (Billerica, MA, USA). Other commercially available products were purchased from Wako Chemicals (Richmond, VA, USA).

4.2.2 Tyrosinase activity assay

Measurements of tyrosinase activity were performed using a technique from previous described in Chapter 2.

4.2.3 Cell culture

Murine melanoma B16-F0 cells (DS Pharma Biomedical, Osaka, Japan) were grown in Dulbecco's modified Eagle medium (DMEM) supplemented with 10% fetal bovine serum, 100,000 unit/L penicillin, and 100 mg/L streptomycin. Cells were cultured at 37°C in humidified atmosphere of 5% CO₂.

4.2.4 Measurement of cellular melanin content

Briefly, confluent cultures of B16 melanoma cells were rinsed in phosphate-buffered saline (PBS) and removed using 0.25% trypsin/EDTA. The cells were loaded into a 24-well plate (5.0×10^4 cells / well) and allowed to adhere at 37 °C for 24 h. Sample compounds prepared at 200–10 μM for synthesized quercetin glycosides and 50–6.25 μM for **12-20** were added and the cells incubated for 72 h. Following incubation, cell medium was collected and 200 μL aliquots were loaded into a 96-well plate. The absorbance of the medium was measured at 510 nm by using a microplate reader and used as a measure of extracellular melanin contents. The cells were washed with PBS following lysis in 600 μL of 1 M NaOH by heating at 100°C for 30 min to solubilize the melanin. A portion of the resulting lysate (250 μL) was loaded into a 96-well microplate, and the absorbance was measured at 405 nm using a microplate reader. Measured absorbance was used as an index of intracellular melanin contents. Each experiment was repeated twice. The melanin-producing activities were expressed as a percentage of the activity measured in the control cells treated with DMSO without sample materials.

4.2.5 Cell viability

Measurement of cell viability was performed according to a previously described method (Arun, 2011b), using the microculture tetrazolium technique (MTT). Cultures were initiated in 24-well plates at 5.0×10^4 cells per well. Following incubation with compounds prepared the same concentrations as described in measurement of cellular melanin content for 72 h, 50 μ L of MTT reagent (5 mg/mL of 3-[4,5-dimethyl-2-thiazolyl]-2,5-diphenyl-2H-tetrazolium bromide in PBS) was added to each well. The plates were incubated in a humidified atmosphere of 5% CO₂ at 37°C for 4 h. After the medium was removed, 1.0 mL of isopropyl alcohol (containing 0.04 N HCl) was added to each well, and a 150 μ L sample were withdrawn and transferred to a 96-well plate. Absorbance was measured at 590 nm by using a microplate reader. Each experiment was repeated twice. Cell viability was expressed as a percentage of the viability measured in control cells treated with solvent DMSO without sample materials.

4.2.6 Western blot analysis

B16 melanoma cells treated with the samples at 12.5–0 μ M for 72h were lysed with radioimmunoprecipitation assay (RIPA) buffer containing protease inhibitor cocktail at 0 °C for 30 min. Protein concentrations were determined using a Bradford protein assay kit (Thermo) and a BSA solution as a standard. Cell lysates were loaded at 10 μ g of protein per lane and separated by sodium dodecyl sulfate-polyacrylamide gel electrophoresis (SDS-PAGE) on 10% polyacrylamide gel. Proteins were subsequently transferred onto a polyvinylidene difluoride (PVDF) membrane (Millipore, Billerica, MA, USA) using a semi-dry transfer system (Atto) run at 150 mA for 30 min. The membrane was blocked with 2% BSA in tris-buffered saline Tween20 (TBST) at 4 °C overnight.

After washing, the membranes were incubated with dilutions of rabbit monoclonal anti-MITF (1: 1000), rabbit polyclonal anti-tyrosinase (1:200), rabbit polyclonal anti-TRP-1 (1:200), rabbit polyclonal anti-TRP-2 (1:100), rabbit polyclonal anti-p38 MAPK (1:100), or mouse monoclonal anti-p-p38 MAPK (1:200) antibodies. Following incubation for 2 h, the membranes were washed and incubated with 1:5000 diluted HRP-conjugated secondary antibody for 2 h. Following addition of the Luminata™ Forte (Millipore), protein density was visualized using enhanced chemiluminescence (ECL) detection system (LAS-3000, Fujifilm, Tokyo, Japan) and quantified using the Multi Gauge V3.0 quantification system (Fujifilm).

4.2.7 Statistical analysis

All data were expressed as means \pm S. D. values. Statistical significance of differences were evaluated using the Student's *t*-test.

4.3 Results and discussion

4.3.1 Melanogenesis activities of quercetin glycosides

The melanogenesis activities by adding the synthesized quercetin glycosides were determined with measuring intra and extracellular melanin content in B16 melanoma cells. The data for cell viability and the melanogenesis activity of B16 melanoma cells are shown in Table 4.1. As shown in Table 4.1, quercetin glycosides **1**, **3**,

and **4** showed intracellular melanogenesis stimulatory activity in a dose-dependent manner, and their activities were higher than that of theophylline used as positive control. These results are described in the previous published (Yamauchi, 2014a). Interestingly, the other quercetin glycosides had little or no melanogenesis stimulatory activity despite their structural similarities. The molecules with 7-*O*-glycoside showed no intracellular melanogenesis stimulatory activity. On the other hand, the molecules with 3-*O*-glucoside, with a free OH group on the B-ring, and the molecules with 3-*O*-cellobioside, with a free OH group or 4'-*O*-glucoside showed intracellular melanogenesis stimulatory activity. Thus, a hydroxyl group on C-7 may play an important role in melanogenesis activity. Additionally, the chemical structure of the sugar connected at the C-4' may also play an important role in the activity. Moreover, it should be noted that the opposite effect was reported that quercetin and quercetin-4'-*O*-glucoside which have the hydroxyl group at C-3 inhibited the melanin biosynthesis (Arung, 2011a). These result indicated that the hydroxyl group at C-3 of quercetin derivatives may be important to suppress the melaninogenesis activity, and the effect for melanin biosynthesis in B16 melanoma cells of quercetin glycosides are varied significantly by the presence or absence of hydroxyl group especially combing to C-3 or C-7 position. Furthermore, the activity may be more complex by the kind, size or polarity of the sugars connecting to the quercetin, therefore it is necessity the further investigations in order to elucidate completely the structure-activity relationships of quercetin glycosides.

The mushroom tyrosinase activities of the quercetin glycosides were also shown in Table 4.2. No stimulated activity of tyrosinase was observed in all of the quercetin glycosides synthesized in this study.

Tyrosinase is transcriptionally regulated by MITF. MITF expression is regulated by kinase pathways such as p38 MAPK, ERK, and JNK as described in Chapter 1.2. Some melanogenesis-enhancing agents have been examined by determining the expression levels of tyrosinase, p38, JNK, ERK, and MITF, as well as tyrosinase activity. Compounds **1**, **3**, and **4** may enhance the activity or expression of MITF by regulating the kinases described above since these compounds showed no tyrosinase stimulatory activities as shown in Table 4.2 but showed high intracellular melanogenesis stimulatory activity in B16 melanoma cells. Moreover, the structures of the synthesized quercetin glycosides could indicate that the hydroxyl group at C-7 may play an important role in intracellular melanogenesis acceleration activity. In future studies, the mechanism underlying the melanogenesis stimulatory activity of **1**, **3**, and **4** should be clarified by measuring tyrosinase and MITF expression in B16 melanoma cells.

Table 4.1 Intra and extracellular melanogenesis activity and cell viability in B16 melanoma cells by the synthesized quercetin glycosides.

	Cell viability and melanogenesis activity (%)		
	200µM	100µM	10µM
1			
Intercellular melanogenesis activity	190.5±10.2*	151.5±8.1*	137.0±0.8*
Extracellular melanogenesis activity	125.5±9.3	116.0±12.6	99.7±21.7
Cell viability	74.8±2.1	86.8±2.0	90.0±6.9
3			
Intercellular melanogenesis activity	206.9±2.3**	157.1±8.6*	116.3±1.3
Extracellular melanogenesis activity	86.1±2.7	85.1±1.7	91.0±4.1
Cell viability	68.4±6.9*	80.9±5.5	105±3.8
4			
Intercellular melanogenesis activity	176.0±9.1*	126.8±9.1*	102.6±2.9
Extracellular melanogenesis activity	85.2±4.9	91.0±6.3	83.3±5.8
Cell viability	81.1±3.0	93.2±0.6	99.6±1.5
5			
Intercellular melanogenesis activity	119.0±7.4	78.9±6.0	91.1±5.5
Extracellular melanogenesis activity	93.3±6.4	105.8±3.3	102.4±2.8
Cell viability	98.7±12.4	112.6±2.6	95.1±1.6
6			
Intercellular melanogenesis activity	99.7±1.8	84.77±2.1	79.7±4.2
Extracellular melanogenesis activity	80.9±3.8	92.3±2.7	91.2±2.0
Cell viability	99.7±1.8	106.0±8.3	106.8±3.4
7			
Intercellular melanogenesis activity	102.6±15.5	97.8±7.2	80.3±2.14
Extracellular melanogenesis activity	96.9±5.4	102.1±0.6	93.0±1.2
Cell viability	95.2±0.4	93.9±7.6	105.3±0.7
8			
Intercellular melanogenesis activity	92.6±0.0	90.4±15.1	89.7±11.9
Extracellular melanogenesis activity	103.2±11.7	95.0±2.3	100.0±3.5
Cell viability	77.4±10.4	104.1±3.5	107.3±6.5
9			
Intercellular melanogenesis activity	86.5±9.1	113.9±14.4	85.0±1.5
Extracellular melanogenesis activity	74.6±9.3	113.7±0.5	103.2±0.1
Cell viability	114.4±4.8	78.0±1.3	97.7±2.5
10			
Intercellular melanogenesis activity	96.3±0.9	90.9±13.3	96.8±7.6
Extracellular melanogenesis activity	87.3±12.6	95.1±5.8	99.9±3.8
Cell viability	105.6±6.4	107.0±2.6	97.8±8.9
11			
Intercellular melanogenesis activity	83.8±1.9	78.9±6.0	91.1±5.5
Extracellular melanogenesis activity	91.9±18.	90.1±2.1	104.5±7.1
Cell viability	111.0±9.6	112.6±2.6	95.1±1.6
Theophylline	500µM	250µM	125µM
Intercellular melanogenesis activity	166.8±31.7*	131.7±1.9	127.6±6.6
Extracellular melanogenesis activity	204±1.6**	183.2±3.2**	170.7±0.7**
Cell viability	91.4±1.3	94.4±4.1	95.5±11.0

Data are expressed as means ± S. D. (n=2). * $p \leq 0.05$ and ** $p \leq 0.01$ compared with respective control values.

Table 4.2 Mushroom tyrosinase activity by the synthesized quercetin glycosides.

	Substrates	Tyrosinase activity (%)		
		200 μ M	100 μ M	50 μ M
1	L-DOPA	101.1 \pm 7.6	103.2 \pm 1.9	100.6 \pm 2.4
	L-Tyrosine	106.4 \pm 1.3	95.9 \pm 6.2	104.7 \pm 2.1
3	L-DOPA	116.0 \pm 3.7	110.2 \pm 0.3	106.6 \pm 1.7
	L-Tyrosine	104.1 \pm 4.2	96.2 \pm 14.3	111.6 \pm 3.2
4	L-DOPA	111.8 \pm 6.0	107.1 \pm 2.5	103.0 \pm 3.0
	L-Tyrosine	82.2 \pm 6.0	95.0 \pm 2.0	97.5 \pm 0.5
5	L-DOPA	104.4 \pm 3.7	103.8 \pm 2.6	102.4 \pm 2.2
	L-Tyrosine	103.8 \pm 2.7	101.9 \pm 3.4	102.6 \pm 3.7
6	L-DOPA	107.6 \pm 0.8	103.4 \pm 4.5	107.2 \pm 11.2
	L-Tyrosine	97.6 \pm 2.6	95.0 \pm 1.0	100.4 \pm 2.7
7	L-DOPA	102.9 \pm 1.6	101.8 \pm 2.5	101.3 \pm 4.1
	L-Tyrosine	101.0 \pm 0.0	104.5 \pm 2.1	104.0 \pm 1.4
8	L-DOPA	99.3 \pm 3.4	99.3 \pm 2.8	101.5 \pm 4.2
	L-Tyrosine	94.3 \pm 10.2	98.8 \pm 3.9	101.2 \pm 0.4
9	L-DOPA	105.6 \pm 2.5	102.8 \pm 0.5	102.8 \pm 4.5
	L-Tyrosine	86.7 \pm 1.7	85.5 \pm 3.3	92.8 \pm 0.3
10	L-DOPA	108.7 \pm 0.3	104.84 \pm 1.0	103.0 \pm 0.8
	L-Tyrosine	82.4 \pm 0.0	85.2 \pm 0.3	88.9 \pm 2.6
11	L-DOPA	110.3 \pm 0.3	104.6 \pm 0.3	107.6 \pm 8.9
	L-Tyrosine	85.6 \pm 4.7	89.0 \pm 4.7	95.2 \pm 3.7

Data are mean \pm S.D

4.3.2 Melanogenesis activities of quercetin methyl ether

The melanogenesis-stimulating activities of synthesized quercetin derivatives were determined by measuring both intra- and extracellular melanin content in B16 melanoma cells. The effects of compounds **12–20** on cell viability and melanogenesis are shown in Table 4.3. We evaluated the modulation of intra and extracellular melanin levels by quercetin methylethers with theophylline as a positive control (Table 4.3). On measuring the melanogenesis activity assay for each compounds, we adopted a concentration which was not shown strong cytotoxicity of the B16 melanoma cells. As shown in Table 4.1, quercetin glycosides **1**, **3**, and **4** stimulated intracellular melanogenesis in a dose-dependent manner. However, none of the synthesized quercetin glycosides increased the extracellular levels of melanin. On the other hand, quercetin methylethers **12–15** increased both intra- and extracellular melanin content (Table 4.3), demonstrating higher melanogenesis-stimulation than theophylline, a positive control. Significant effects were observed on the extracellular melanin levels. Comparing the activities of compounds **12–15**, medium of cells incubated with 50 μM of compound **12** showed 224.9% higher extracellular melanin levels compared to controls. The increases of melanin levels following incubation with compounds **13–15** were higher than 220%, even at 6.25 μM , indicating the most potent stimulation of extracellular melanin levels in this study. Furthermore, the 3-hydroxyl quercetin methylethers such as **16–18**, 3-*O*-acetylquercetin (**19**), and quercetin-3-*O*- β -D-2,3,4,6-tetra-*O*-acetoglucoopylanoside (**20**) showed no stimulatory effect on the extracellular melanin levels, suggesting that the 3-methoxyl group of compounds **12–15** is an essential moiety for stimulation activity. Additionally the 4' and/or 7-methoxyl group may further increase the melanogenesis-stimulating activity. Compounds **13–15** showed more potent melanogenesis-stimulating activity

compared to **12**. Importantly, **13** and **14** were associated with high cell cytotoxicity in the cell viability studies, while **15** exhibited high cell viability. These differences in cell cytotoxicity between the quercetin methylethers may depend on the presence of both 4' and 7-methoxyl groups. These results are described in the previous published (Yamauchi, 2014b).

In order to understand the involvement of the tyrosinase enzyme in the stimulation of melanogenesis, the activity of mushroom tyrosinase was measured following incubation with quercetin derivatives. However, no effect on tyrosinase activity was observed with any of the quercetin derivatives synthesized in this study (data not shown). Therefore, the quercetin methylethers may contribute to the expression of tyrosinase or related genes in B16 melanoma cells.

Table 4.3 Intra and extracellular melanogenesis activity and cell viability in B16 melanoma cells by the synthesized quercetin derivatives **12-20**.

	Cell viability and melanogenesis activity (%)			
	50µM	25µM	12.5µM	6.25µM
12				
Intercellular melanogenesis activity	157.3±8.4*	146.5±15.3	137.0±23.6	-
Extracellular melanogenesis activity	224.9±18.2*	130.8±5.8*	124.1±1.4	-
Cell viability	74.4±3.8	88.1±4.1	98.2±6.7	-
13				
Intercellular melanogenesis activity	-	166.6±0.0**	178.8±9.6**	132.3±8.1*
Extracellular melanogenesis activity	-	346.7±2.9**	309.5±14.5**	229.5±17.6**
Cell viability	-	63.2±2.1**	50.0±0.5**	75.6±2.9**
14				
Intercellular melanogenesis activity	-	187.6±2.5**	171.2±0.0**	134.0±4.3*
Extracellular melanogenesis activity	-	265.5±5.9**	304.3±4.0**	222.8±12.8**
Cell viability	-	54.1±0.55**	60.4±4.2**	80.4±0.5**
15				
Intercellular melanogenesis activity	-	203.4±3.4**	181.4±9.0**	127.7±4.3*
Extracellular melanogenesis activity	-	298.7±3.7**	228.0±7.0**	225.5±10.8**
Cell viability	-	90.2±4.3	101.9±2.2	95.3±1.8
16				
Intercellular melanogenesis activity	-	106.9±7.1	133.5±4.4	125.6±5.7
Extracellular melanogenesis activity	-	97.9±0.0	95.1±0.2	97.5±2.2
Cell viability	-	100.9±1.3	103.0±4.3	103.6±3.6
17				
Intercellular melanogenesis activity	-	75.8±12.9	87.6±2.6	102.4±12.0
Extracellular melanogenesis activity	-	114.3±1.1	105.2±1.3	105.5±1.4
Cell viability	-	91.6±4.5	99.4±5.1	92.7±0.5
18				
Intercellular melanogenesis activity	-	100.5±10.0	106.1±8.1	110.2±2.5
Extracellular melanogenesis activity	-	100.1±0.3	98.0±0.0	100.5±0.5
Cell viability	-	101.3±3.7	101.4±1.9	99.7±1.2
19				
Intercellular melanogenesis activity	104.6±3.1	114.3±3.6	99.0±8.3	-
Extracellular melanogenesis activity	126.6±2.3	102.6±6.2	87.6±5.1	-
Cell viability	110.0±7.9	120.4±0.3	110.0±3.8	-
20				
Intercellular melanogenesis activity	148.4±1.4**	121.4±17.1	122.4±2.1	-
Extracellular melanogenesis activity	96.1±1.8	101.5±1.4	89.3±0.4	-
Cell viability	103.7±1.1	101.8±0.2	113.5±8.1	-
Theophylline	500µM	250µM	125µM	
Intercellular melanogenesis activity	166.8±31.7*	131.7±1.9	127.6±6.6	
Extracellular melanogenesis activity	204±1.6**	183.2±3.2**	170.7±0.7**	
Cell viability	91.4±1.3	94.4±4.1	95.5±11.0	

Data are expressed as means ± S. D. (n=2). * $p \leq 0.05$ and ** $p \leq 0.01$ compared with respective control values. -: not done.

4.3.3. Effect of compounds **12** and **15** on the expression of proteins involved in melanin biosynthesis

In general, the signaling pathway modulating the expression of melanogenic enzymes in melanoma cells comprises the following steps. First, extracellular messengers, such as α -MSH and histamine, interact with receptors on the melanocyte. Receptor stimulation increases intracellular cAMP levels in the melanocyte, stimulating a number of intracellular kinase pathways, such as the p38 MAPK, ERK, and JNK. These kinase signaling cascades regulate the expression of MITF, which acts as a transcriptional factor regulating the expression of tyrosinase, TRP-1, and TRP-2 (Chapter 1.2).

Some studies have reported that melanogenesis-modulating agents regulate the expression of tyrosinase, TRP-1, and TRP-2 by regulating the expression of p38 MAPK, ERK, JNK, and MITF. For example, the components isolated from *Nardostachys chinensis* and *Rhodiola rosea* crude extracts were reported to inhibit melanin biosynthesis by suppressing the expression of MITF and tyrosinase in B16 melanoma cells (Chiang, 2014 and Jang, 2011). Similarly, the compounds showing melanogenesis-stimulating activity in this study may also control the levels of tyrosinase and the proteins that modulate its expression, as suggested by the observation that the stimulatory activity does not depend on the tyrosinase activity.

As presented in Table 4.3, compound **15** showed significant intra- and extracellular melanogenesis-stimulating activity, with low cytotoxicity. The effects of compound **15** on the expressions of proteins related to melanin biosynthesis, such as tyrosinase, TRP-1, TRP-2, MITF, p-p38 MAPK, and p38 MAPK were investigated in order to identify the specific biosynthetic step associated with its activity. As shown in Fig.4.2C and D, **15**

increased the expression of tyrosinase, TRP-1, TRP-2, MITF, and p-p38 MAPK in a dose dependent manner in B16 melanoma cells. Conversely, the expression of p38 MAPK was not increased by **15**, indicating that it stimulates melanin biosynthesis by stimulating the p38 MAPK phosphorylation. Furthermore, the melanogenesis-stimulating effects of **12** were determined in order to compare the activity on the expression of the proteins. Comparing the activities of **12** and **15** on the expression of proteins related to melanin biosynthesis, **12** was found to increase the expression ratio of the tyrosinase and TRP-1 to a greater extent than **15** (Fig.4.2B and D). Nevertheless, extracellular melanogenesis-stimulating activity of **12** was lower than that of **15** (Table 4.3), suggesting that melanogenesis in melanoma cells is not solely dependent on the expression of tyrosinase and TRP-1. Furthermore, **15** significantly stimulated the expression of MITF and p-p38 MAPK, which enhance the expression of tyrosinase, TRP-1, and TRP-2. Conversely, **12** did not alter the expression of MITF and p-p38 MAPK, despite enhancing the expression of tyrosinase, TRP-1, and TRP-2. Except for MITF, no transcriptional factors controlling tyrosinase expression have been reported thus far. These results may therefore indicate that **12** enhances the expression of tyrosinase, TRP-1, and TRP-2 by stimulating transcriptional factors that are yet to be identified. The levels of melanogenic enzymes in the melanocyte are also regulated by protein degradation by proteasome through ubiquitination (Bellei, 2010). Fatty acids, a major component of the cell membranes, were previously reported to regulate melanin biosynthesis by controlling the degradation of tyrosinase, TRP-1, and TRP-2 (Ando, 2004). Therefore, in addition to the possible effect on a transcriptional factor, an alternative explanation for the enhancing activity of **12** on the levels of melanogenic enzymes may involve the inhibition of the degradation of melanogenic enzymes through ubiquitination. Compared to **15**, **12** increased the expression

of melanogenic enzymes, but showed less melanogenesis-stimulating activity, as described above. Additionally, the levels of p-p38 MAPK and MITF were not increased by the addition of **12**. If the two phenomena were related to each other, MITF and/or p-p38 MAPK may play an important role in the regulation of melanogenesis not only by enhancing the expressions of the enzymes, but also through affecting other factors, such as the transportation and/or degradation of melanogenic enzymes. These results and discussions are described in the previous published (Yamauchi, 2014b).

Tyrosinase, TRP-1, and TRP-2 are expressed through a MITF-regulated process and transported to the melanosome. Melanin is biosynthesized in the melanosome by the action of the melanogenic enzymes. The mature melanosome is specifically transported to the periphery of the cell from the perinuclear region of the melanocytes through a process that involves a wide variety of cellular transport proteins, including actin, myosin Va, Rab27A, and Slac2-a (Chapter 1.3). Compound **15** may accelerate the transportation of melanogenic enzymes to the melanosome and/or transportation of melanosome to the outside of the cells by regulating the expression of proteins related to cellular transport. However, **12** may elicit less potent stimulation of the transportation of melanogenic enzymes to the melanosome and/or the transportation of melanosome as compared to **15**.

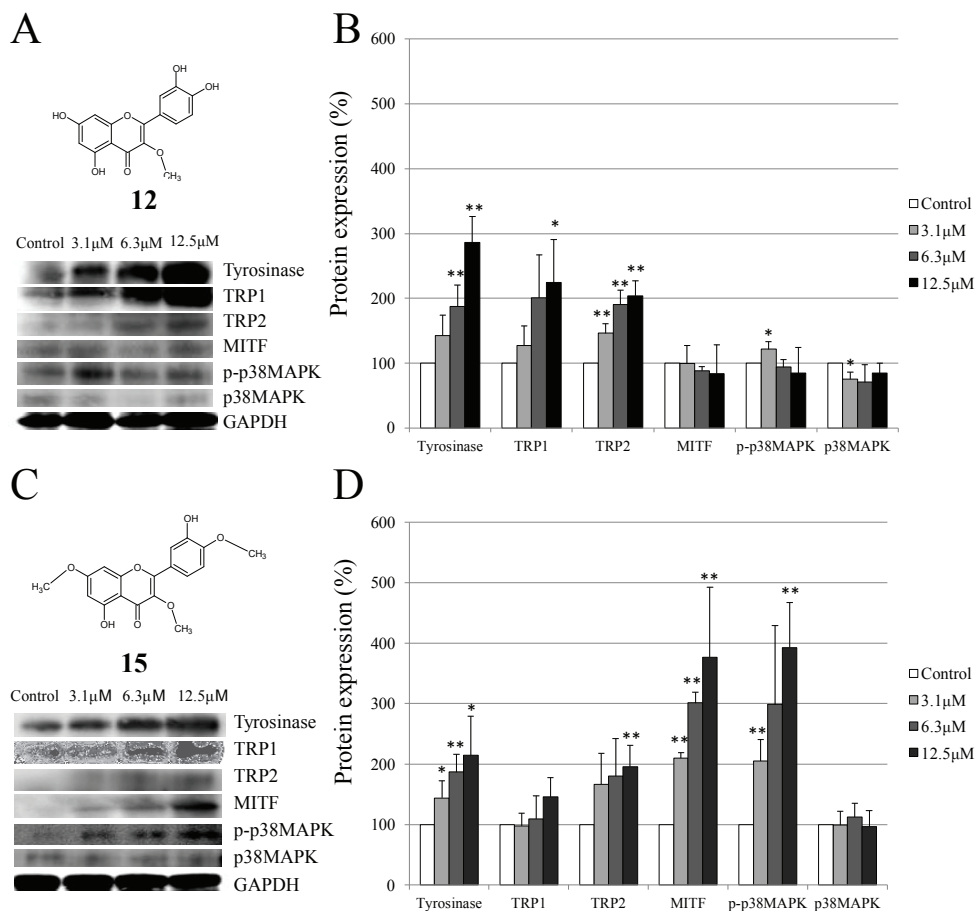
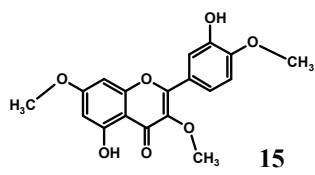


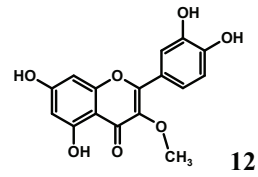
Fig.4.2 Effect of **12** and **15** on the expression of Tyrosinase, TRP1, TRP2, MITF, p-p38MAPK, and p38MAPK in B16 melanoma cells. (A) Representative blots of **12**. (B) Quantification of the ratio of protein expressions in melanoma cells treated by **12**. The data show the means \pm S.D. from three independent experiments. (C) Representative blots of **15**. (D) Quantification of the ratio of protein expressions in melanoma cells treated by **15**. The data show the means \pm S.D. from three independent experiments. * $p \leq 0.05$ and ** $p \leq 0.01$ compared with control values.

4.4 Summary

Among the nineteen synthesized compounds, **1**, **3**, and **4** which are quercetin glycosides exhibiting intracellular melanogenesis stimulatory activity. While they showed no effect on extracellular melanogenesis. On the other hand, **12** and **15** increased both intra and extracellular melanin contents more potently than the positive control theophylline, with exhibiting low cytotoxicity. Compound **12** exhibited less melanogenesis-stimulating activity than compound **15**. However, **12** increased the expression of tyrosinase and TRP-1 to a greater extent than **15**, thereby suggesting that melanogenesis in melanoma cells does not depend solely on the expression of the enzymes catalyzing melanin biosynthesis. Furthermore, **15** also stimulated the expression of the MITF and p-p38 MAPK, while they were not increased by **12** (Fig.4.3). These results suggest that **12** may enhance the expression of tyrosinase and TRP-1 by regulating the proteasomal degradation of melanogenic enzymes and/or by activating other transcriptional factors regulating enzyme expression.



Stimulate melanogenesis by enhancing of MITF and p-p38



Stimulate melanogenesis without enhancing of MITF and p-p38

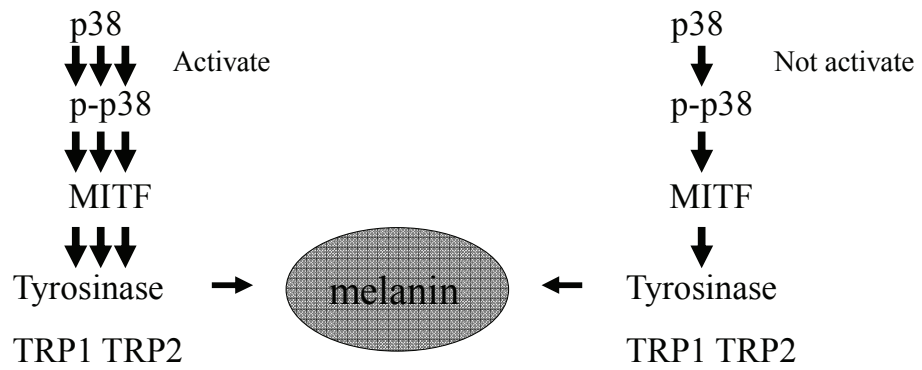


Fig.4.3 Effects of compound **12** and **15** on expression of melanogenic enzymes

Chapter 5

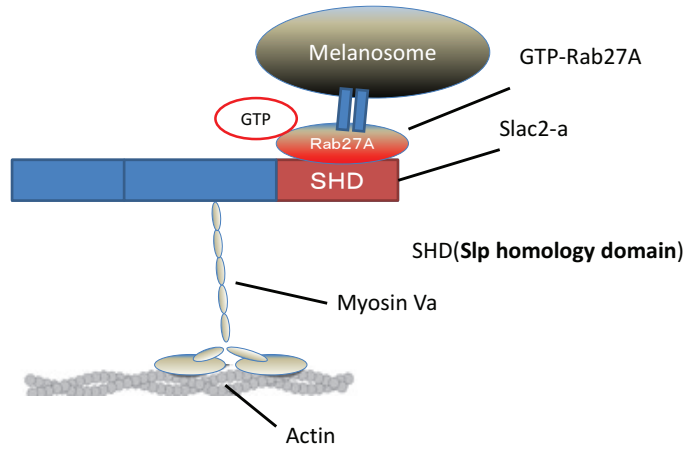
Quercetin derivatives regulate transportation of melanosome *via* EPI64

5.1 Introduction

Two novel quercetin glucosides namely 4'-*O*- β -D-glucopyranosyl-quercetin-3-*O*- β -D-glucopyranosyl-(1 \rightarrow 4)- β -D-glucopyranoside (**1**) and 4'-*O*- β -D-glucopyranosyl-(1 \rightarrow 2)- β -D-glucopyranosyl-quercetin-3-*O*- β -D-glucopyranosyl-(1 \rightarrow 4)- β -D-glucopyranoside (**2**) were isolated from *H. zeylanica* root 50% EtOH extract which is described in Chapter 2 (Yamauchi, 2013). Compound **1** exhibited intracellular melanogenesis stimulatory activity, while **2** showed no effect even the structural similarity of the two compounds. This result indicates the involvement of the substituent group attached quercetin on melanogenesis. In order to understand the structure-activity relationships of quercetin derivatives, nineteen quercetin derivatives were synthesized from rutin in Chapter 3 (Yamauchi, 2014a and 2014b). As the result of bioassay using synthesized nineteen quercetin derivatives in B16 melanoma cells, **1**, **3**, and **4**, the quercetin glycosides, stimulates the intracellular melanogenesis, while they elicits no stimulatory activity on extracellular melanogenesis. On the other hand, the quercetin methyl ether, **12** and **15** increase the both intra and extracellular melanin contents with no cytotoxicity (Chapter 4) (Yamauchi, 2014a and 2014b). This results suggests that **12** and **15** may stimulate the transportation of melanosomes in B16 melanoma cells. In this Chapter, the effects of **12** and **15** on the transportation of melanosomes in B16 melanomacells were investigated *via* focusing on the elongation effect of the cells and expression of EPI64, a suppressor of actin transportation by inactivating the Rab27A on melanosomes.

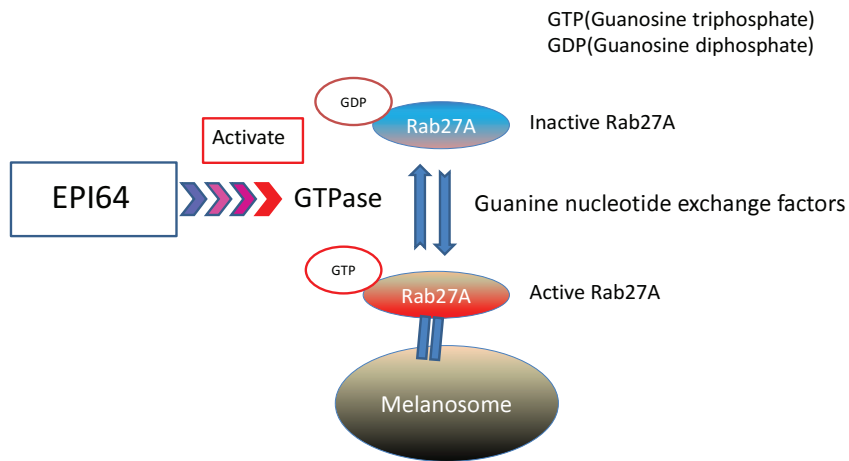
The dendrite elongation of melanocyte, involved in the transportation of melalnogenic enzymes and melanosomes (Tamura, 2009 and Ohbayashi, 2012b), plays an important role to transfer melanosomes to the keratinocytes or hair matrix cells.

Melanosome transportation is composed of microtubule and actin transportation. Rab1A on the melanosome is involved in the anterograde microtubule transportation (Ishi, 2012) and Mreg localized on the mature melanosome relates to retrogradely transportation of melanosomes on microtubule (Ohbayashi, 2012a) (Chapter 1.3.1). Besides Rab27A on the melanosomes acts to compose the transportation complex with Slac2-a and myosin Va (Fig.5.1). The GTP-bound active Rab27A is localized on the melanosome which elicits actin transportation. The EPI64 inactivates the Rab27A and the inactive Rab27A is excluded from the surface of melanosome (Fig.5.2). In order to understand the effect of **12** and **15** on the transportation of melanosomes, the shapes as well as the contents of EPI64 of the B16 melanoma cells treated with quercetin derivatives were determined. Furthermore the distribution of Rab27A and melanosomes in B16 melanoma cells were examined by immunofluorescence microscopy to support the results on EPI64 contents.



Fukuda M. et al., 2002, Journal of Biological chemistry, 277, 12432-12436.
 Itoh. et al., 2006, Journal of Biological chemistry, 281, 31823-31831.

Fig.5.1 Complex for actin transportation



Itoh. et al., Journal of Biological chemistry, 2006; 281: 31823-31831

Fig.5.2 Active/inactive switch of Rab27A on melanosomes. Rab27A is inactivated by EPI64 and activated by guanine nucleotide exchange factors.

5.2 Material and methods

5.2.1 General

Bovine serum albumin (BSA) was purchased from Sigma-Aldrich (St. Louis, MO, USA). Antibodies against tyrosinase (H-109), EBP50-PDZ interactor of 64kDa (EPI64) (M-120), and Rab27A (H-60) were purchased from Santa Cruz Bio technology (Santa Cruz, CA, USA). Horseradish peroxidase (HRP)-conjugated anti-rabbit IgG donkey antibody (NA934) were purchased from GE Healthcare (Piscataway, NJ, USA), while glyceraldehyde-3-phosphate dehydrogenase (GAPDH)-specific antibody (GTX100118) were purchased from GeneTex (Irvine, CA, USA). Goat anti-rabbit IgG antibody (Alexa Fluor®594) and 4',6-diamidino-2-phenylindole dihydrochloride (DAPI) (p36941) was purchased from Life technologies (Grand Island, NY, USA). Radioimmunoprecipitation assay (RIPA) buffer (ab156034) and protease inhibitors cocktail (539134) were purchased from Abcam (Cambridge, MA, USA) and Merck Millipore (Billerica, MA, USA). Other commercially available products were purchased from Wako Chemicals (Richmond, VA, USA).

5.2.2 Cell culture

The manner of cell culture is described in Chapter 4.2.3. Murine melanoma B16-F0 cells (DS Pharma Biomedical, Osaka, Japan) were grown in Dulbecco's modified Eagle medium (DMEM) supplemented with 10% fetal bovine serum, 100,000 unit/L penicillin, and 100 mg/L streptomycin. Cells were cultured at 37°C in humidified atmosphere of 5% CO₂.

5.2.3 Observation of cell shapes

Briefly, confluent cultures of B16 melanoma cells were rinsed in phosphate-buffered saline (PBS) and removed using 0.25% trypsin/EDTA. The cells were loaded into a 24-well plate (5.0×10^3 cells / well) and allowed to adhere at 37 °C for 24 h. Sample compounds prepared at 200–25 μM for **1** and 25–3.125 μM for **2** and **3** were added and the cells incubated for 72 h. The cell shapes treated with the samples for 42h and 72h were examined by using microscope (Olympus, DP20-5). The average of cells length were compared with control cells treated with DMSO without sample materials.

5.2.4 Western blot analysis

Western blot analysis was performed according to a previously described method²⁶. B16 melanoma cells treated with the samples at 12.5–0 μM for 72h were lysed with radioimmunoprecipitation assay (RIPA) buffer containing protease inhibitor cocktail at 0 °C for 30 min. Protein concentrations were determined using a Bradford protein assay kit (Thermo) and a BSA solution as a standard. Cell lysates were loaded at 10 μg of protein per lane and separated by sodium dodecyl sulfate-polyacrylamide gel electrophoresis (SDS-PAGE) on 10% polyacrylamide gel. Proteins were subsequently transferred onto a polyvinylidene difluoride (PVDF) membrane (Millipore, Billerica, MA, USA) using a semi-dry transfer system (Atto) run at 150 mA for 30 min. The membrane was blocked with 2% BSA in tris-buffered saline Tween20 (TBST) at 4 °C overnight. After washing, the membranes were incubated with dilutions of rabbit polyclonal anti-

GAPDH (1:5000), rabbit polyclonal anti-tyrosinase (1:200) or rabbit polyclonal anti-EPI64 (1:200) antibodies. Following incubation for 2 h, the membranes were washed and incubated with 1:5000 diluted HRP-conjugated secondary antibody for 2 h. Following addition of the Luminata™ Forte (Millipore), protein density was visualized using enhanced chemiluminescence (ECL) detection system (LAS-3000, Fujifilm, Tokyo, Japan) and quantified using the Multi Gauge V3.0 quantification system (Fujifilm).

5.2.5 Immunofluorescence Microscopy

B16 melanoma cells solution (20 μ L) were loaded on 24-well glass slide at 1.0×10^4 cells/ml allowed to adhere at 37 °C for 24 h. After 24h, the medium was replaced with 20 μ L medium containing 0.2% DMSO and samples at 100 μ M for **1** and 25 μ M for **2** and **3**. The cells were incubated for an additional 72h. Following removed the medium, cells were washed with PBS and fixed in 4% paraformaldehyde for 20 min at 4 °C. After washing with PBS, the cells were made permeable by treatment with 10 μ L MeOH at 4 °C for 2min. Cells were blocked with 20 μ L 2% BSA/PBS solution for 1h at room temperature, and washed with PBS five times. The cells were then incubated with a rabbit polyclonal Rab27A antibody (1:50) in PBS containing 2% BSA for 1h at room temperature. After five washes in PBS, the polyclonal antibody was reacted with goat anti-rabbit IgG labeled Alexa®594 dye (1:1000) in PBS containing 2% BSA for 1h at room temperature. After five further washes in PBS, the nuclear was stained with DAPI. All preparations were examined with a confocal microscope (LSM710 ZEISS).

5.2.6 Statistical analysis

Data were expressed as means \pm S. D. values. Statistical significance of differences were evaluated using the Student's *t*-test.

5.3 Results and discussion

5.3.1 Effects on cell shapes treated with **1**, **12**, and **15**

As shown in Fig.5.3-5 the effects on cell shapes treated with **1**, **12**, and **15** for 42h and 72h were examined by microscopy, and the ratio of cell length was shown in Fig.5.6 On measuring the melanogenesis activity assay for each compounds, we adopted a concentration which was not shown strong cytotoxicity of the B16 melanoma cells as shown in Chapter 4. The shapes of cells treated with **1** exhibited no dendrite elongation effect at 200-25 μ M (Fig.5.6C). On the other hand, **12** and **15** elongated the dendrite in a dose dependent manner (Fig.5.6 A and B). The elongations took place for the 48h treatment with **12** or **15**, and the ratio of cell length was not increased by the further 24h treatment (total 72h treatment). Comparing the activity of **12** and **15**, the ratio of cell length treated at 25 μ M was approximately 200% that are the almost the same effect on **12** and **15**. On the 12.5-3.125 μ M, **15** elongated cell shape more potently than **12**. Our previous paper indicates that **15** increases the extracellular melanin contents much more than **12**, then the elongation effect may relate to the extracellular melanogenesis stimulatory activity and/or transportation of melanosome. Recently many proteins, involved in the transportation of melanosome, have been identified, and Slp2-a is reported to relate to the cell shapes (Kuroda and Fukuda, 2004). Slp2-a also reported to interact

with Rab27A on the periphery of the cell and capable to interact with plasma membrane to transfer melanosome to the keratinocytes or hair matrix cells (Fukuda, 2005 and 2006). **12** and **15** may be involved in the expression or the activity of Slp2-a and may stimulate the transportation of melanosome to the plasma membrane *via* the effect of Slp2-a. Furthermore, the function of vacuolar protein sorting 9 (VPS9)–ankyrin-repeat protein (Varp), a Rab21, Rab32, and Rab38 effector, have been reported to stimulate the transportation of melanogenic enzyme and elongation of dendrite in melanocyte (Tamura, 2009, 2011 and Ohbayashi, 2012). Melanogenic enzymes, tyrosinase, TRP-1, and TRP-2, are synthesized and transported to the melanosome, and melanin is biosynthesized by the melanogenic enzymes in melanosome. The transportation of melanogenic enzyme to the melanosome is elicited by Rab32/38 binding Varp, and the dendrite elongation is occurred in melanocyte by Rab21 binding Varp (Fig.5.7). Then Varp regulates the melanogenesis by controlling the two essential points in melanocyte. In our previous report, **12** stimulates expression of tyrosinase, TRP-1, and TRP-2 more potently than **15** even though **12** elicits less potent extracellular melanogenesis activity than **15**. This phenomenon may relate to the transportation of melanogenic enzymes to the melanosomes by Rab32/38 binding Varp. Additionally the dendrite elongation activity of **12** was less potent than **15**. This phenomenon may be elicited by the regulation of expression and/or activity of Rab21 binding Varp, hence **15** may contribute to stimulate the expression and/or activity of Varp more potently than **12**. Considering the stimulatory activity of **15** on expressions of p-p38 MAPK and MITF which is not exhibited on **12** (Chapter 4), p-p38 MAPK or MITF may stimulate the Varp contents in B16 melanoma cells. However it is needed to more experiments to understand completely the phenomenon caused by **12** and **15**.

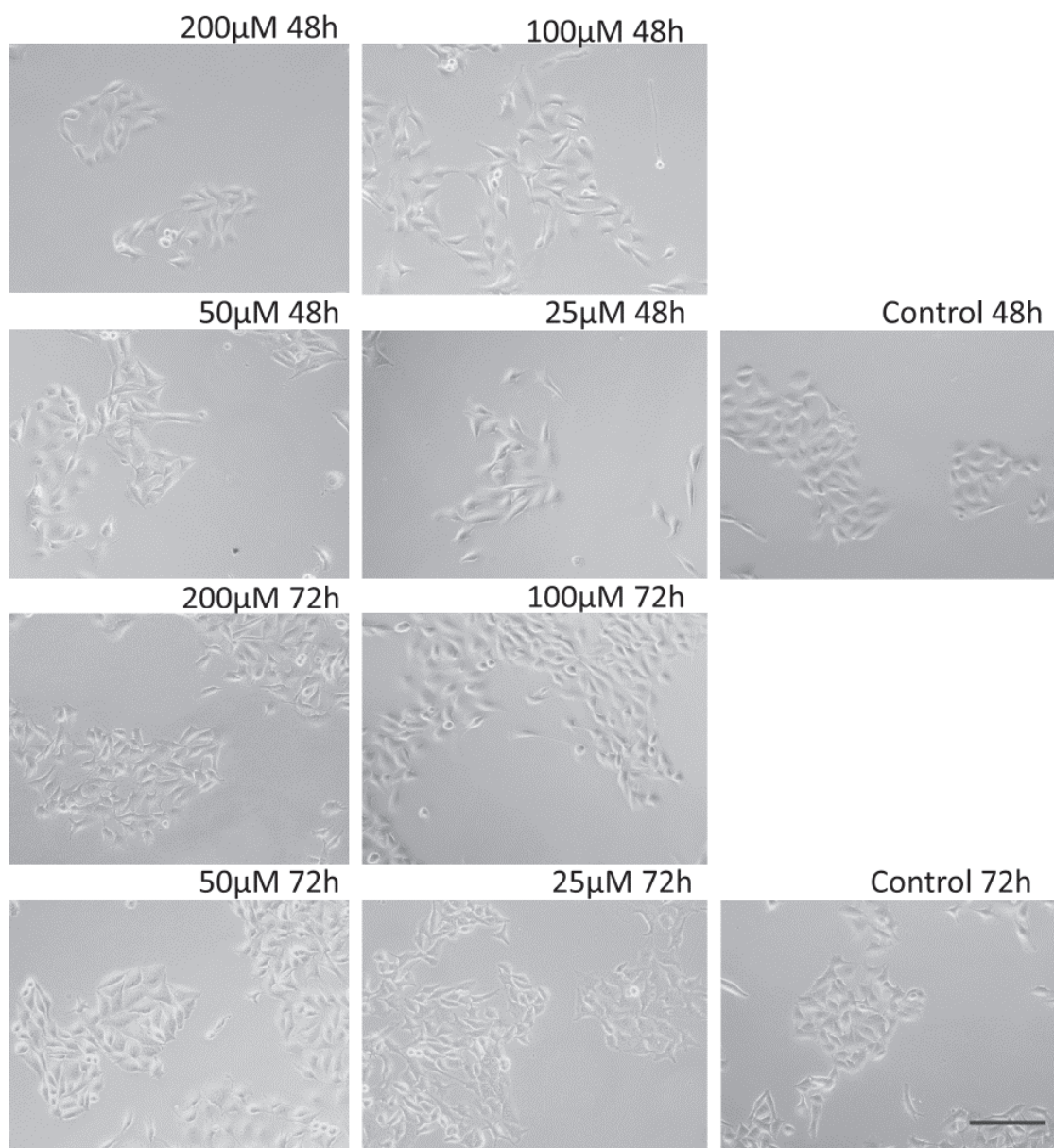


Fig.5.3 Cell shapes treated with **1** at 200-0µM for 42h or 72h. Scale bar shows 100µm.

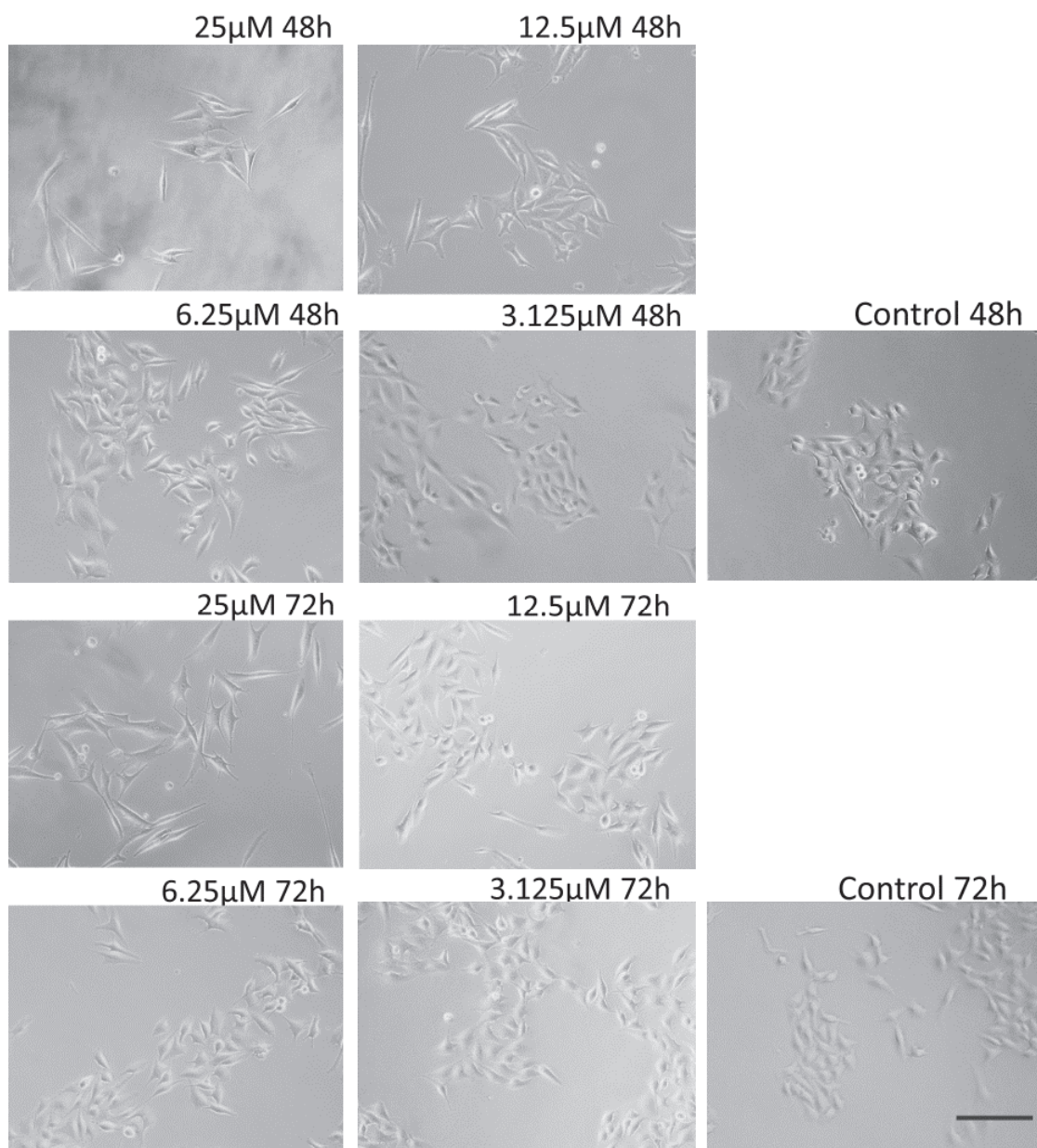


Fig.5.4 Cell shapes treated with **12** at 25-0µM for 42h or 72h. Scale bar shows 100µm.

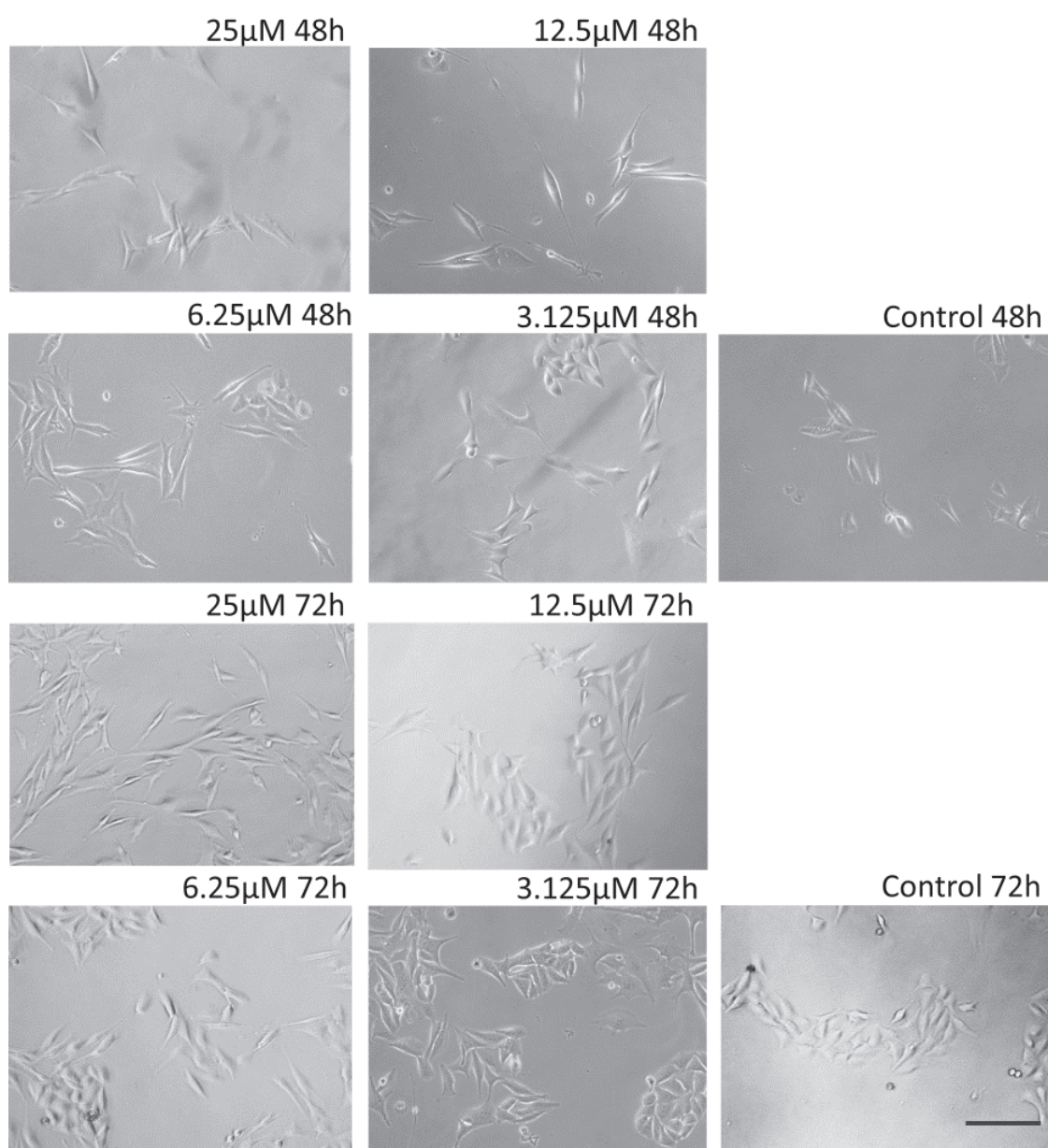


Fig.5.5 Cell shapes treated with **15** at 25-0µM for 42h or 72h. Scale bar shows 100µm.

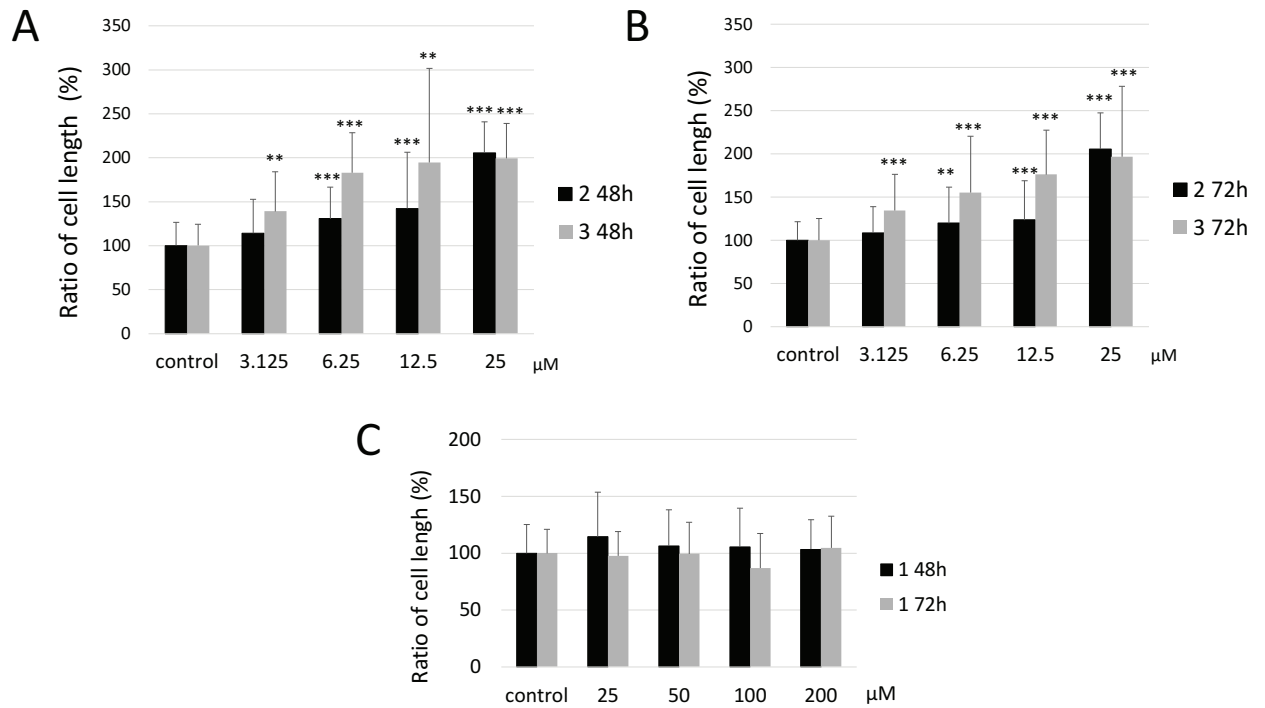
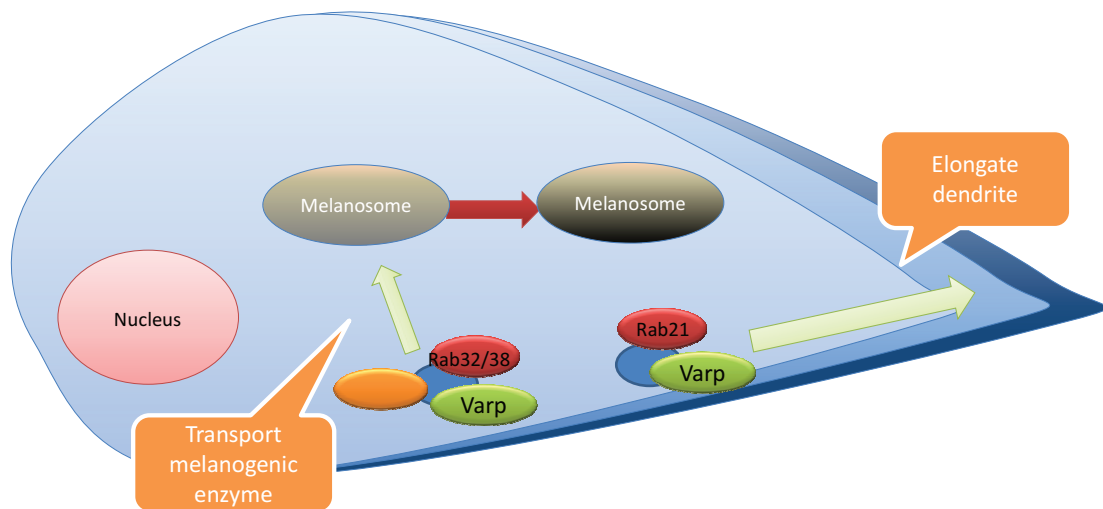


Fig.5.6 Ratio of cell length. A: Ratio of cell length treated with **12** or **15** for 48h. B: Ratio of cell length treated with **12** or **15** for 72h. C: Ratio of cell length treated with **1** for 48h and 72h. Data are expressed as means \pm S. D. against the ratio of cells length in Fig.5.3-5.5. ** $p \leq 0.01$ and *** $p \leq 0.001$ compared with respective control values.



Tamura K. et al., 2009, *Mol. Biol. Cell.* 20, 2900-2908.
 Ohbayashi N. et al., 2012, *Mol. Biol. Cell.* 23, 669-678.

Fig.5.7 Effect of Varp on melanogenesis in melanocyte. The transportation of melanogenic enzyme to the melanosome is elicited by Rab32/38 binding Varp, and the dendrite elongation is occurred in melanocyte by Rab21 binding Varp.

5.3.2 Effects of **1**, **12**, and **15** on transportation of melanosome

Mature melanosomes in melanocytes are specifically transported by transporter proteins through the microtubule and actin transportation. Activated Rab27A is localized on melanosome and interacted with its effectors, Slac2-a and Slp2-a (Kuroda and Fukuda, 2004 and Fukuda, 2005). Slac2-a is also interacted with myosin Va, a motor protein, and the melanosome/Rab27A/Slac2-a complex is transported to the periphery of the cell from the perinuclear region by the myosin Va on the actin cable (Fukuda, 2002, Wu, 2001, Kuroda, 2003, and Ito, 2006) (Chapter 1.3.2). Rab27A occurs in a guanosine triphosphate (GTP)-bound active state and a guanosine diphosphate (GDP)-bound inactive state. The active Rab27A is localized on the surface of melanosome to transport by interacting with Slac 2-a and myosin Va, while inactivate Rab27A is released from the surface of melanosome. Then the active and inactive cycling of Rab27A plays an essential role to regulate the melanosome transportation. Guanine nucleotide exchange factors deprives the GDP and stimulates GTP loading to Rab27a. Conversely EPI64, a GTPase-activating protein of Rab27A, promotes the GDP-bounding and inactivates Rab27A (Itoh and Fukuda, 2006). Compounds **12** and **15** were reported as potent extracellular melanogenesis stimulator described in Chapter 4, suggesting **12** and **15** stimulate the transportation of melanosome in B16 melanoma cells. In order to demonstrate the hypothesis, the expression of EPI64 in B16 melanoma cells treated with **12** and **15** was determined. Compound **1** was used as comparison target since it showed no stimulatory activity on extracellular melanogenesis even though it increases the intracellular melanin content in previous. As shown in Fig.5.8C and E, the expression of EPI64 was decreased by treating with **12** and **15**. Compound **12** significantly decreased the expression ratio of EPI64, 57% and 49% at 6.25 μ M and 12.5 μ M respectively, while the significant difference

was not shown at 3.125 μ M (Fig.5.7 D). Compound **15** also decreased the expression of EPI64 in a dose dependent manner. Compound **15** exhibited significant decrease on EPI64 expression even at 3.125 μ M (Fig.5.7 F). The IC₅₀ values which shows the concentrations of the samples exhibiting 50% inhibition were 11.0 μ M and 9.4 μ M by treating with **12** and **15** respectively. These result indicated that the inhibitory activity on EPI64 expression of **15** was more potently than **12**. The inhibition activates Rab27A and stimulate transportation of melanosomes (Fig.5.11). The EPI64 expression inhibitory activity of **12** and **15** supports the result that extracellular melanogenesis stimulatory activity of **15** was stronger than **12**. In case of **1**, the ratio of EPI64 expression was 170%, 262%, and 290% at 25 μ M, 50 μ M, and 100 μ M respectively (Fig.5.8 B), suggesting that **1** stimulates the inactivation of Rab27A and inhibits the transportation of melanosomes. This may result in the intracellular melanogenesis stimulatory activity of **1** (Fig.5.10).

Activated Rab27A is localized on the surface of melanosome and excess expression of EPI64 induces exclusion of Rab27A on melanosomes (Itoh, 2006). In order to confirm the colocalization of Rab27A and melanosomes in the cells treated with **12** or **15**, the distributions of melanosomes and Rab27A in melanoma cells were examined by immunofluorescence microscopy. Fig.5.9 shows the distribution of Rab27A (red stain) and melanosomes (shown by arrows) in melanoma cells. The Rab27A is ubiquitously distributed regardless the distribution of the melanosomes in the cells treated with **1** and control cells (Fig.5.9 A and B). On the other hand, **12** and **15** elicited the colocalization of Rab27A (shown by arrowheads) and melanosomes (Fig.5.9 C and D), indicating that Rab27A was activated and existed on the melanosomes by inhibiting the expression of EPI64. This colocalization between Rab27A and melanosomes supports the result on the inhibitory activity of EPI64 expression after treatment with **12** and **15**.

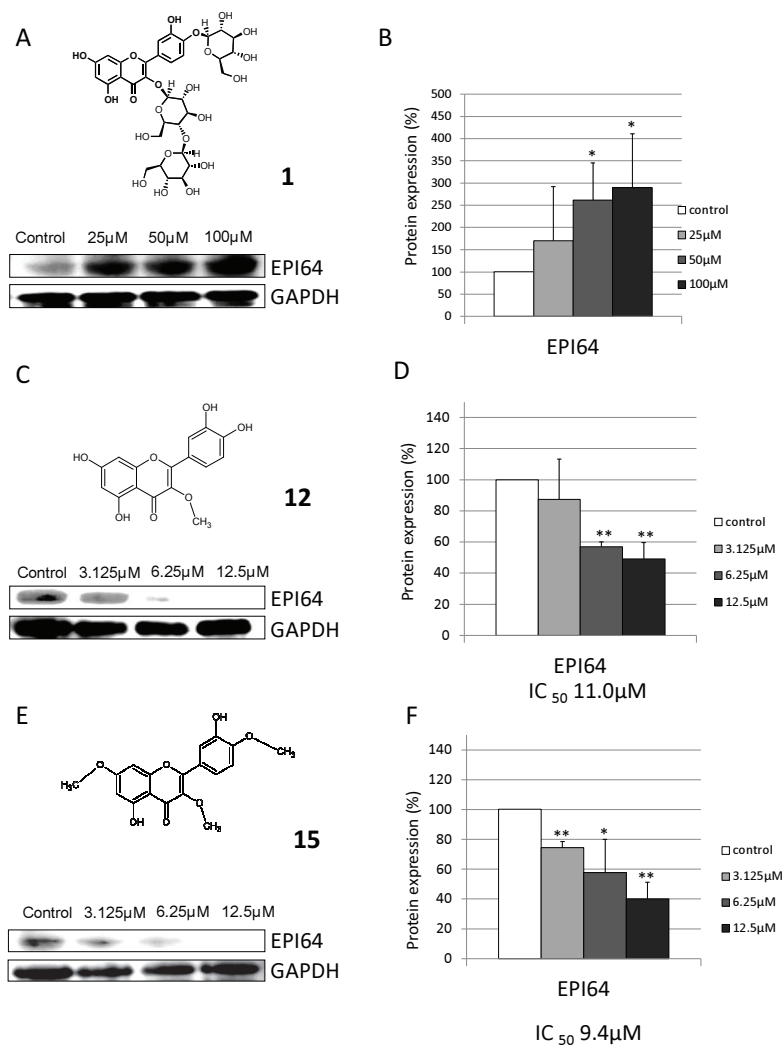


Fig.5.8 Effect of **1**, **12**, and **15** on the expression of EPI64 in B16 melanoma cells. (A) Representative blots of **1**. (B) Quantification of the ratio of protein expressions in melanoma cells treated by **1**. The data show the means \pm S.D. against the ratio of EPI 64 expression from three independent experiments. (C) Representative blots of **12**. (D) Quantification of the ratio of protein expressions in melanoma cells treated by **12**. Data are expressed as means \pm S. D. against the ratio of EPI64 expression from three independent experiments. (E) Representative blots of **15**. (F) Quantification of the ratio of protein expressions in melanoma cells treated by **15**. The data show the means \pm S.D. against the ratio of EPI 64 expression from three independent experiments. * $p \leq 0.05$ and ** $p \leq 0.01$ compared with control value.

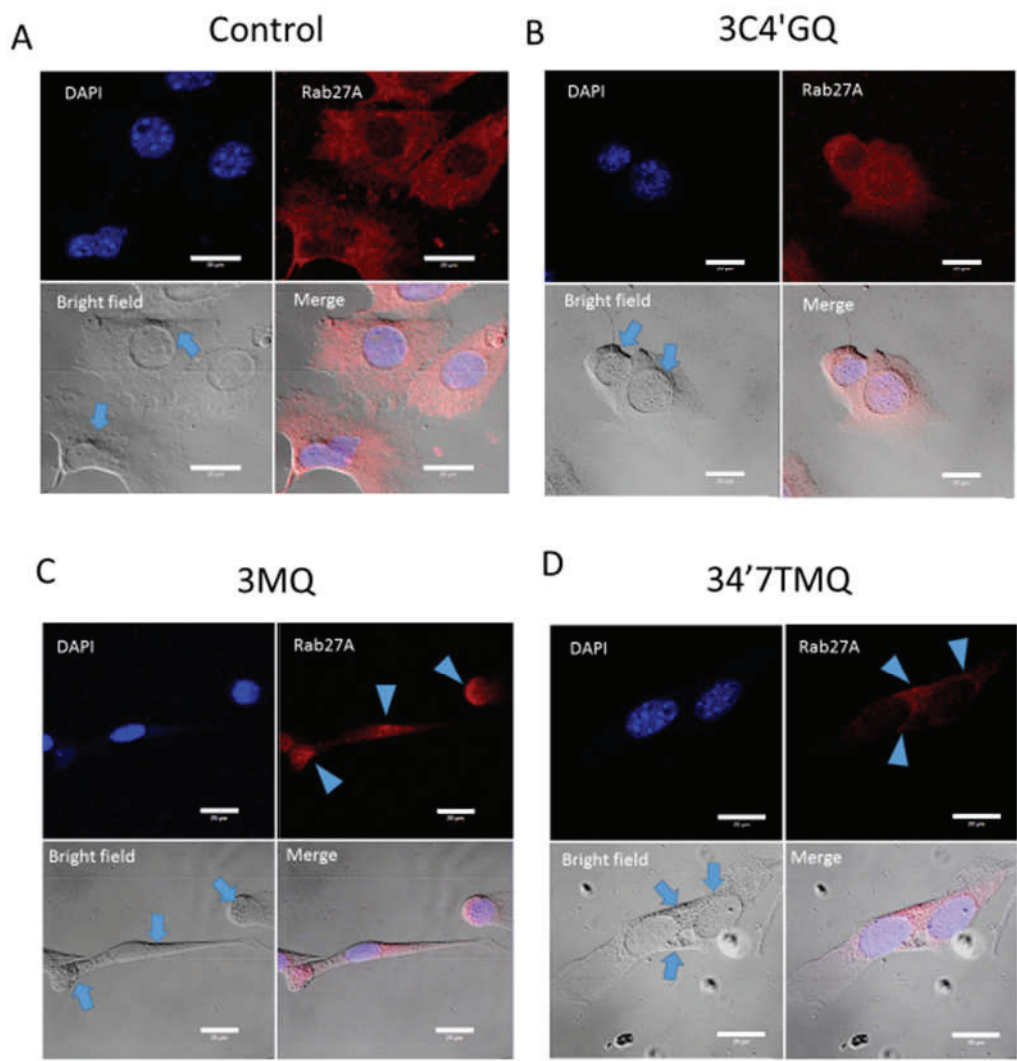


Fig.5.9 Immunofluorescence confocal microscopy showing the distribution of Rab27A and melanosomes. Cells were treated with **1** (100 μ M) (B), **12** (25 μ M) (C), and **15** (25 μ M) (D) for 72h. Cells were stained with Rab27A antibody (red) and DAPI (blue). Arrowheads point the localization of Rab27A. Arrows point the melanosomes in the cells. Scale bar shows 20 μ m.

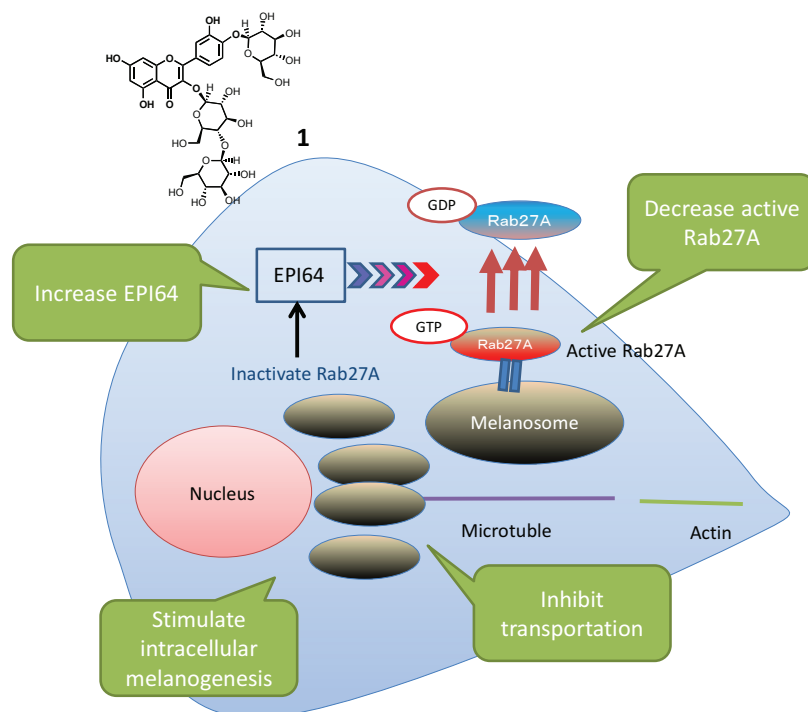


Fig.5.10 Effect of **1** on transportation of melanosome. **1** inhibits transportation of melanosomes and increases intracellular melanin contents *via* stimulation of EPI64 expression.

5.4 Summary

Compound **1** was isolated from *Helminthostachys zeylanica* root extract and synthesized as an intracellular melanogenesis stimulation compound. Synthesized **12** and **15**, quercetin methyl ethers, increased extracellular melanin content more potently than the positive control. The formation of dendrite and the expression of EPI64 that inactivates the melanin transportation were investigated using B16 melanoma cells treated with **1**, **12**, or **15** in order to understand the mechanism underlying the observed activity. Compound **1** that increases intracellular melanin contents increased the expression of EPI64 and exhibited no dendrite elongating activity, suggesting **1** inhibits the transportation of melanosome which may results in the intracellular melanogenesis stimulatory activity. Compound **12** and **15** that increases extracellular melanin contents inhibited the expression of EPI64 and elongated the dendrite, suggesting **12** and **15** stimulate the transportation of melanosome.

Conclusions

Two novel quercetin glycosides namely 4'-*O*- β -D-glucopyranosyl-quercetin-3-*O*- β -D-glucopyranosyl-(1 \rightarrow 4)- β -D-glucopyranoside (**1**) and 4'-*O*- β -D-glucopyranosyl-(1 \rightarrow 2)- β -D-glucopyranosyl-quercetin-3-*O*- β -D-glucopyranosyl-(1 \rightarrow 4)- β -D-glucopyranoside (**2**) were isolated from *H. zeylanica* root 50% EtOH extract. Compound **1** exhibited intracellular melanogenesis stimulatory activity, while **2** showed no effect even the structural similarity of the two compounds. Nineteen quercetin derivatives were synthesized from rutin on the purpose of understanding the structure-activity relationships of quercetin derivatives. Among the synthesized nineteen quercetin derivatives, **1**, **3**, and **4**, the quercetin glycosides, stimulates the intracellular melanogenesis, while they elicits no stimulatory activity on extracellular melanogenesis. On the other hand, the quercetin methylether, **12** and **15** increase the both intra and extracellular melanin contents with no cytotoxicity. Compound **15** stimulated the phosphorylation of p38 MAPK, which regulates the expression of tyrosinase, TRP-1, and TRP-2. Compound **12** enhanced the expression of melanogenic enzymes while it was lack of any stimulation of the expression of MITF and p-p38 MAPK. This result indicates that **12** may stimulate the expression of melanogenic enzymes by stimulating currently unidentified transcriptional factors and/or by regulating the degradation of melanogenic enzymes.

In order to investigate the effect of **12** and **15** on transportation of melanosomes, the cells length and the expression of EPI64 in B16 melanoma cells after treatment of **12** and **15** were examined. Compounds **12** and **15** elongated the dendrite in a dose dependent manner. Furthermore, **12** and **15** stimulated the transportation of melanosome

via inhibiting the expression of EPI64. This results may relate to the potency of extracellular melanogenesis stimulatory activity of **12** and **15**. The investigation of distributions of Rab27A and melanosomes in melanoma cells treated with the samples by immunofluorescence microscopy were support the result on inhibitory activity of expression of EPI64 after treatment of **12** and **15**. The discoveries of the novel melanosome transportation modulating activity of quercetin methylethers in B16 melanoma cells supports further research into its potential anti-graying applications or into possible uses for such compounds as cosmetic products that regulate skin pigmentation.

References

Adewole S.O., Ojewole J.O. (2007) Hyperglycaemic effect of *Artocarpus communis* Forst. (Moraceae) root bark aqueous extract in Wistar rats: cardiovascular topic. *Cardiovasc. J. Afr.*, 18: 221-227.

Aksan I., Goding C. R. (1998) Targeting the Microphthalmia Basic Helix-Loop-Helix–Leucine Zipper Transcription Factor to a Subset of E-Box Elements In *Vitro* and In *Vivo*. *Mol. Cell Biol.* 18: 6930-6938.

Alvaro F.S., Jos R.L.N., Francisco C.G. (1995) Tyrosinase: a comprehensive review of its mechanism. *Biochimica et Biophysica Acta*, 1247: 1-11.

Arung E.T., Furuta S., Ishikawa H., Kusuma W.I., Shimizu K., Kondo R. (2011a) Anti-melanogenesis properties of quercetin- and its derivative-rich extract from *Allium cepa*. *Food Chemistry* 124: 1024-1028.

Arung E.T., Matsubara E., Kusuma I.W., Sukaton E., Shimizu K., Kondo R. (2011b) Inhibitory components from the buds of clove (*Syzygium aromaticum*) on melanin formation in B16 melanoma cells. *Fitoterapia* 82: 198-202.

Ando H., Watabe H., Valencia J. C., Yasumoto K., Furumura M., Funasaka Y., Oka M., Ichihashi M., Hearing V. J., (2004) Fatty acids regulate pigmentation via proteasomal degradation of tyrosinase: a new aspect of ubiquitin–proteasome function. *J. Biol. Chem.*, 279: 15427-15433.

Batubara I., Darusman L.K., Mitsunaga T., Rahminiwati M., Djauhari E. (2010) Potency of Indonesian Medicinal Plants as Tyrosinase Inhibitor and Antioxidant agent. *J. Biol. Sci*

10: 138-144.

Bellei B., Maresca V., Flori E., Pitisc, A., Larue L., Picardo M. (2010) p38 regulates pigmentation via proteasomal degradation of tyrosinase. *J. Biol. Chem.* 285: 7288–7299.

Bertolotto C., Abbe P., Hemesath T. J., Bille K., Fisher D. E., Ortonne J. P., Ballotti R. (1998a) Microphthalmia Gene Product as a Signal Transducer in cAMP-Induced Differentiation of Melanocytes. *J. Cell Biol.* 142: 827-835.

Bertolotto C., Bile K., Ortonne J.P., Ballotti R., (1998b) In B16 melanoma cells, the inhibition of melanogenesis by TPA results from PKC activation and diminution of microphthalmia binding to the M-box of the tyrosinase promoter. *Oncogene* 16: 1665-1670.

Bertolotto C., Buscà R., Abbe P., Bile K., Aberdam E., Ortonne J.P., Ballotti R. (1998c) Different cis-acting elements are involved in the regulation of TRP1 and TRP2 promoter activities by cyclic AMP: pivotal role of M boxes (GTCATGTGCT) and of microphthalmia. *Molecular and Cellular Biology* 18: 694-702.

Bouktaib M., Lebrun S., Atmani A., Rolando C. (2002) Hemisynthesis of all the O-monomethylated analogues of quercetin including the major metabolites, through selective protection of phenolic functions. *Tetrahedron* 58: 10001-10009.

Bu J., Ma P.C., Chen Z.Q., Zhou W.Q., Fu Y.J., Li L.J., Li C.R. (2008) Inhibition of MITF and tyrosinase by paeonol-stimulated JNK/SAPK to reduction of phosphorylated CREB. *Am. J. Chin. Med.* 36, 245-263.

Buscà R., Abbe P., Mantoux F., Aberdam E., Peyssonnaud C., Eychène A., Ortonne J. P.,

Ballotti R. (2000) Ras mediates the cAMP-dependent activation of extracellular signal-regulated kinases (ERKs) in melanocytes. *EMBO J.* 19, 2900-2910.

Chan Y. Y., Kim K. H., Cheah S. H. (2011) Inhibitory effects of *Sargassum polycystum* on tyrosinase activity and melanin formation in B16F10 murine melanoma cells. *Journal of Ethnopharmacology* 137: 1183-1188.

Chen C.H., Chan H.C., Chu Y.T., Ho H.Y., Chen P.Y., Lee T.H., Lee C.K. (2009) Antioxidant activity of some plant extracts towards xanthine oxidase, lipoxygenase and tyrosinase. *Molecules* 14: 2947-2958.

Chen Q.X., Kubo I.J. (2002) Kinetics of mushroom tyrosinase inhibition by quercetin *Agric Food Chem.* 50: 4108-4112.

Chiang H. M., Chien Y.C., Wu C.H., Kuo Y.H., Wu W.C., Pan Y.Y., Su Y. H., Wen K.C. (2014) Hydroalcoholic extract of *Rhodiola rosea* L. (Crassulaceae) and its hydrolysate inhibit melanogenesis in B16F0 cells by regulating the CREB/MITF/tyrosinase pathway *Food and Chemical toxicology* 65: 129-139.

Chiu N.Y., Chang K.H. (1992) *The illustrated medicinal plants of taiwan.* 3, SMC Publishing Inc, Taipei. 18.

Cooksey C.J., Garratt P.J., Land E.J., Ramsden C.A., Riley P.A. (1998) Tyrosinase kinetics: failure of the auto-activation mechanism of monohydric phenol oxidation by rapid formation of a quinomethane intermediate. *Biochemical Journal* 333: 685-691.

Diwakar G., Rana J., Scholten D.J. (2012) Inhibition of melanin production by a combination of Siberian larch and pomegranate fruit extracts. *Fitoterapia* 83: 989-995.

Englaro W., Bertolotto C., Busca R., Brunet A., Pages G., Ortonne J.P., Ballotti R., (1998) Inhibition of the mitogen-activated protein kinase pathway triggers B16 melanoma cell differentiation. *J. Biol. Chem.* 273: 9966-9970.

Elfahmi Woerdenbag J.H., Kayser O. (2014) Jamu: Indonesian traditional herbal medicine towards rational phytopharmacological use. *Journal of herbal medicine* 4: 51-73.

Fuji T., Saito M. (2009) Inhibitory effect of quercetin isolated from rose hip (*Rosa canina* L.) against melanogenesis by mouse melanoma cells. *Biosci. Biotechnol. Biochem.* 9: 1989-1993.

Fukuda M. (2005) Versatile role of Rab27 in membrane trafficking: focus on the Rab27 effector families. *J. Biochem.*, 137: 9-16.

Fukuda M. (2006) Rab27 and its effectors in secretory granule exocytosis: a novel docking machinery composed of a Rab27 · effector complex *Biochem. Soc. Trans.*, 34: 691-695.

Fukuda M., Kuroda T.S., Mikoshiba K. (2002) Slac2-a/melanophilin, the missing link between Rab27 and myosin Va: Implications of a tripartite protein complex for melanosome transport. *J. Biol. Chem.* 277: 12432-12436.

Gibellini L., Pinti M., Nasi M., Roat B.S. DeE., Bertoncelli L., Cossarizza A. (2009) Interfering with ROS metabolism in cancer cells: the potential role of quercetin. *Cancers* 2: 1288-1311.

Guo H., Fang Y. K., Jixing D., Yizhan Y., Yuhong X., Xiaohua L., Yang T.L. (2012)

Wnt3a promotes melanin synthesis of mouse hair follicle melanocytes. *Biochemical and Biophysical Research Communications* 420: 799-804.

Hertog G.L.M., Hollman H.P.C., Katan M.B. (1992) Intake of potentially anticarcinogenic flavonoids and their determinants in adults in the Netherlands. *J. Agric. Food Chem.* 40: 2379-2383.

Hirata N., Naruto S., Ohguchi K., Akao Y., Nozawa Y., Inumac M., Matsuda H. (2007) Mechanism of the melanogenesis stimulation activity of (-)-cubebin in murine B16 melanoma cells. *Bioorganic & Medicinal Chemistry* 15: 4897-4902.

Hollman C.H.P., Katan B.M. (1999) Dietary Flavonoids: Intake, Health Effects and Bioavailability. *Food Chem. Toxicol.* 37: 937-942.

Huang Y.L., Yeh P.Y., Shen C.C., Chen C.C. (2003) Antioxidant flavonoids from the rhizomes of *Helminthostachys zeylanica*. *Phytochemistry* 64: 1277-1283.

Huang Y.T., Hwang C., Chang Y., Yang C., Shen W., Liao S., Chen C., Liaw (2009) Antiinflammatory flavonoids from the rhizome of *Helminthostachys zeylanica*. *J Nat Prod* 72: 1273-1278.

Ikawati Z., Wahyuono S., Maeyam K. (2001) Screening of several Indonesian medicinal plants for their inhibitory effect on histamine release from RBL-2H3 cells. *Journal of Ethnopharmacology* 75: 249-256.

Ishida M., Ohbayashi N., Maruta Y., Ebata Y. Fukuda M. (2012) Functional involvement of Rab1A in microtubule-dependent anterograde melanosome transport in melanocytes. *J. Cell Sci.*, 125: 5177-5187.

Itoh T., Fukuda M.J. (2006) Identification of EPI64 as a GTPase-activating Protein Specific for Rab27A. *Biol. Chem.*281: 31823-31831.

Jang Y.J., Kim N.H., Kim R.Y., Choi W.Y., Choi H.Y., Shin K.H., Choi T.B. (2011) Partially purified components of *Nardostachys chinensis* suppress melanin synthesis through ERK and Akt signaling pathway with cAMP down-regulation in B16F10 cells. *Journal of Ethnopharmacology* 137: 1207-1214.

Jian D., Jiang D., Su J., Chen W., Hu X., Kuang Y., Xie H., Li J., Chen X. (2011) Diethylstilbestrol enhances melanogenesis via cAMP-PKA-mediating up-regulation of tyrosinase and MITF in mouse B16 melanoma cells. *Steroids* 76: 1297-1304.

Jiang Z., Xu J., Long M., Tu Z., Yang G., He G. (2009) 2,3,5,4'-tetrahydroxystilbene-2-O- β -D-glucoside (THSG) induces melanogenesis in B16 cells by MAP kinase activation and tyrosinase upregulation. *Life Sci.* 85: 345-350.

Kamiya K., Saiki Y., Hama T., Fujimoto Y., Endang H., Umar M., Satake T. (2001) Flavonoid glucuronides from *Helicteres isora* . *Phytochemistry* 57:297-301.

Kajjout M., Rolando C. (2011) Regiospecific synthesis of quercetin O- β -d-glucosylated and O- β -d-glucuronidated isomers. *Tetrahedron* 67: 4731-4741.

Kajjout M., Zemmouri R., Rolando C. (2011) An expeditious synthesis of quercetin 3-O- β -D-glucuronide from rutin. *Tetrahedron Letters* 52: 4738-4740.

Karin M. (1995) The regulation of AP-1 activity by mitogen-activated protein kinases. *J. Biol. Chem.* 270: 16483-16486.

Kim S.S., Kim M.J., Choi Y.H., Kim K.S., Park K.J., Park S.M., Lee N.H., Hyun C.G.

(2013) Down-regulation of tyrosinase, TRP-1, TRP-2 and MITF expressions by citrus press-cakes in murine B16 F10 melanoma. *Asian Pacific Journal of Tropical Biomedicine*, 3: 617-622.

Koz O., Bedir E., Masullo M., Ozgen A.C., Piacente S. (2010) Triterpene glycosides from *Agrostemma gracilis*. *Phytochemistry* 71: 663–668.

Kurkin V., Zapesochnaya G. (1985) Chemical composition and pharmacological characteristics of *Rhodiola rosea* [review]. *J. Med. Plants*. 1231-1445.

Kubo I., Murai Y., Soediroa I., Soetarnoa S., Sastrodihardjoa S. (1992) Cytotoxic anthraquinones from *Rheum palmatum*. *Phytochemistry* 31: 1063-1065

Kuroda T.S., Ariga H., Fukuda M. (2003) The Actin-Binding Domain of Slac2-a/Melanophilin Is Required for Melanosome Distribution in Melanocytes. *Mol. Cell. Biol.* 23: 5245-5255.

Kuroda T.S., Fukuda M. (2004) Rab27A-binding protein Slp2-a is required for peripheral melanosome distribution and elongated cell shape in melanocytes. *Nat. Cell Biol.*, 6: 1195-1203.

Lan W.C., Tzeng C.W., Lin C.C., Yen F.L., Ko H.H. (2013) Prenylated flavonoids from *Artocarpus altilis*: Antioxidant activities and inhibitory effects on melanin production. *Phytochemistry* 89: 78-88.

Lee C.H., Huang Y.L., Liao J.F., Chiou W.F. (2011) Ugonin K promotes osteoblastic differentiation and mineralization by activation of p38 MAPK- and ERK-mediated expression of Runx2 and osterix. *Eur. J. Pharmacol.* 668: 383-389.

Lee C.H., Huang Y.L., Liao J.F., Chiou W.F. (2012) Ugonin K-stimulated osteogenesis involves estrogen receptor-dependent activation of non-classical Src signaling pathway and classical pathway. *Eur. J. Pharmacol.* 676: 26-33.

Lopez-Bergami P. (2011) The role of mitogen- and stress-activated protein kinase pathways in melanoma. *Pigment Cell Melanoma Res* 24: 902-21.

Lukiewicz S. (1972) The biological role of melanin. I. New concepts and methodological approaches. *Folia Histochemica Cytochemica* 10: 93-108.

Nagata H., Takekoshi S., Takeyama R., Homma T., Osamura Y.R. (2004) Quercetin enhances melanogenesis by increasing the activity and synthesis of tyrosinase in human melanoma cells and in normal human melanocytes. *Pigment Cell Res.* 17: 66-73.

Nerya O., Vaya J., Musa R., Izrael S., Ben-Arie R., Tamir S. (2003) Glabrene and Isoliquiritigenin as Tyrosinase Inhibitors from Licorice Roots *J. Agric. Food. Chem.*, 51: 1201-1207.

Manach C., Scalbert A., Morand C., Rémésy C., Jimenez L. (2004) Polyphenols: food sources and bioavailability. *Am. J. Clin. Nutr.* 79: 727-747.

Mendoza-Wilson A.M., Santacruz-Ortega H., Balandrán-Quintana R.R. (2011) Relationship between structure, properties, and the radical scavenging activity of morin *Journal of Molecular Structure* 995: 134-141.

Mingo-Sion, A.M., Marietta, P.M., Koller, E., Wolf, D.M., & Van Den Berg, C.L. (2004) Inhibition of JNK reduced G2/M transit independent of p53, leading to endoreduplication, decreased proliferation, and apoptosis in breast cancer cells. *Oncogene* 23(2): 596-604.

Moon J.H., Tsushida T., Nakahara K., Terao J. (2001) Identification of quercetin 3-O-beta-d-glucuronide as an antioxidative metabolite in rat plasma after oral administration of quercetin. *Free Radical Biology and Medicine* 30: 1274-1285.

Murakami T., Hagiwara M., Tanaka K., Chen C.M. (1973a) Chemische untersuchungen U ber die inhaltsstoffe von *Helminthostachys zeylanica* (L.) Hook. I. *Chemical & Pharmaceutical Bulletin* 21: 1849-1851.

Murakami T., Hagiwara M., Tanaka K., Chen C.M. (1973b) Chemische untersuchungen U ber die inhaltsstoffe von *Helminthostachys zeylanica* (L.) Hook. II. *Chemical & Pharmaceutical Bulletin* 21: 1851-1852.

Ohbayashi N., Maruta Y., Ishida M., Fukuda M. (2012a) Melanoregulin regulates retrograde melanosome transport through interaction with the RILP-p150Glued complex in melanocytes. *J. Cell Sci.*, 125: 1508-1518.

Ohbayashi N., Yatsu A., Tamura K., Fukuda M. (2012b) The Rab21-GEF activity of Varp, but not its Rab32/38 effector function, is required for dendrite formation in melanocytes. *Mol. Biol. Cell* 23: 669-678.

Oh E.Y., Jang J.Y., Choi Y.H., Choi Y.W., Choi B.T. (2010) Inhibitory effects of 1-O-methyl-fructofuranose from *Schisandra chinensis* fruit on melanogenesis in B16F0 melanoma cells. *J. Ethno.* 132: 219-224.

Olejniczak S., Potrzebowski M.J. (2004) Solid state NMR studies and density functional theory (DFT) calculations of conformers of quercetin. *Org. Biomol. Chem.* 2: 2315-2322.

Rees J.L. (2003) Genetics of hair and skin color. *Annual Review of Genetics* 37: 67-90.

Park S.Y., Kim Y.H., Kim Y.H., Park G., Lee S.J., (2010) Beta-carboline alkaloids harmaline and harmalol induce melanogenesis through p38 mitogen-activated protein kinase in B16F10 mouse melanoma cells. *BMB Rep.* 43: 824-829.

Prota G. (1995) The chemistry of melanins and melanogenesis. *Fortsch Chem. Organ. Natur.* 64: 93-148.

Roberts P.J., Der C.J. (2007) Targeting the Raf-MEK-ERK mitogen-activated protein kinase cascade for the treatment of cancer. *Oncogene* 26: 3291-3310.

Saaby L., Rasmussen H.B., Jager A.K. (2009) MAO-A inhibitory activity of quercetin from *Calluna vulgaris* (L.). *Journal of Ethnopharmacology* 121: 178-181.

Saratikov A., Krasnov E., Khnikina L., Duvidson L. (1967) Isolation and chemical analysis of individual biologically active constituents of *Rhodiola rosea*. *Proc. Siberian Acad. Sci. Biol.*, 1: 54-60.

Shimizu K., Kondo R., Sakai K. (2000) Inhibition of Tyrosinase by Flavonoids, Stilbenes and Related 4-Substituted Resorcinols: Structure-Activity Investigations. *Planta Med.* 66: 11-15.

Shimizu K., Kondo R., Sakai K., Lee S.H., Sato H. (1998) The Inhibitory Components from *Artocarpus incisus* on Melanin Biosynthesis. *Planta Med.* 64: 408-412.

Slominski A., Paus R. (1993) Melanogenesis is coupled to murine anagen: toward new concepts for the role of melanocyte and the regulation of melanogenesis in hair growth. *J. Invest. Dermatol.* 90S-97S.

Slominski A., Paus R., Plonka P., Chakraborty A., Maurer M., Pruski D., Lukiewicz S.

(1994) Melanogenesis during the anagen-catagen-telogen transformation of the murine hair cycle. *Journal of Investigative Dermatology*. 102: 862-869.

Slominski A., Wortsman J., Plonka P.M., Schallreuter K.U., Paus R., Tobin D.J. (2005) Hair follicle pigmentation *J. Invest. Dermatol.* 124: 13-21.

Suja S.R., Latha P.G., Pushpangadan P., Rajasekharan S. (2004) Evaluation of hepatoprotective effects of *Helminthostachys zeylanica* (L.) Hook against carbon tetrachloride-induced liver damage in Wistar rats. *Journal of Ethnopharmacology* 92: 61-66.

Tachibana M., Takeda K., Nobukuni Y., Urabe K., Long J.E., Meyers K.A., Aaronson S.A., Miki T. (1996) Ectopic expression of MITF, a gene for Waardenburg syndrome type 2, converts fibroblasts to cells with melanocyte characteristics. *Nat. Genet.* 14: 50-54.

Tamura K., Ohbayashi N., Ishibashi K., Fukuda M. (2011) Structure-function analysis of VPS9-ankyrin-repeat protein (Varp) in the trafficking of tyrosinase-related protein 1 in melanocytes. *J Biol Chem.* 286: 7507-7521.

Tamura K., Ohbayashi N., Maruta Y., Kanno E., Itoh T., Fukuda M. (2009) Varp is a novel Rab32/38-binding protein that regulates Tyrp1 trafficking in melanocytes. *Mol. Biol. Cell* 20: 2900-2908.

Tobin D.J., Slominski A., Botchkarev V., Paus R. (1999) The fate of hair follicle melanocytes during the hair growth cycle. *Journal of Investigative Dermatology Symposium Proceedings* 4: 323-332.

Tobin D.J., Hagen E., Botchkarev V.A., Paus R. (1998) Do hair bulb melanocytes undergo

apoptosis during hair follicle regression (catagen)? *Journal of Investigative Dermatology* 111: 941-947.

Uzgare R.A., Isaccs T.J. (2004) Enhanced redundancy in Akt and Mitogen-activated protein kinase-induced survival of malignant *versus* normal prostate epithelial cells. *Cancer Research* 64: 6190-6199.

Wagner H., Chari V.M., Sonnenbichler J. (1976) ¹³C-NMR-spektren natürlich vorkommender flavonoide. *Tetrahedron lett.* 21: 1799-1802.

Wang Y., Zhang G., Yan J., Gong D., (2014) Inhibitory effect of morin on tyrosinase: Insights from spectroscopic and molecular docking studies. *Food chemistry* 163: 226-233.

Wang H., Pan Y., Tang X., Huang Z. (2006) Isolation and characterization of melanin from *Osmanthus fragrans*' seeds. *LWT-Food Science and Technology* 39: 496-502.

Wei B., Zhang Y.P., Yan H.Z., Xu Y., Du T.M. (2014) Cilostazol promotes production of melanin by activating the microphthalmia-associated transcription factor (MITF). *Biochemical and Biophysical Research Communications* 443: 617-621.

Weston C.R., Davis R.J. (2007) The JNK signal transduction pathway. *Curr. Opin. Cell Biol.* 19: 142-149.

Wu X.S., Rao K., Zhang H., Wang F., Sellers J.R., Matesic L.E. Copel N.G., Jenkins N.A., Hammer J.A. III (2002) Identification of an organelle receptor for myosin-Va. *Nat. Cell Biol.* 4: 271-278.

Yang Y.M., Son Y.O., Lee S.A., Jeon Y.M., Lee J.C. (2011) Quercetin Inhibits α -MSH-stimulated Melanogenesis in B16F10 Melanoma Cells. *Phytotherapy Research* 25: 1166-

1173.

Yamauchi K., Mitsunaga T., Batubara I. (2011) Isolation, identification and tyrosinase inhibitory activities of the extractives from *Allamanda cathartica*. *Natural Resources*, 2:167-172.

Yamauchi K., Mitsunaga T., Batubara I. (2013) Novel quercetin glucosides from *Helminthostachys zeylanica* root and acceleratory activity of melanin biosynthesis. *J. Nat. Med.* 67: 369-374.

Yamauchi K., Mitsunaga T., Batubara I. (2014a) Synthesis of quercetin glycosides and their melanogenesis stimulatory activity in B16 melanoma cells. *Bioorganic & Medicinal Chemistry* 22: 937-944.

Yamauchi K., Mitsunaga T., Inagaki M., Suzuki T. (2014b) Synthesized quercetin derivatives stimulate melanogenesis in B16 melanoma cells by influencing the expression of melanin biosynthesis proteins MITF and p38 MAPK. *Bioorganic & Medicinal Chemistry* 22, 3331-3340.

Ye Y., Chou G.X., Wang H., Chu J.H., Yu Z.L. (2010a) Flavonoids, apigenin and icariin exert potent melanogenic activities in murine B16 melanoma cells. *Phytomedicine* 18: 32-35.

Ye Y., Chu J.H., Wang H., Xu H., Chou G.X., Leung A., Fong I.K.M., W.F, Yu Z.L., (2010b) Involvement of p38 MAPK signaling pathway in the anti-melanogenic effect of San-bai-tang, a Chinese herbal formula, in B16 cells. *Journal of Ethnopharmacology* 132: 533-535.

Yoon S., Seger R. (2006) The extracellular signal-regulated kinase: multiple substrates regulate diverse cellular functions. *Growth Factors* 24: 21-44.

Yoshida M., Takahashi T., Inoue S. (2000) Histamine induces melanogenesis and morphologic changes by protein kinase A activation *via* H₂ receptors in human normal melanocytes. *J Invest Dermatol.* 114: 334-342.

Acknowledgments

I'm highly appreciated to Professor Dr. Tohru Mitsunaga, United Graduate School of Agricultural Science, Gifu University for the supervision and encouragement through the ph. D. study period. He gave me the opportunity to proceed ph. D. course, and he also gave me the knowledge and suggestions on my study. We have discussed everyday about the improvement of the experiment methods, future plans, collaborations with the abroad, and even administration of the laboratory. All of the discussions support me to behave as researcher as well as to proceed my study.

I also would like to thank to Professor Dr. Shingo Kawai, United Graduate School of Agricultural Science, Shizuoka University, and Professor Dr. Tohru Suzuki, United Graduate School of Agricultural Science, Gifu University, for their valuable comments and suggestions.

I gratefully acknowledges to Dr. Mizuho Inagaki supporting the experiments and discussing my study on molecular biology area.

I would like to thank to all laboratory member, Kazuya Onoe, Megumi Ogawa, Yasuko Ogata, Miyuki Nagai, Wang Xiaoyu, Sun Hao, Ryuta Suzuki, and Syoko Sakamoto, Master course students, and Hiroyuki Hattori, Yuki Takahashi, and Wakaho Nakashima, under graduate students, for supporting the study and for keeping the good an atmosphere in our laboratory. Also, I appreciate to the already graduated laboratory members studied together.